UNIVERSITÀ POLITECNICA DELLE MARCHE

DIPARTIMENTO DI SCIENZE DELLA VITA E DELL'AMBIENTE

CORSO DI LAUREA MAGISTRALE IN

BIOLOGIA MARINA

Nannofossili calcarei per la ricostruzione paleoceanografica del Mar Mediterraneo Orientale al tempo della deposizione del sapropel S6 (180 ka)

Calcareous nannofossils to reconstruct the Eastern Mediterranean Sea paleoceanography at the time of sapropel S6 deposition (180 ka ago)

Tesi di Laurea di:
Aiudi Laura

Relatore:
Chiar.ma Prof.ssa **Negri Alessandra**

Sessione Straordinaria
Anno Accademico 2018/2019

TABLE OF CONTENTS

ABSTRACT

The Mediterranean Sea is defined as a perfect “laboratory" to study the effect of climate change. In fact, it is a semi-closed basin and is more sensitive to the climate variation and also to the undergoing high anthropic pressure.

In the past, the Mediterranean Sea has been affected by major environmental changes, which are useful to understand the ongoing changes.

The geological records show that the deposition of oxygenated hemipelagic sediment periodically alternated with dark-black anoxic sediment layers, called sapropels

These layers are the effect of environmental changes that periodically affected the Mediterranean basin (last 5.3 Ma).

The analysis of these layers provides an excellent tool in the study of paleoclimate and paleoceanography and allows to better understand what are the natural forces that can be expressed during climate change.

The sapropels are the object of this thesis, in particular the sapropel S6, defined "cold" because it is the only sapropel, together with S8, to have settled in a glacial period, about 180 ka.

The aim of this work is to investigate the causes of the deposition of this unusual sapropel.

In fact, since their discovery, an intense debate on the causes of the deposition

of sapropels is taking place within the scientific community. The two main theories proposed are: the stagnation model (the anoxic condition is the dominant cause of the preservation of organic matter) and the productivity model (increase in primary production that triggered flow of organic carbon on the seabed).

The area studied in this work the Ionian Sea, where in 1993 the core M25/4-12 was taken.

Calcareous nannofossil have been chosen as tool tackle the causes of S6 deposition. The quantitative and qualitative analysis of calcareous nannofossils allows the investigation of environmental conditions throughout geological history. Thanks to the collaboration with the Australia National University and the University of Utrecht, were also available for this work stable oxygen isotope data and dinocyst and pollens analyses obtained for the same core.

RIASSUNTO

Il Mediterraneo viene definito come perfetto “laboratorio" per studiare l'effetto dei cambiamenti climatici in quanto soggetto a questi più di altre zone.

Essendo infatti un bacino semichiuso è più sensibile alle variazioni del clima e soprattutto all'elevata pressione antropica a cui è soggetto.

Anche in passato il Mediterraneo è stato interessato da grandi cambiamenti ambientali, utili alla comprensione degli attuali cambiamenti globali.

I record geologici evidenziano come la deposizione di sedimento emipelagico ossigenato si sia periodicamente alternato a strati di sedimento anossico di colore scuro-nero, chiamati Sapropel.

Questi strati sono l'impronta di un netto cambiamento ambientale verificatosi più volte, in maniera ciclica, nel bacino del Mediterraneo, negli ultimi 5.3 Ma.

L'analisi di questi strati fornisce alla ricerca un ottimo strumento nello studio del paleoclima e della paleoceanografia, e permette, in ottica futura, di comprendere meglio quelle che sono le forzanti naturali che possono esprimersi durante i cambiamenti climatici.

I sapropel sono l'oggetto di questa tesi, in particolare il Sapropel S6, definito "freddo" poiché è l'unico dei sapropel, insieme a S8, ad essersi depositato in un periodo glaciale, circa 180 ka.

L'obiettivo del presente lavoro è quello di indagare le cause della deposizione

di tale inusuale sapropel. Infatti, dalla loro scoperta, è in atto all'interno della comunità scientifica, un acceso dibattito sulle cause della deposizione dei sapropel. Le due teorie principali proposte sono: il modello della stagnazione (ovvero formazioni in condizioni di anossia) da un lato e il modello della produttività (che incrementa il flusso di materiale organico verso il fondo) dall'altro.

L'area studiata in questo lavoro è quella del Mar Ionio, in cui nel 1993 è stata prelevata la carota M25/4-12.

Come mezzo per lo studio delle cause della deposizione del S6 sono stati utilizzati i nannofossili calcarei, ovvero fossili di Coccolitoforidi che si sono depositati sul fondale marino. L'analisi quantitativa e qualitativa dei nannofossili calcarei permette di investigare le condizioni ambientali nel corso della storia geologica.

I Coccolitoforidi sono un importante gruppo del fitoplancton ed elemento chiave della produzione primaria e dei principali cicli biogeochimici marini. La loro distribuzione è influenzata da variazioni ambientali come temperatura, salinità, nutrienti e luce e infatti in base alle loro preferenze ecologiche si può risalire alle variazioni paleoambientali avvenute in tempi passati, in particolar modo in questo lavoro durante la deposizione di S6.

L'analisi quantitativa dei nannofossili calcarei è stata effettuata tramite una

metodologia sperimentale, teorizzata da Flores *et al*. (1997), che permette di conoscere il numero di nannofossili calcarei per grammi di sedimento all'interno di un campione. Nonostante sia un metodo vantaggioso per quanto riguarda l'effettiva analisi delle abbondanze assolute dei nannofossili calcarei, risulta essere alquanto macchinoso e lungo, la cui preparazione rischia di compromettere la qualità dei campioni. Ulteriori prove sono quindi necessarie per confermare la validità di questo metodo.

Insieme ai dati delle abbondanze assolute e relative dei nannofossili calcarei, grazie alla collaborazione con Australian National University e l'Università di Utrecht, sono stati utilizzati anche i dati sugli isotopi stabili dell'ossigeno $\delta^{18}O$ e le analisi di dinocisti e di polloni.

Questi dati hanno permesso di evidenziare diverse caratteristiche in termini di associazioni e loro significato paleoceanografico del sapropel S6. Esso può essere diviso in 3 intervalli: la base S6a, S6b intervallo tra due interruzioni e S6c che comprende il top del sapropel. In generale le abbondanze ci mostrano un andamento decrescente verso il top della carota.

L'intervallo pre-sapropel è caratterizzato da basse temperature (12°C) e infatti la specie che mostra picchi di abbondanza è *Coccolithus pelagicus* definita "cold species". La base del sapropel è caratterizzata invece da temperature più elevate (16/17°C), come ipotizzato per gli altri sapropel da Emeis *et al.,* (2003).

S6a mostra un generale raffreddamento verso il top, ma un aumento di *Florisphaera profunda*, ci permette di identificare la formazione di un DCM. Infatti, tutto il sapropel S6 è caratterizzato da un'alta produttività. Questa produttività è suggerita anche dall'alternanza di *C. pelagicus* e *Helicosphaera carteri* che indicano alta produttività rispettivamente a temperature basse e a temperature un po' più calde e condizioni di torbidità, probabilmente dovute ad un apporto di acque dolci da costa.

Nell'intervallo S6b e S6c, *F. profunda* ci mostra un andamento opposto, decresce a discapito di *H. carteri*. Probabilmente ciò è dovuto ad una condizione generale di apporto di acque provenienti da sbocchi fluviali e quindi da costa che crea torbidità e non permette la formazione di DCM, come nella parte bassa del S6.

L'aumento dell'apporto di acque di origine fluviale è anche suggerito dalle abbondanze delle specie "rimaneggiate", infatti ci troviamo in una zona di scarpata e al momento della deposizione. Si possono anche ipotizzare eventi di cascading o torbiditici innescati a seguito di piene fluviali con conseguente trasporto in profondità di sedimenti deposti originariamente in zone di piattaforma. L'analisi delle dinocisti supporta l'ipotesi di condizioni di alta produttività e di trasporto di nutrienti. Mentre l'analisi sull'associazione pollinica rivela che questo sapropel non si è depositato in condizioni così aride,

come si dovrebbe supporre dal periodo glaciale, ma probabilmente la sua formazione è avvenuta in un periodo di intermedio tra un clima arido e uno più umido.

In conclusione, la temperatura non sembra aver un ruolo decisivo sulla deposizione di questo sapropel, ma solo sul comportamento delle masse d'acqua: scarico di acque dolci e scioglimento di ghiaccio, dovuto alle fluttuazioni di temperatura, hanno permesso la creazione di un "blanket" superficiale che ha verosimilmente inibito il rimescolamento delle acque profonde, portando ad anossia.

I trend espressi dalle differenti specie di Coccolitoforidi evidenziano che sapropel si è iniziato a depositare dopo un primo picco di produttività e formazione di un DCM che ha innescato un alto consumo di ossigeno. Successivamente si sono stabilizzate le condizioni lungo la colonna d'acque e il continuo apporto di acque dolci ha creato le condizioni per l'inibizione del rimescolamento in profondità e quindi il mantenimento di condizioni anossiche anche in assenza di DCM.

Si può quindi dire che questo sapropel, confermato essere "freddo", non si è formato solo per un evento di anossia o di alta produttività, ma che piuttosto queste due condizioni abbiano interagite e supportato la sua deposizione.

Chapter One

MEDITERRANEAN SEA AND SAPROPELS

1.1 THE MEDITERRANEAN SEA: OCEANOGRAPHY AND CLIMATE

The Mediterranean Sea is an enclosed basin composed of two similar basins and different sub-basins. It is a concentration basin, where evaporation exceeds precipitation. The Mediterranean is furthermore the site of water mass formation processes, which can be studied experimentally because of their easy accessibility. There are two main reasons why the Mediterranean is important. The first one is the impact of the Mediterranean on the global thermohaline circulation; the second reason is that the Mediterranean basin can be considered as laboratory for investigating processes occurring on the global scale of the world ocean. (Bergamasco, Malanotte-Rizzoli, 2010).

1.1.1 *Oceanography*

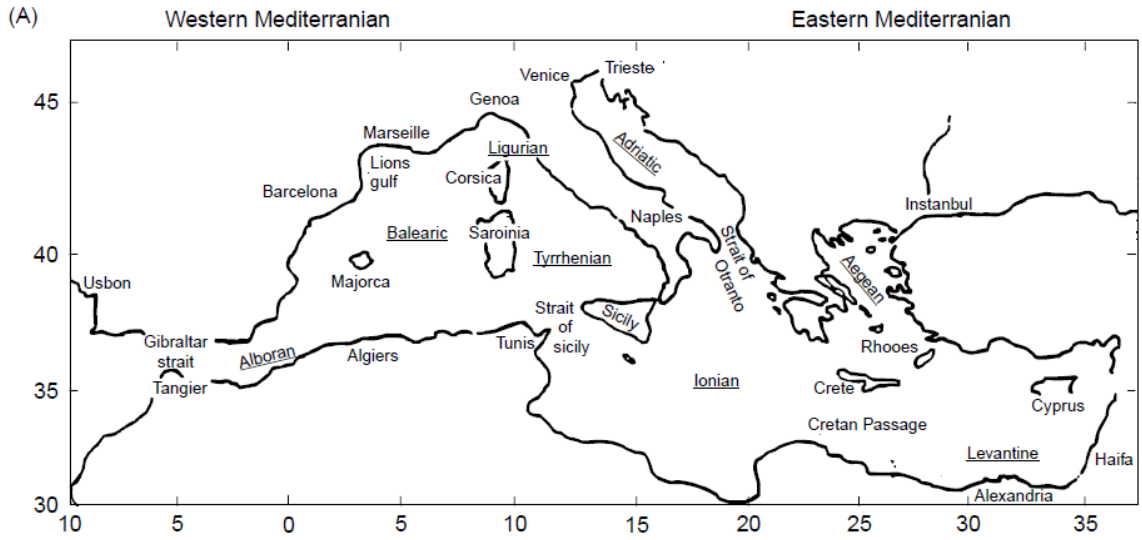

Figure 1.1: *The Mediterranean Sea geography and nomenclature of major sub-basins and straits* (Robinson *et al.*, 2001)

The Mediterranean Sea is a residual intercontinental basin of a paleo-ocean interposed between Eurasia and Africa, called Tethys.

It covers an area of about 2.5 million km^2, with a maximum depth of 4900 m.

It is connected to the West with the Atlantic Ocean, through the Strait of Gibraltar; to the East with the Black Sea, through the Sea of Marmara and the Strait of Dardanelli and the Bosphorus; and to the South East with the Red Sea through the Suez Canal.

The Mediterranean Sea is divided into two main basins, the Western Basin and the Eastern Basin, which can also be considered semi-closed.

Western Med includes the Alboran Sea, the Algerian-Provençal basin and the Tyrrhenian basin. It is connected to the east by the channel of Sicily and is characterized by wide abyssal plains.

The Eastern Med includes the Adriatic Sea, Ionian Sea, Aegean Sea and the Levantine Sea.

One of the main characteristics of the Mediterranean Sea is its vertical thermal profile: even at maximum depths, the temperature does not fall below 12.8°C, while in the oceans the temperature at corresponding altitudes is about 2°C. This characteristic is due to the shallow depth of the Strait of Gibraltar, which prevents the cold and deep waters of the Atlantic Ocean to penetrate the Mediterranean basin, while the input flow consists of warmer surface waters (13-14°C) also in winter.

The Mediterranean Sea is a basin with strong evaporation rate, in fact the average values are about 130 cm/year in September and 65 cm/year in May, with extremely high values in the southern area with 500 cm/year (Ovchinnikov, *et al*., 1976).

In summer the evaporation is relatively reduced due to the not too frequent winds and high humidity. On the contrary, in winter the evaporation is very high due to the cold air and the prevalence of dry winds of continental origin.

Evaporation and reduced river water supply mean that Mediterranean is in constant water deficit.

As a consequence of evaporation, the salinity values of the water ranging from 37 to 39 ‰. The minimum values are found on the surface for the inflow of water from the Atlantic Ocean while the maximum values are about 250-500 m (Ovchinnikov *et al.,* 1976).

1.1.2 The Mediterranean circulation

The circulation of water masses is usually explained by two models: due to wind action and thermoaline properties.

Wind-induced circulation is mainly responsible for horizontal movements in the surface layer of the oceans, while thermoaline circulation explains vertical movements and the mixing of water masses.

The water balance of the Mediterranean Sea is characterized by a negative delta of heat at the air-sea interface. In fact, the heat acquired in the summer months is less than the losses in the winter months. As indicated by Pinardi and Masetti (2000) this deficit could justify the antiestuarine character of the thermoaline circulation. By antiestuarine we mean the surface entry of less dense Atlantic waters and exit in depth of denser waters from the Strait of Gibraltar.

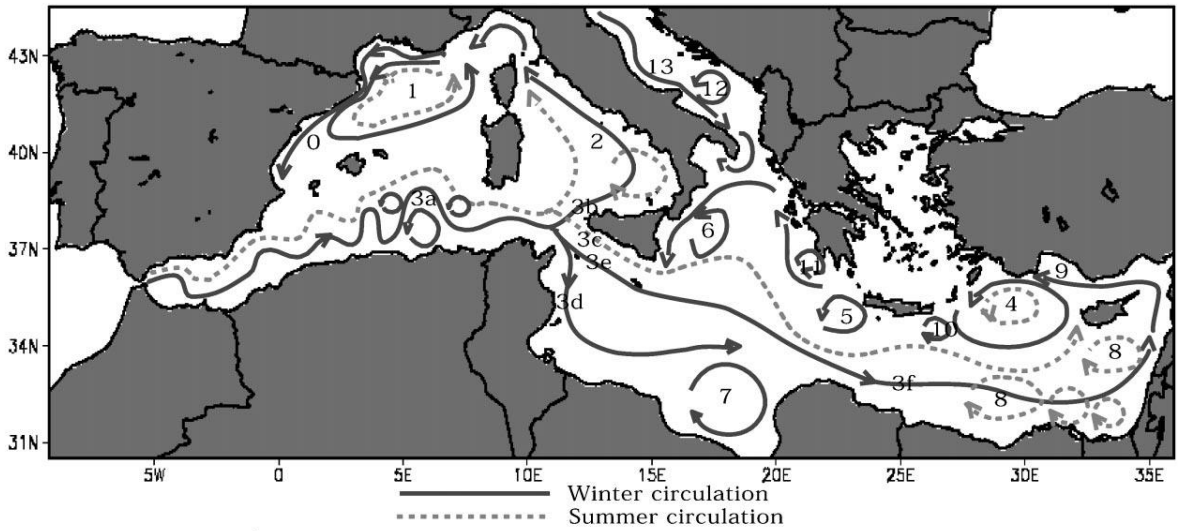

0 Ligurian–Provencal current
1 Lion Gyre
2 Thyrrhenian cyclonic circulation with summer weakening and eastern anticyclone
3 Algerian Current (3a) and eddies, Atlantic–Ionian Stream (3e) branching of the Atlantic–Ionian Stream (3b, 3c, 3d) and Mid–Med. Jet (3f)
4 Rhodes Gyre
5 Western Cretan Gyre
6 Western Ionian Gyre
7 Anticylone in the Gulf of Syrte
8 Shikmona and Mers a–Matruh gyres system
9 Cilician and Asia Minor Current
10 Iera–Petra gyre
11 Pelops gyre
12 Southern Adriatic gyre
13 Western Adriatic Coast al Current

***Figure 1.2**: The Mediterranean Sea circulation* (Pinardi & Masetti, 2000)

Surface waters from the Atlantic are currently moving eastwards, evaporating drastically and increasing their salinity. When these surface waters, become Modified Atlantic Water (MAW), arrive in the most eastern sector of the Mediterranean Sea, the salinity overcome the 39 psu units, reaching a value significantly higher than that of the surface Atlantic waters of origin (about 36,5 psu units) or the average global salinity of the oceans (34,5 psu units). This area of the eastern basin, Levantine Sea, is the site of the formation of the Levantine Intermediate Water (LIW), which from here will retrace backwards, to the West

and to intermediate depths, the path of the Atlantic waters entering from Gibraltar.

Figure 1.3: *Circulation of the Levantine Intermediate Water (Menna and Poulain, 2010, adapted from Millot and Taupier-Letage, 2005)*

The formation of LIW is due to the progressive increase of salinity caused by the evaporation of the Atlantic waters as they proceed from west to east. During the summer, the increase of salinity, up to 39 psu units, is balanced by the parallel increase in temperature that keeps the density low. During winter, however, with the surface cooling of the water, the density increases rapidly, the heavier ones sink up to a depth between 200-600 meters, and head west, affecting the middle layer of all the Mediterranean. Finally, they cross the Strait of Gibraltar and disperse into the Atlantic, contributing their salinity to global circulation.

In the Western and Eastern basins, thermoaline cells are reproduced where the LIW is preconditioned and participates in the formation of deep waters respectively in the Gulf of the Lion and in the northern Adriatic.

In winter the cold and dry continental winds determine the strong cooling of the surface waters and from their sinking form the deep-water mass of the Eastern Basin, Eastern Mediterranean Deep Water EMDW. Later, this last one flows to depth through the strait of Otranto and supplies the Ionic Basin and the Levantine one with a mass of oxygenated and dense water (Löwemark *et al.,* 2006).

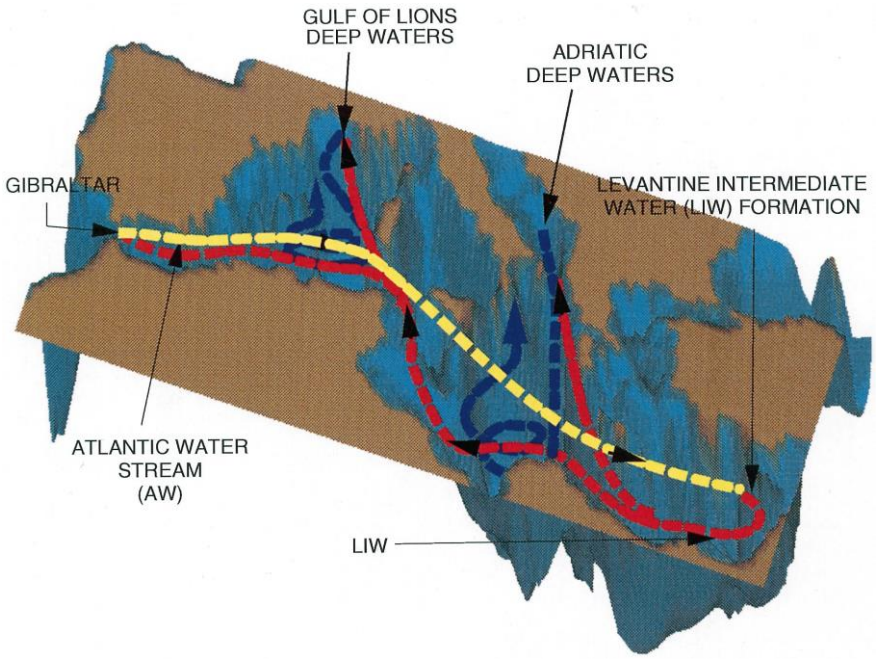

Figure 1.4 *The schematic of thermoaline circulation (Pinardi and Masetti, 2000)*

1.1.3 Chemical, physical and trophic condition of the Mediterranean Sea

Atlantic surface waters directly influence the physical and chemical characteristics of surface waters of the Mediterranean Sea. Water entering the Gibraltar Strait has a relatively low phosphate content (3 μ/l) (Berland *et al.*, 1988). This content gradually decreases along the path of the surface waters to the East. The Mediterranean is therefore characterized by generalized oligotrophy, particularly marked in the eastern region.

The nitrate and phosphate content found by Berland et al 1988 shows some peculiarities: both nutrients are depleted to the point of being irrelevant in the first 100 m of the water column and in a Levantine station, phosphates are irrelevant up to 300 m.

Another characteristic of the Eastern basin is the lower depth of nitratocline compared to phosphatocline. These two “chemical structures” usually appear at the same depth; in some cases, phosphatocline has also been detected at lower depths than nitratocline, indicating nitrates as limiting compounds for surface water systems.

In the oceans, a rich and diversified phytoplanktonic community that takes nutrients and carbon from the environment and uses solar energy to form new biomass through photosynthesis with oxygen production represents the base of the marine trophic net, which is the autotrophic plant organisms.

In the Mediterranean, the light needed for photosynthesis penetrates up to a maximum depth of about 120 m, which limits the presence of phytoplankton to the surface layer of the water column.

Most of the carbon and nutrients originally fixed in the biomass with photosynthesis are released into the water column through the process of photorespiration. However, in illuminated surface layers, the concentration of nutrients remains low, as the released nutrients are immediately reused for photosynthesis. In deep water, where photosynthesis does not occur, the dissolved nutrients are not reused, and their concentration increases over time.

In the water column, the oxygen concentration is inversely proportional to the nutrients concentration: it is high in the surface layer in equilibrium with the atmosphere. Below the surface layer, where the oxygen input is limited to that provided by the deep-water formation process, the oxygen levels decrease rapidly from saturation values in newly formed background water to progressively lower values in older waters. The concentrations of oxygen in deep water therefore reflect a precarious balance between the ventilation of the new deep water and the oxygen consumption through breathing (Rohling, 2001).

Some nutrients are lost from the ocean system and trapped in the ocean floor by the sedimentation process. This loss is balanced by the supply of nutrients

to the ocean through the atmosphere, especially nitrogen, and through rivers especially phosphorus. The river supply, unlike the atmospheric one, is not uniform, but mainly limited to the coastal waters, close to rivers. Here the release of nutrients through rivers is impressive and results in intensive phytoplankton production. In the open ocean, processes that redistribute nutrients are needed (Rohling, 2001). The nutrients in it, released by breathing, accumulate in the intermediate and deep waters constituting a reservoir of enormous volume. In order to make these nutrients available again for photosynthesis, it is necessary to bring them inside the photic zone, whose lower limit in the Mediterranean is about 120 meters (the lower limit is defined as the depth at which 1% of the incident solar radiation penetrates).

In the Mediterranean, an efficient transport of the deep nutrient reservoir is achieved in winter, when intense surface currents in the Gulf of Lyon pump the intermediate water from a depth of about 200 m up to 100 m, causing fertilization at the base of the photic layer. The result is the bloom of a specific phytoplankton combination called Deep Chlorophyll Maximum (DCM).

The second level of the trophic network consists of the secondary producers, also forming a specific association regulated by a complex interaction of parameters, such as food preferences, temperature, depth, competition and

reproductive strategies. The level of specialization increases in the upper trophic levels.

Phytoplanktonic biomass consists essentially of: Diatoms, Dinoflagellates, Coccolithophyceae and numerous unidentifiable microflagellate organisms.

The specific diversity decreases from West to East: the number of phytoplankton cells per liter varies from about $1x10^3$ to about $26,7x10^3$ for the Eastern basin and from about $1x10^3$ to about $164x10^3$ for the Western basin (Berland *et al*., 1988).

Diatoms are almost absent in the first 50 meters of the water column, while they have a maximum of presence at about 100 m of depth, in summer, where they often constitute the almost entire phytoplanktonic biomass.

Dinoflagellates have a clear tendency to concentrate in the first 80 meters of the water column, where they constitute a good part of the total biomass.

Coccolithophyceae also seem to concentrate mainly in the most superficial part of the photic zone, but they are also present in the deeper zone.

An interesting fact is the report of an almost total disappearance of Coccolithophyceae in conjunction with a relative bloom of diatoms, in the Eastern Mediterranean (Berland *et al*., 1988). Diatoms are rather rare in the Eastern basin due to the physico-chemical characteristics of surface water, dominated by oligotrophic conditions and the prevalence of a primary

productivity of the recycled type or based on the recycling of nutrients within the photic zone and not on the injection of nutrients from deeper depths.

1.1.4 Climate

The classic Mediterranean climate is characterized by hot, dry summers and mild, rainy winters.

The Mediterranean climate regime reflects the interplay between the climatic conditions of westelies winds dominating the central and northern areas of Europe and the high-pressure belt of North Africa. (Boucher, 1975; Lolis *et al*., 2002). This last in summer moves northward, consequently most of the Mediterranean is subject to drought. During winter, however, the subtropical conditions are shifted to the south and the Mediterranean passes under the influence of cold and dry polar ad continental air masses, which are carried to the basin through the lower Rhone Valley towards the Gulf of Lion ("Mistral") and also across the Adriatic and the Aegean Sea ("Bora" and "Vardar"), causing strong evaporation and cooling of the sea surface (Leaman and Schott, 1991; Saaroni *et al*., 1996; Maheras, 1999; Casford *et al.*, 2003).

The low surface pressure conditions during winter are the direct consequence of the high sea surface temperatures due to the high thermal capacity of the basin water masses (Lolis *et al*., 2002).

Cold and relatively dry air flows to the north above the warm sea surfaces cause intense cyclogenesis (formation of new depressions) in the northern sectors of the Mediterranean Sea. Although cyclones from the Atlantic can penetrate into the basin, most tend to grow in preferred areas of cyclogenesis (Rumney, 1968). These areas are more frequent in the Western basin, in particular in the Gulf of Genoa. In winter also the Cyprus area becomes a significant centre of cyclogenesis (Trewartha, 1966; Rumney 1968; Boucher, 1975; Furlan, 1977). Most of the Genoese depressions move southeast under the Italian coasts, then east or northeast through the Aegean Sea and the northern Levantine (Trewartha, 1966; Rumney, 1968; Trigo *et al*., 1999; Lolis *et al*., 2002). These depressions cause the winter rainfall which are all over the current Mediterranean climate. The ratio of hydrogen and oxygen stable isotopes characterizing these precipitations identifies the Mediterranean Meteoric Water Line MMWL, which differs from the Meteoric Water Line MWL, at a global level due to the contribution of low humidity air masses derived from the evaporation of Mediterranean waters (Matthews *et al.,* 2000).

The Mediterranean depressions are considered secondary “depressions”, often related to wider disturbances north of the Alps, since their central pressures are considerably higher than those associated with Atlantic storms (Trewartha, 1966; Boucher 1975).

In summer the South-Eastern Mediterranean is affected by the circulation of the “Etesians”, dry winds generated by a branch of the Asian depression, characteristic of the summer circulation of the south-eastern Europe up to the Levantine area, in response to counterclockwise circulation around the dominant monsoons (Mariopoulos, 1961; Furlan 1977).

The summer that currently characterizes the climate of the Eastern basin has presumably developed in the late Paleogene in response to climatic changes induced by the lifting of the Tibetan Plateau. This event would have resulted in a slight increase in winter humidity and a more substantial and significant increase in summer drought (Ruddiman & Kutzbach, 1989; Su *et al.*, 2018).

1.2 SAPROPELS

The term sapropel, originating from the Greek *sapros* (rotten) and *pelos* (soil), was widely cited following the work of the German chemist Wasmund who qualitatively described the composition of sapropel, gyttja (a freshwater decomposition of plant material) and bitumen from lacustrine sediments (Wasmund, 1930).

In 1938, Bradley hypothesized that organic-rich sediments could have been deposited in the Mediterranean as a result of fluctuations in Pleistocene sea levels (Bradley, 1938).

During the Swedish Expedition (1947) sapropels were first recovered from the Mediterranean Sea (Kullenberg, 1952). The term "sapropelic" was later introduced by Olausson (1961) to describe group of late Quaternary organic-carbon-rich marine sediments recovered from the Eastern Mediterranean. Then Kidd *et al.* (1978) proposed a quantitative definition of sapropels defining them as being similar marine deposits containing "between 0.5 and 2% organic carbon by weight" (Cramp & O'Sullivan, 1999).

Later, during the Leg 42A of the Deep Sea Drilling Program (DSDP) sapropel were defined as being: "a discrete layer, greater than 1 cm in thickness, set in open marine pelagic sediments containing greater than 2% organic carbon by weight". In the early 1990s Hilgen (1991a) proposed a less restrictive definition

describing sapropel as “simply brownish, often laminated interbeds”, but his definition cannot be applied to many Plio-Pleistocene sapropels (Cramp, 1999). The nomenclature of sapropels is therefore subject to change as research progresses.

The first main campaigns have allowed the recovery and the study of sapropel sequences in the Mediterranean Sea are the Deep Sea Drilling Projetct (DSDP) and Ocean Drilling Project (ODP).

Currently sapropels recovered date back to the Early Pliocene, though the earliest reported occurrence is from the Middle Miocene (Kidd *et al*., 1978; Taylforth *et al.,* 2014) and are intercalated within and below evaporite sequences.

The data acquired during the ODP confirmed that in all the area of the Mediterranean more than 80 sapropel have settled, during the Pliocene and the Pleistocene (Emeis *et al*, 1996).

Sapropels found in the Eastern Mediterranean region show significant differences from those found in the Western Mediterranean, evidence that these two macro-compartments of the same basin respond differently to the forces that cause sapropel formation, and the forces that drive the formation of sapropel act differently to the East and West of the Mediterranean (E. J. Rohling *et al*., 2015). The Eastern of the Mediterranean appears more prone to anoxic

or disoxic phenomena, showing sapropel with higher TOC content ranging from 1-12%, and peaks even to 30% (Emeis *et al*., 1996), compared to 1-2% of the sapropel of the West (Cita e Grignani, 1982). Moreover, the deposition of sapropel is not synchronous in the two sub-basins.

The processional cycles, characterized by alternate phases of hot/cold and dryness/humidity are evidently the most strongly expressed external forcing in the Mediterranean (Rossignol-Strick, 1985; Lourens, 1994; Wehausen e Brumsack, 1998). However, the recurrence pattern of sapropel in Eastern Mediterrean, suggests that the processional influence is modulated by the cycles of glaciation. Before the start of the glaciations in the Northern hemisphere, sapropels were deposited more frequently in all sites in the Eastern Mediterranean regardless of the depth of the water, while after the beginning of the glaciation the frequency of formation of sapropels has decreased considerably. Alpine meltwater contributions may be essential for early onsets of western Mediterranean sapropel deposition during deglaciations. Outside deglaciations, western Mediterranean sapropels likely are mechanistically related to eastern Mediterranean sapropels (Rohling *et al.*, 2015).

To explain why sapropels occur more frequently in the eastern than in the western basin Rohling and Grant suggested that the eastern Mediterranean is more sensitive to development of deep-sea anoxia than the western basin, because of differences in the efficiency of deep-water renewal. In the eastern basin, deep-water renewal is governed by a single process, namely formation of new deep water of sufficient density. While in the western basin deep-water renewal is governed by two major processes namely both injection of new deep waters of sufficient density, and effective Bernoulli aspiration of deep waters into outflow from the basin through the Strait of Gibraltar (Rohling *et al.*, 2015).

1.2.1 Models of Sapropel formation

Since the first discovery of sapropels of the Late Quaternary in the Mediterranean (Kullenberg, 1952), many hypotheses have been put forward for the explanation of their deposition. However, the precise mechanism that determines these accumulations of organic matter is still debated. Despite the rather clear evidence that sapropels coincide with the minima of the terrestrial precession cycle, that is with periods of increased humidity (Rossignol-Strick *et al*., 1983; Eelco J. Rohling, 1991) and that their presence is related to hydrographic regimes associated with heavy rainfall and river flows.

Currently the opinions on the formation of sapropels are:

1. Stagnation model: the anoxic condition is the dominant cause of the preservation of organic matter (Oulasson, 1961; Demaison and Moore, 1980).
2. Productivity model: an increase in primary production that triggered an increased flow of organic carbon on the seabed (Pedersen and Calvert, 1990).
3. Mixed theory: according to which a same basic mechanism would cause an increase in productivity and an impoverishment of oxygen in the deep waters.

Bradley (1938) was the first to propose the water column anoxia as a cause of deposition of sediments rich in organic carbon.

Many authors have suggested anoxia as the primary cause for sapropelic formation, focusing on the explanation of the causes of anoxia (Stanley, 1977). These authors believe that anoxia is triggered by massive flows of fresh water in the Mediterranean, producing a layer of shallow water with low salinity. This flow of fresh water produces strong stratification of density in the water column resulting in a slowing down or even a pause in the circulation of background water: such a situation may result in anoxia if the oxygen consumed in the degradation of organic matter is not replaced.

Two hypotheses have been proposed for the formation of the freshwater: confluence of glacial melting water during deglaciation and large-scale river flows.

The first hypothesis is based on the fact that in the last 400,000 years most sapropels have been deposited during periods of global warming, with the exception of sapropel S6 and S8. During such periods the temperature increase would have caused the melting of the ice caps north of the Mediterranean region, resulting in an influx of glacial melting water entering the Mediterranean, and consequently a freshwater flow and a strong stratification of density that would inhibit the vertical mixing, and therefore the oxygenation of the background water, which would then become stagnant and anoxic (Ryan, 1972; Ryan *et al*., 1976; Vergnaud-Grazzini *et al*., 1977; Williams et al., 1979; Mangini and Dominik, 1979; Williams and Thunell, 1979; Muerdter *et al*., 1984; Thunell and Williams, 1989).

However, studies conducted at high temporal resolution, thanks to astrochronological scales (Hilgen, 1991), have definitively demonstrated that the formation of sapropel has also occurred in the late Neogene (there are in fact deposits of this type also on the Earth-surface) and in last case did not occur at deglaciation periods, so the theory of "glacial melting" was rejected by many authors.

The main supporters of the second hypothesis (Rossignol-Strick *et al*.,1983) believe that along the mid-latitudes, a sharp increase in rainfall in the run-up to the formation of S1 and that the inflow of fresh water from the African highlands across the Nile has spilled into the Mediterranean, forming a shallow salt layer. The causal mechanism of high levels of African rainfall is attributed to fluctuations in the intensity of the African monsoon in response to changes in the Earth's climate due to changes in the Earth's orbital cycle.

Rohling (1994) argues that an increase in intensity of the summer monsoon of the Indian Ocean would manifest itself in the Mediterranean through increased inputs of the Nile and an increased activity of Mediterranean atmospheric depressions. That would result in a reduction, but not a complete reversal, of the current anti-estuarine pattern of circulation. The theory of Rohling is supported by isotopic and microfaunistic evidence obtained in sedimentary successions from the Strait of Gibraltar and Sicily suggesting an anti-circulation during the deposition of sapropel.

Rohling also considers that current oligotrophic conditions are abnormal and that the Mediterranean was more productive in the past. The results of $\delta^{15}N$ obtained from a core recovered in the Nile basin indicate that the deposition of sapropel occurred at a time when surface water was enriched with

nutrients, while marl, poor in organic matter, deposited in nutrient depletion conditions like current oligotrophic conditions (Calvert *et al*.,1992).

The other mechanism alternative to anoxia, for the formation of sapropel, is intensified productivity of the water column, which is an increase in the production rate of organic matter rather than a decrease in the rate of degradation. Many authors have supported the productivity models theory as the primary cause of sapropel formation (Schrader and Matherne, 1981; Ganssen and Troelstra, 1987; Parisi, 1987). These authors, who support the theory, mainly based on geochemical evidence, do not necessarily dispute the presence of anoxia, but they declare that anoxia alone cannot be the cause of the deposition of large quantities of organic matter, but only a symptom. (Henrichs and Reeburg, 1987; Pedersen and Calvert, 1990; Calvert and Pedersen, 1992).

The Black Sea is usually cited to support this theory, as although it is an anoxic reservoir it does not accumulate sediments rich in organic matter (Calvert and Fontugne, 1987) and geochemical evidence suggests that the Holocenic sapropel of the Black Sea was deposited in oxygenated conditions in response to the increased productivity of the photic zone (Calvert, 1990).

Other evidence in support of productivity theory comes from the areas of "upwelling", where local river flow regimes are neither stagnant nor anoxic (Pedersen and Calvert, 1983; Pedersen, 1991).

Sancetta,(1994) proposed an original model to explain the trend of productivity in the Mediterranean: diatom mats could highlight the presence of a DCM (Deep Chlorophyll Maximum), whose existence during the period of sapropel formation has been documented by studies on associations to nannofossils and foraminifera. This model is consistent with the presence of stratified conditions, where nutrients trapped in depth can be exploited by vertically migrating diatoms.

Canfield (1994) presents a balanced approach to the anoxia versus productivity thesis, suggesting a third scenario in which organic carbon in sediments is the product of the equilibrium between the flow of organic carbon and the dilution of "input" clastic. He states that in the absence of a "input" clastic, a high flow of organic carbon would result in the deposition of sediments rich in organic carbon regardless of the redox state of the water. The Canfield approach was poorly supported, as a mechanism capable of inducing the formation of sapropel basin, in fact there is evidence that during the formation of S1 in the Aegean an increase of territorial flow occurred. Therefore, during the formation of the most recent layers rich in organic

matter, it could result in the deposition of sapropelic sediments rather than sapropel proper, as defined by Kidd *et al*., 1978.

1.2.2 Milankovitch cycles

The fluctuations across time of $\delta^{18}O$ performed on planktonic foraminifers in marine sediments deposited in the last 780,000 years (Lisiecki and Raymo, 2005) show periodic characteristics in accordance with changes in Earth's orbit illustrated by Milankovitch (1930). These variations are able to influence the Earth's climate.

The fundamental orbital parameters considered by Milankovitch to elaborate his theory on cyclicity are three: precession, axial tilt and eccentricity.

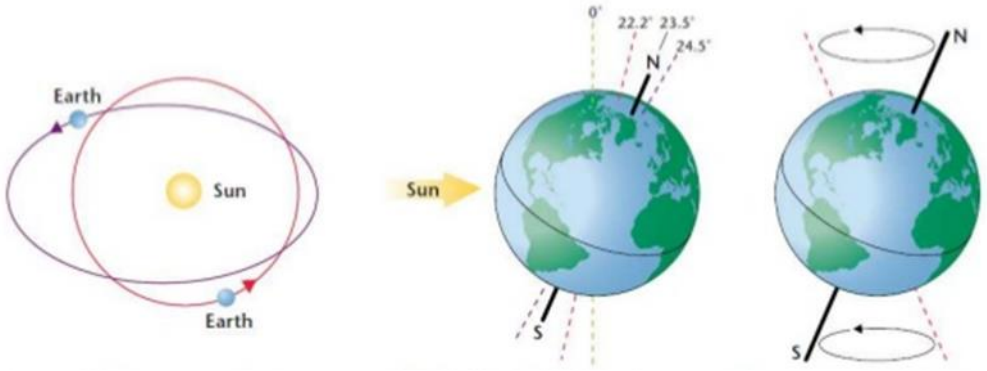

Figure 1.5*: Graphic description of the Milankovitch cycle: precession; axial tilt; eccentricity (www.nibiru2012.it)*

Precession consists in the rotation of the terrestrial axis around the perpendicular passing through the center of the Earth.

This rotation leads to a continuous change in the time of the year in which the Earth reaches its perihelion (point of the Earth's orbit closest to the Sun), in a cycle that lasts between 19,000 and 24,000 years.

The terrestrial axis makes a conical path that leads to each semi cycle an alternation of those which are the days of equinoxes and solstices. This cyclicality drastically changes the amount of incident solar radiation that a certain area of the Earth's surface receives during the year, depending on the latitude to which it is placed. Thus, affecting the regulation of those factors which are the annual climatic cycles such as summer/winter and consequently all the ecological factors related to them.

The second type of cyclicity highlighted by Milankovitch's theory is axial tilt (obliquity): the oscillation between 22.1° and 24.5° of the angle of the terrestrial axis in relation to the equatorial plane which varies with a cyclicity close to 41000 years and modifies the angle of exposure of the terrestrial surface to the solar rays by altering the amount of radiation to which certain areas are exposed. The variation in the amount of total solar radiation certainly has a greater effect in the regions placed at the high latitudes as these regions are the ones that are most affected by the variation of the incidence of solar radiation in relation to the Earth's surface. In fact, the lower the angle of incidence at

which a radiation hits a surface, the greater will be the energy absorbed by the surface itself.

Finally, the third parameter is relative to the variations of the eccentricity. The variations of the eccentricity of the Earth's orbit in its motion of revolution around the sun, varies with a deviation from a perfect circular orbit between +0.005% (almost perfect) to +0.058% (elliptical). The cycles to which eccentricity is subject are two: one "short" 100,000 years and one long 400,000 years. However, eccentricity does not greatly change the amount of radiation affecting the globe (about 0.1%). However, if combined with the other two parameters, in particular with precession, it can lead to a considerable difference in what is the amount of solar radiation incident to the earth (Rossignol-Strick, 1999).

In fact, these cycles modify both the distance of the Earth from the Sun, and the variation of the angle of incidence of solar radiation: during the period of maximum irradiation of the northern hemisphere the radiation hits the atmosphere and the Earth's surface with a greater intensity and angle, but with less intensity compared to the perpendicular to the surface. This increases the ratio of absorbed energy to reflected energy. The consequence of this variation, has an effect then on the increase in what is the ability of the Earth/Atmosphere system to convert the radiation into heat, thus going to a heating process.

This correlation has been demonstrated by comparing the reconstruction of the variation of incident solar radiation at 65° North with data from historical records taken from polar ice or marine sediments. These records allow an analysis of the variation in the ratio of oxygen isotopes ($\delta^{18}O/\delta^{16}O$) and the content of CO_2.

This allowed a historical reconstruction of the evolution of the Earth's temperatures. The CO_2 rates in the atmosphere and of the extension of the polar ice on the surface of the globe, showing an almost constant periodicity in the alternation of ice cycles with interglacial periods (Hilgen, 1991; Hilgen *et al*., 1995; Lourens *et al*., 1996) and at the same time allow a good correlation between changes in Earth's orbital cycles and the deposition of sapropels (Cita e Grignani, 1982; Mangini and Schlosser 1986; Rohling, 1994; Emeis *et al*., 2003).

1.2.3 African monsoon

The change in the exposure of the Earth's surface to solar radiation accidents in relation to the cycles of Milankovitch leads to changes in the intensity of climatic processes both on a regional and global scale. As solar radiation is

the engine that moves wind processes and sea currents allowing the climate to perform its cycles, so a positive or negative modification of the incident solar energy can change the intensity with which these same processes occur (Rossignol-Strick, 1999).

An important climatic phenomenon affected by these variations, which insists on an area close to the Mediterranean, is the African monsoon.

This atmospheric phenomenon has global importance both for its intensity and for the very large area on which it acts and has annual cyclicality. These are winds with a South/West-North/East trend in the summer and North/East-South/West in the winter period, which arise from an intense process of heating of water and air at the level of the Atlantic Ocean.

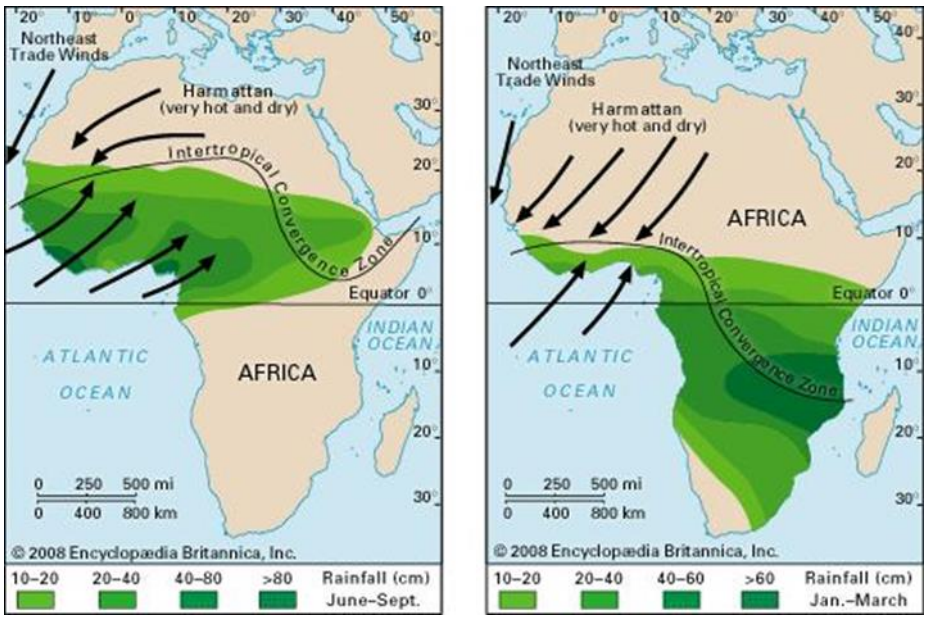

***Figure 1.6**: S/W-N/E trend of the summer African monsoon and N/E-S/W of the winter African monsoon. The areas in green report an estimate of the values in cm of rainfall in the two different periods (www.clivar.org/african-monsoon)*

The air, whose water vapor content resulting from evaporation is very high, is directed towards the low-pressure zones above the deserts of North Africa, where, as a result of convective processes, a considerable quantity of water in the form of intense rainfall is cooled and released on the underlying territories. The African monsoons are the only fresh water supply for some of these regions and therefore determine the presence of human and animal life in these areas.

Studies to determine the correlation between the possible intensifications of the monsoon and the consequent intensification of the fluvial contribution to the sea (Rossignol-Strick *et al*., 1982; Rossignol-Strick, 1983) show how a small variation in intensity can result in significant effects.

In fact, based on simulations carried out with climatic models it has been calculated that during the period of maximum solar radiation of the northern hemisphere, this atmospheric phenomenon may have increased by about 25% compared to its current intensity. At the same time, a migration was estimated from about 23°N to about 30°N of the maximum latitude to which the monsoon activity on the African continent would have been expressed (Kutzbach and Liu, 1997).

Sapropel are deposited when the maximum insolation index exceeds a threshold value.

Specifically, in the Mediterranean Sea, sapropels can form during an intensification of the African monsoon associated with the increased Nile range (Rossignol-Strick, 1983, 1985; Rohling, 1994; Mercone, 2001). Moreover, the increase of Indian monsoon activities would have favored the stationing of depressions in the Mediterranean area, making it more humid, and thus encouraging the increase of rainfall and river flows (Rohling, 1994).

1.2.4 Mediterranean Sapropels

In the Late Quaternary, the occurrence of at least twelve sapropels have been recorded, S1-12, with S2 being a ghost sapropel. The youngest one, S1, has been dated at 7000-9000 years B.P. (Ten Haven *et al*., 1987). The oldest one, S12, has been dated at approximately 464.000 years B.P. (Lourens, 2004). Sapropel S1 and S5 are the most studied. S1 being the most recent one enables us to compare the paleo environmental condition during its deposition with present day conditions. Since circulation during the time of deposition is likely similar to present day circulation, this can be taken into consideration when discussing the cause of organic matter accumulation (de Groot, 2017).

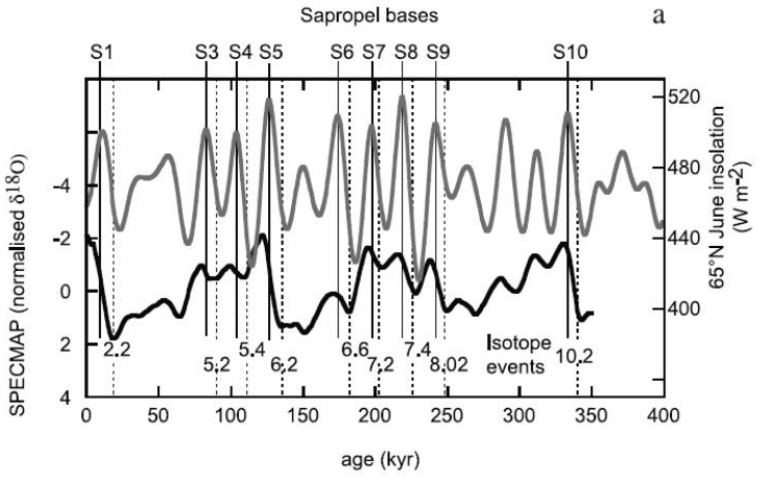

***Figure 1.7**: Sapropel occurrence in relation to oxygen isotope values and insolation (Emeis et al., 2003)*

Following the analysis proposed by Castradori (1993) we can describe the Mediterranean sapropels, based on their stratigraphic position, as follow.

- Sapropel S1 was deposited in the Holocene, formed during the Marine Isotopic Stage 1 (MIS 1) during the last deglaciation or immediately after it (Rossignol-Strick *et al*., 1977). It is about 20 cm thick (Stanley and Maldonado, 1977) and is the only one to have been radio metrically dated with the ^{14}C method.
- Sapropel S2 is generally 5 cm thick, but is often not very visible, in literature it is called *ghost sapropel*. Its deposition occurred during Marine Isotopic Stage 3 (MIS 3).

- Sapropel S3, S4 and S5 are very close (80, 100, and 124 Ka) and were deposited during MIS 5. S3 and S4 have a thickness of about 10-15 cm with C org content equal to 2%.
- Sapropel S5 shows clear laminations. Its color is very dark, and Its thickness is greater than 22 cm (Cramp *et al.,* 1999) The planktonic foraminifera assemblage is dominated by "warm" microfossils (G*lobigerinoides ruber*). It also has a C org content of about 7% (Oggioni and Zandini, 1987) and corresponds to the isotopic sub-stage 5e.
- Sapropel S6 (object of this work) is often divided into two or three superimposed layers. It was deposited during a glacial phase of the isotope stage 7. The C org content is between 2.2 and 4.4% (Cita *et al.,* 1982) and the organic matter has been estimated to be for 60-70% of marine origin (Cita e Grignani, 1982). S6 is the only sapropel in which large populations of benthic foraminifera (Vismara Schilling, 1986) have been found to indicate that the background waters during deposition were not completely anoxic (Parisi, 1987b).
- Sapropel S7 is deposited in MIS 7a, it has limited thickness and in some cases is absent. The C org content is between 4.7 and 5.3% (Cita *et al.,* 1982; Murat 1984).

- Sapropel S8 was deposited during the isotopic subs-stadium 7d during a low glacial phase. The content in C org is 1.5% and 2.5% (Cita *et al.,* 1982).
- Sapropels S9 to S12 are less known due to the fact that they have been recovered in rather limited number of cores. They are about 1-2cm thick and very bioturbated (Cita *et al.,* 1982).

Chapter Two

COCCOLITHOPHORES

Coccolithophores are planktonic algae, unicellular, flagellated, essentially marine, belonging to the phylum Haptophyta in the class of Prymnesiophyceae. They are characterized by a composite cellular cover, the coccosphere, formed by microscopic calcite plates, coccoliths.

The size of coccoliths varies from 1 to 30 μm, while the overall size of the alga is between 5 and 30 μm.

In deep ocean sediments, coccoliths are extraordinarily abundant, as single elements, above the carbonates compensation depth (CCD). More rarely, the whole coccosphere can be found. For this reason, the Haptophyta account among the most abundant fossil record phyla. Moreover, such fossil record is continuous from their first appearance, in the late Triassic, to today.

Due to their abundance and the importance of the photosynthetic and calcification processes, Haptophyta provides a significant contribution to global biogeochemical cycles.

2.1 BIOLOGY

2.1.1 Cellular structure

Haptophyta, initially included in the division Chrysophyceae along with the silicoflagellates and other algae (equipped with yellow-brown chloroplasts), now they constitute a distinct phylum, characterized by the possession of a unique structure: the haptonema.

The haptonema is an appendix like the flagella, among which it is inserted, but which differs from them at the ultrastructural level. It is not formed by the typical structure (9+2) microtubular universally present in the flagella but by seven microtubules; moreover, unlike the flagella, it presents a spiral winding and seems to possess a range of functional adaptations to swimming, adhesion and particle capture (Inouye and Kawachi, 1994).

Another distinctive characteristic of the phylum is the organic and calcareous gills (coccoliths) forming the outer lining of the plasma membrane, which is formed by an internal layer of organic nature and an external one of calcareous nature. Although many flagellates are endowed with exoskeletons formed by organic gills, calcareous or siliceous, the organic gills of the Haptophyta are peculiar and the calcareous ones seem to be exclusive of the phylum. Moreover, the process of calcification of the coccoliths is also very particular as it exists in a lamellar structure but does not continue as for example that of some dinoflagellates.

Organic lamellae and coccoliths are closely related structures: both are formed in the Golgi apparatus, moreover, the coccoliths rest on a basal lamella.

At the ultrastructural level, gills have a proximal face consisting of micro-fibrils with a radial and distal structure formed by microfibrillas with a concentric structure.

The inside of the cell is dominated by chloroplasts and by a single nucleus covered by a double perforated membrane, which represent the sites, respectively, of photosynthesis and genetic material. Mitochondria are also easily identifiable. The apparatus Golgi apparatus is well developed, consisting of a set of interconnected vesicles where important biosynthetic processes take place and, in particular, the formation of organic gills and coccoliths. Typically, there are vesicles in Golgi which are stacked and in which it is possible to see gills and coccoliths in the various stages of the formation process.

The cell is surrounded by a multilayered membrane, known as plasmalemma. Two smooth flagella of equal length protrude from the plasmalemma, and between them, there is the haptonema.

During the movement of the alga, characterized both by rotation and by revolution around the direction of displacement, the flagella are normally directed back and the haptonema is tightly wound. In other cases, the movement occurs with the flagella directed forward and the haptonema rigidly extended in the same direction. Since the movement of these algae, although rapid in relation to the size of the organism, is still less than that of an oceanic current, they are normally considered passive.

The characteristic brown-golden color of the Haptophyta is due to the presence of a high quantity of fucoxanthin, dark orange pigment.

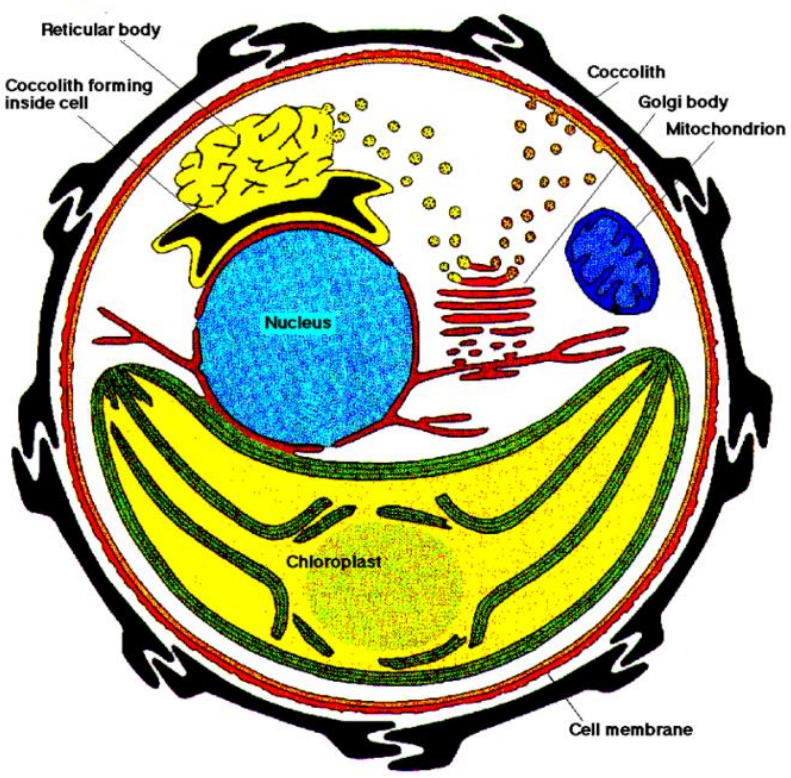

***Figure 2.1**: Cell structire of Coccolithophores*

2.1.2 Morphology and formation of coccoliths

Coccolithophores can produce two types of coccoliths: heterococcoliths and holococcoliths, which differ in morphology, mode of formation and stage of the life cycle in which they are formed.

The production of coccoliths is closely associated with the photosynthesis activity: laboratory experiments (Brand and Guillard, 1981) have shown that coccoliths formation is inhibited almost completely in the absence of light, while light production rate can be very high. Experiments with ^{14}C, under conditions of light intensity and variable wavelengths, they have also shown that the production of coccoliths is catalyzed by two different photochemical reactions, one linked to the pigments of plastids, the other to a pigment that specifically absorbs in the blue region of the spectrum or perhaps a combination of chlorophyll a and c and carotenoids.

Based on detailed TEM observations of the intracellular structure of coccoliths, SEM, LM and MET analyses of individual coccoliths and biochemical investigations, the coccoliths formation process can be divided into three stages (Westbroek et al 1989; Pienaar 1994):

1) Formation of an organic basal lamella;
2) Nucleation: formation of a cycle of simple crystals around the margin of the basal organic lamella (Protococcolith);

3) Growth of crystals in 3 dimensions (Coccolith)

The formation of the coccoliths can take place outside or inside the cell: in the first case the result is a holococcolith, in the second a heterococcolith.

Holococcoliths are formed by an extracellular calcification process that takes place on the organic cladding plates extruded by the apparatus of Golgi.

They are in the form of a disk or dome and consist of numerous, small equal-dimensional crystals (0.1 μm) of calcite of simple shape, arranged with the faces aligned according to a precise geometric model. In this case the calcite crystals undergo little or no changes in their overall shape and their orientation is precisely regulated.

Heterococcoliths instead are formed with the same modalities of the organic plates that is inside the cell, in connection with the apparatus of Golgi and are then extruded to form a composite exoskeleton (coccosphere). In this case the calcite crystals are modified in the form of the complicated genetic process that often involves the overlapping of the different crystal. Heterococcoliths are generally circular or elliptical and have a disk formed by one or more radial cycles of crystalline units of various shapes, which encloses an open central area, closed or with various structures.

The different forms of formation are also reflected in the preservation potential, which is worse in the holococcoliths, which therefore have a more

sporadic and scattered fossil record so that better-preserved taxa tend to have forms that are more atypical.

2.1.3 Nannoliths

Nannoliths are a heterogeneous group, almost certainly artificial, which includes a wide range of forms.

Although many of them have characteristics similar to heterococcoliths, such as rotational symmetry, complex shape of crystalline units and chirality, the differences are sufficient to make their relations with them uncertain.

However, it is believed that many nannoliths may be heterococcoliths modified (eg *Nannotetrina, Discoaster, Florisphaera*), others would appear to be holococcoliths modified (*Ceratolithus*) others could have been produced by Haptophyta with completely different calcification mechanisms (*Braarudosphaera, Nannoconus*) or even by non-haptophyta (*Schizosphaerella*).

2.1.4 Function of coccoliths

Although many hypotheses have been made about the function of coccoliths, no definitive explanation has been uniformly accepted (Young, 1987, 1994).

The most obvious function would appear to be the protection of the delicate cellular membrane from various agents:

- mechanical damage
- bacterial/viral attack
- grazing of herbivorous zooplankton
- chemical shocks

However, there is no clear evidence that coccoliths represents an effective defense against predation, especially by the herbivorous zooplankton.

Another common explanation concerns the buoyancy of the cell: the loss or addition of coccoliths could regulate the buoyancy of the cell in relation to the uptake of nutrients. Floating is in fact a critical point for phytoplankton, as it needs to maintain a position within the photic zone avoiding water depleted of nutrients.

Other interesting explanations suggest that the function of coccoliths is related to the regulation of light. Coccoliths would seem to be able both to reflect the UV rays from the cell, allowing life in the upper photic zone, or to refract sunlight, favoring the life of the organism in the lower photic zone; in both cases there is evidence to support this hypothesis:

- *Florisphaera profunda,* still existing species, has an atypical asymmetric coccosphere, which seems to have the refractive function of sunlight, this

would justify the presence of this species in an unusual niche of the lower photic zone, where few other algae can grow (Bown and Young, 1997).

- *Emiliania huxleyi,* responsible for intense bloom in the upper photic zone, produces an enormous number of coccoliths, many of which are released in the water column. The production of a high number of coccoliths for the cell could, favor the presence of this species in its sub-superficial niche, according to the hypothesis of the reflection of sunlight (Holligan *et al*, 1993).

The fact that coccoliths can have different functions in different species suggests that the morphological differentiation has led to the adaptation to different functions that can be considered in size, shape and number of coccoliths. However, coccoliths may have had initially a common function, such as protection.

Finally, there is also a biochemical explanation: coccoliths could be intermediate products of cellular biochemical processes or would serve to intensify the energy efficiency.

However, none of these theories has been proven and further in-depth studies will be necessary to explain the origin of this group, which, unfortunately, is generally poorly considered by the biologists.

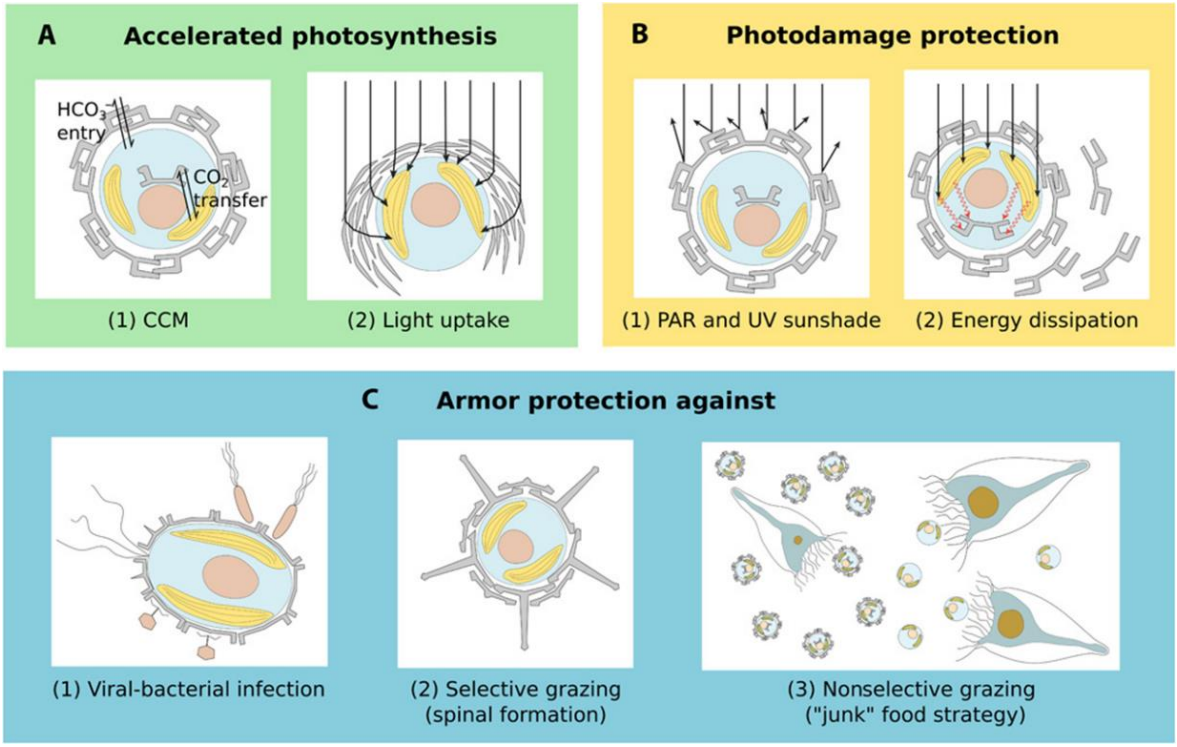

***Figure 2.2**: Main benefits of calcification in coccolithophores (Monteiro et al, 2016)*

2.1.5 Coccolithophores life-cycle

Our knowledge of the vital cycles of the Haptophyta is limited to the few species regularly kept in cultivation and even for these observations are incomplete.

Most Haptophyta show an alternation of two distinct stages during their life, dimorphic life cycle: the motile and non-motile stages.

Both stages can be characterized by a coating of small organic plates, coccoliths, or both.

When both the motile and the non-motile stages are covered by coccoliths, these can be of different type in the two stages. For example, in the coastal

species *Pleurochrysis carterae,* the non-motile phase seems to be benthic, while the motile one is planktonic (Rayns 1962; Paasche 1968; Klaveness and Paasche 1979). In the case of *Coccolithus pelagicus,* both phases produce different types of coccoliths; the fact that only the planktonic stage possesses heterococcoliths suggests that they play an important role in the planktonic life. Although only a few species have been studied, it is likely that most coastal species will spend part of their life cycle in a benthic state during the periods of the year when environmental conditions are hostile, while ocean species are probably planktonic at all stages of their life cycle.

Coccolithophores essentially reproduce asexually by binary fission. In conditions of illumination and saturation of nutrients, *Emiliania huxleyi* and *Pleurochrysis carterae* may divide 2.5 times a day, *Gephyrocapsa* oceanica twice a day, and *Calcidiscus leptoporus* once (Brand and Guillard 1981).

This reflects the choice of two different strategies: high growth rates in species characteristic of coastal and eutrophic waters (r-selection), low growth rates in tropical oligotrophic waters (k-selection).

In general, asexual reproduction rates in Coccolithophores are higher than in cyanobacteria and dinoflagellates, but lower than in diatoms.

Mitosis is similar to that found in most eukaryotic cells and each daughter cell inherits about half of the cuddles. The sexual reproduction is known only for some species but is not yet well studied.

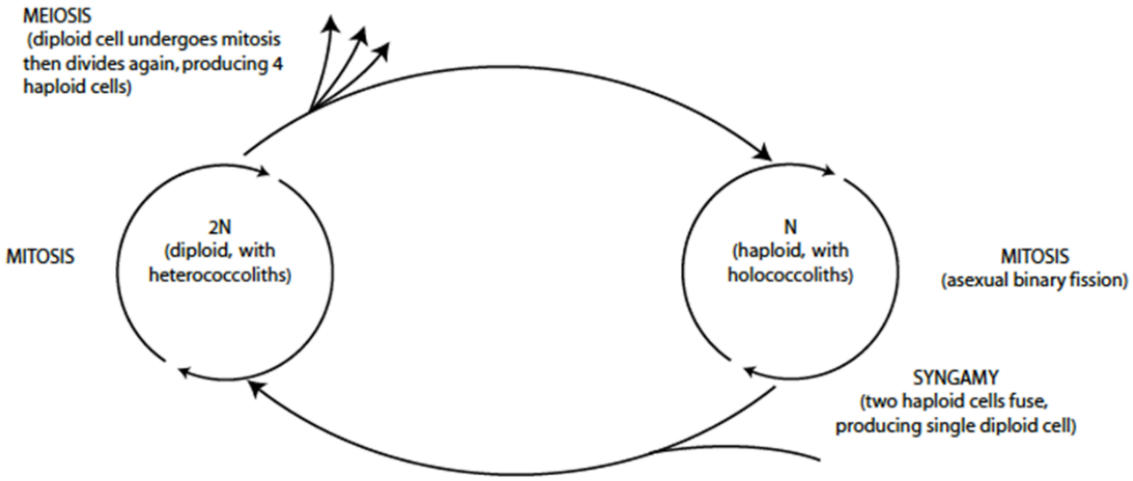

***Figure 2.3**: Example of a life cycle* (Young *et al*., 2003)

2.2 ECOLOGY AND DISTRIBUTION

The distribution of Coccolithophores as a phylogenetic group has undergone significant changes over the geological time.

The first appearance dates to about 220 million years ago, to reach the peak of abundance in the upper Cretaceous, period in which they were cosmopolitan, well diversified (Tappan, 1980) and very abundant in ocean and coastal waters, polar or equatorial.

At the end of the Cretaceous, most of the species of this group were extinct, in favour of the Diatoms, which occupied many of the habitats previously occupied by the Coccolithophores.

Currently in the coastal and polar waters Diatoms still dominate, while the Coccolithophores have regained their dominance in the temperate and tropical waters.

2.2.1 Biogeographical distribution

Coccolithophores currently has a wide ocean distribution. They live in the photic zone reaching high densities at low latitudes. In general, they are not found at latitudes greater than 70° and they bloom in warm, stratified and oligotrophic waters. However, several species are very tolerant: for example, *Emiliania huxleyi* adapts to a wide temperature range (1-31°C) and salinity (11-41‰) (Brand, 1994).

Coccolithophores show distinct patterns of geographic distribution, which define wide latitudinal bands or zones (Winter *et al*., 1994), characterized by different associations of species rather than by high endemicity, because most species are cosmopolitan.

Their biogeographical distribution depends on the surface temperature of the water and the distribution of nutrients, which in turn are related to ocean

circulation characteristics, such as zones of divergence, upwelling, gyres and seasonal mixes.

Diversity is greatest in seasonally stable environments, oligotrophic, tropical and subtropical, where the biomass is instead low, as a result of the modest reproduction rates. Under eutrophic conditions, instead, due to upwelling or seasonal mixing of the water column, biomass is high and specific diversity low. In such condition, Diatoms predominate, while Coccolithophorid's bloom generally follows silica depletion in surface waters. In addition, continental shelf environments tend to be unstable and eutrophic, supporting characteristic associations that include taxa that do not live in the open ocean.

Currently five main latitudinal zones of distribution are identified (McIntyre & Be 1967; Okada & Honjo, 1973; Winter & Siesser, 2006): Subarctic; Temperate; Subtropical; Tropical; Subantartic. The boundaries of these zones are not at all static or net but in continuous movement, because they are associated with the movements of the greater water masses.

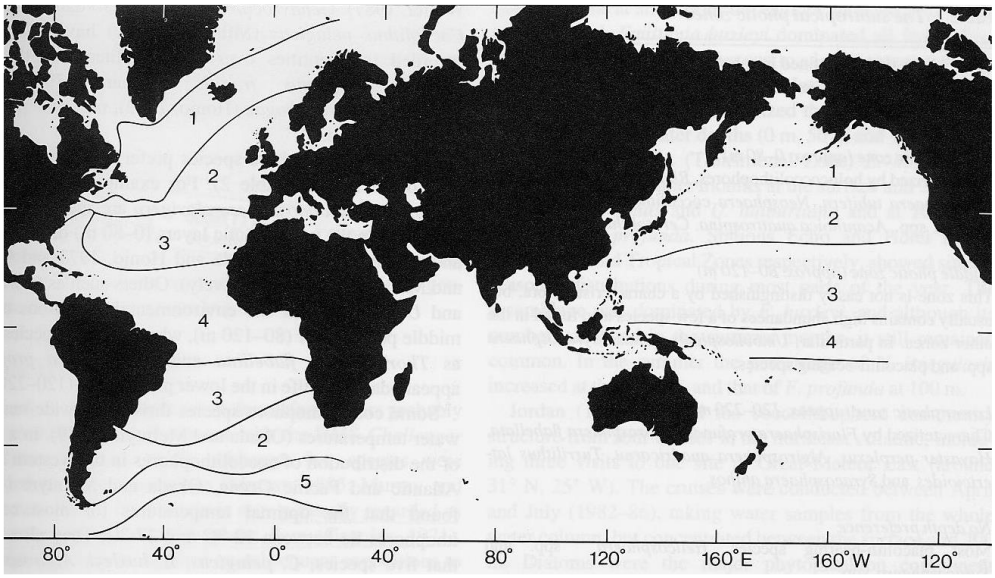

***Figure 2.4**: Biogeographic coccolithophores zone from the Atlantic and Pacific Ocean (McIntyre and Bè, 1967; Okada and Honjio, 1973)*

The vertical distribution is quite limited: they are usually confined in the upper photic zone, with the exception of characteristic associations that exploit conditions of reduced light intensity, low temperature, but high concentrations of nutrients, occupying a less competitive niche, for example the species *Florisphaera profunda* (Winter *et al.*, 1994).

In stratified waters, the vertical distribution of species tends to be quite clear. Vendrick (1982) has shown that some species are mainly confined in the upper photic zone, while others live in the lower photic zone, for example, *Anthosphaera sp. Thorosphaera flabellata* and *Florispheara profunda* live exclusively between 100 and 200 m of depth, therefore below the photic zone.

We do not know whether they are able to photosynthesize with such low light levels, or whether they have heterotrophy.

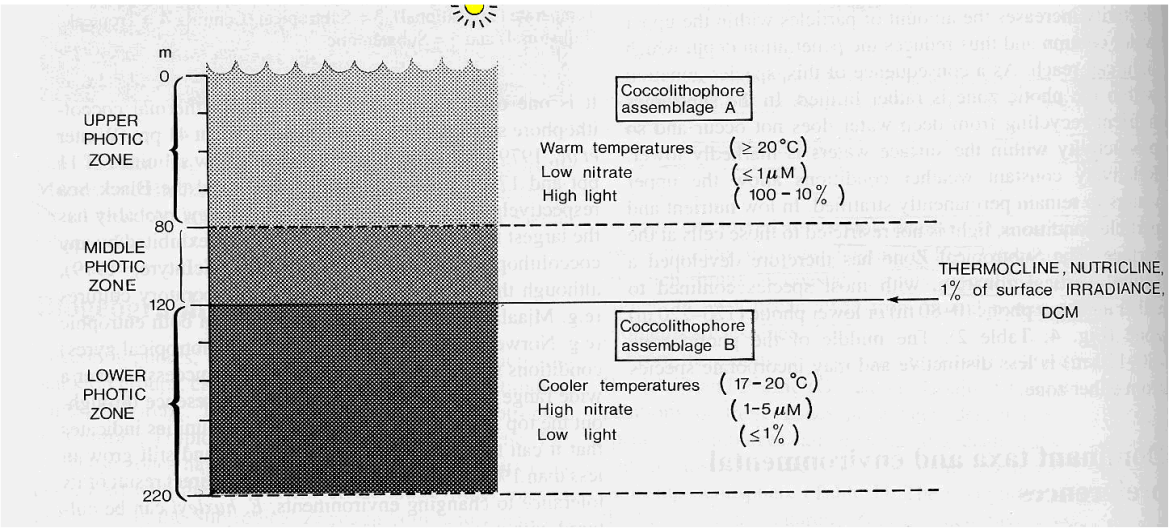

***Figura 2.5**: Schematic diagram of subtropical photic zone (R. Jordan, unpub data)*

2.2.2 Seasonal distribution

The seasonal patterns reflect quite well the geographical distribution.

In winter, during periods of greatest vertical mixing, cosmopolitan species such as *E. huxleyi* bloom in the open ocean, while tropical species are rather rare (Okada and McIntyre, 1979). During the summer stratification, however, the tropical communities predominate. In the temperate regions, where the stratification is interrupted during winter *E. huxleyi* and *G. oceanica* are the main components of the spring blooms, when the water column returns to be

stratified (Hulburt *et al.*, 1960). In the coastal waters *E. huxleyi* is the prevailing species during the summer stratification (Marshall, 1978).

2.2.3 Envoironmental factors influencing the distribution

Factors affecting living of Coccolithophorids are:

- Water depth and temperature: Mcintyre & Be (1967) showed that most common species had relatively narrow temperature ranges, although subsequent workers extended these ranges. Thus, temperature seems to play a role in controlling the largest scale distribution of species, largely defining broad latitudinally arranged biogeographical zones. However, on smaller scales temperature ranges are less informative and important, as no water masses has annual temperature fluctuations covering an extremely large range. For subtropical populations temperature change is perhaps unimportant, whereas for subpolar communities, temperature plays a more prominent role due to the formation and breakdown of the seasonal thermocline (Andruleit *et al*, 2003).
- Salinity: Most species of coccolithophores live in the open ocean and so are adapted to salinities of 32-37 ppt. However, several species have a wider salinity tolerance (Brand, 1994) and are known from low salinity environments, such as fjords. Coccolithophorid species diversity is

highest in stratified, warm oligotrophic environments, where salinity values are relatively high.

In areas characterised by lower salinities, such as the coastal areas, coccolithophorid diversity is relatively low, and the species may be specialised (Baumann *et al*., 2005).

- Nutrients: As part of phytoplankton, Coccolithophores also require certain nutrients for their growth and biochemical reactions. The most important nutrients are considered nitrate and phosphate. Nitrate is essential for growth and calcification; however, at unnatural high nutrient concentrations calcification is inhibited. Phosphate seems to act as a controlling agent for calcification. It has been shown that phosphate concentrations were lower in waters where coccolithophores, mainly *E. huxleyi*, bloomed (Townsend *et al,* 1994; Van der Wal *et al,* 1995; Baumann, 2005).

  In eutrophic environments coccolithophores are often outcompeted by diatoms forming relatively minor components of the total communities. Nonetheless, many coccolithophores are K-selected, adapted to oligotrophic conditions. Coccolithophores as a group achieve their highest relative abundances within phytoplankton communities in such

oligotrophic environments (Baumann, 2005). The nutrient availability in controlled by the depth of the nutricline which can be monitored by the abundance of *F. profunda:* if the nutricline is shallow, Coccolithophores production in the upper euphotic zone is enhanced and the abundance of *F. profunda* is minimal.

- Light: They require light for carbon fixation. Most species therefore live in the upper photic waters (<50-80 m). In contrast, some species, such as *Florisphaera profunda*, inhabit the lower photic zone (LPZ), which is characterised by low light levels (<1% to 4% of the surface irradiance). The LPZ is usually a permanent feature of the subtropical gyres but may develop in well-stratified waters in equatorial and temperate regions during summer months. Thus, it is not surprising that the LPZ flora is rare or absent in turbulent waters, in coastal or upwelling areas. (Bauman, 2005).
- Photoperiod and day-night cycle: Brand & Guillard (1981) theorized that the partition of the various physiological processes is so strong in oceanic phytoplankton that a light-dark cycle is necessary for cellular metabolism. On the contrary, the daily periodicity is probably not so advantageous for coastal species exposed to wider luminous

- fluctuations on temporal scales lower than the daily one, due to the vertical mixing.
- Toxic metals: inhibits the growth of Coccolithophores: Sunda & Huntsman (1983) assumed that enrichment in Cu of upwelling areas is toxic to phytoplankton, only *E. huxleyi* is present in these areas, since it is adapted to tolerate high concentrations of Cu (Brand *et al*., 1986).

2.2.4 Dominant taxa and environmental preferences

Emiliania huxleyi is the most abundant and ubiquitous coccolithophore living in today's oceans, often occurring at a relative abundance of 60-80%. It is one of the most euryhaline and eurythermal coccolithophore species. It thrives in the Red Sea at 41‰ (Winter et al, 1979) and can easily withstand the low salinities of 11 ppt and 17-18‰ in the Sea of Azov and the Black Sea respectively (Burky, 1974). *E. huxleyi* probably has the largest temperature range (1-30°C) exhibited by any coccolithophores species (Okada and McIntyre, 1979), although this is not always reflected in laboratory cultures (e.g. Mjaaland, 1956). Its ability to grow both in eutrophic and oligotrophic condition suggest that this species can be successful over a wide range of nutrient levels. Equally, its presence throughout the top 200m in coccolithophores communities indicates that it can tolerate fluctuating light

levels and still grow in less than 1% of the surface irradiance. Evidence from the sedimentary record has indicated that *E. huxleyi* has dominated the coccolithophore assemblages for approximately 73,000 years and probably evolved from the *Gephyrocapsa* species complex about 268,000 years ago (Thierstein, 1998). The genus *Gephyrocapsa* may also dominate coccolithophore population. *Gephyrocapsa oceanica*, is abundant in warm marginal seas (Okada and Honjo, 1975), is also found in upwelling areas (Mitchell-Innes and Winter, 1987; Kleijine et al, 1989). *Gephyrocapsa muellerae* (Jordan, 1988) and *Coccolithus pelagicus* (Milliman, 1980) have also recorded in quantities over 10^6 cells/liter, and the two species *Oolithotus fragilis* (Bernard, 1948) and *Umbilicosphaera sibogae* (Honjo, 1982) may also produce large population.

Many coccolithophore species prefer to live within specific depth ranges:

- *Discosphaera tubifera* and *Rhabdosphaera clavigera* are species that prefer to live in the upper photic layers (0-80m) of the Pacific and Atlantic Oceans (Okada and Honjo, 1973; Okada and McIntyre, 1979).
- *Oolithotus fragilis* and *U. tenuis* prefer the environmental condition of the middle photic layer (80-120m).
- *F. profunda* and *G. flabellatus* appear adapted to life in the lower photic zone (120-220m).

Some coccolithophores species thrive in a wide range of water temperatures (Okada and McIntyre, 1979). In a study of a distribution of coccolithophores in the western North Atlantic and Pacific Ocean, Okada and McIntyre (1979) found that the optimal temperatures for most coccolithophores lie between 12°C and 27°C. They also found that five species *C. pelagicus, E. huxleyi, Algirosphaera robusta, Calciopappus caudatus* and *Syracosphaera borealis* are able to survive in temperatures as low as 1°C. *Coccolithus pelagicus* may survive temperatures as low as -1,7°C (Braarud, 1979). On the other hand, 11 species can live in temperatures up to 30°C. One species, in particular, *U. irregularis*, thrives in temperature from 25°C to 30°C.

2.2.5 Distribution of modern coccolithophores in Mediterranean Sea

Knappertsbusch *et al.*, 1997 and Kleijine (1991) conducted quantitative studies on the distribution of coccolithophores in the entire Mediterranean in the early 90's. The results of Knappertbusch were based on two cruises along the entire length of the Mediterranean in the fall of 1986 and the late winter of 1988. Distribution of coccolithophores from 21 stations at six different water depth from 0 to 200 m were compared to physical and chemical parameters. Fluctuations in species abundances were attributed to the seasonal

hydrological changes of the Mediterranean. In summer, the water is highly stratified, whereas in winter the water column is well mixed due to increased winds (Winter *et al.,*1994). Assemblages from the summer period seem to reflect strong hydrological gradients between the eastern and western basins whereas blooms of *E. huxleyi* dominated assemblages during the winter period. Cell abundances in winter were 10^4 to $3x10^5$ per liter, which is 10 times greater than in summer. Kleijine (1991) collected surface water samples along an east-west transect of the Mediterranean during the summer of 1985. Her results concerned only the contribution made by the holococcolithophores, which times reached 50-70% of the total coccolithophores count. However, even at these high percentage stations the abundance of coccolithophores was low ($<10^4$ per liter), corroborating the earlier findings of Knappertsbusch (1990). Kleijine also noted a strong east-west gradient, with higher absolute frequencies of holococcolithophores increasing westward with decreasing salinity (Winter 1994).

Malinverno *et* al., 2003 investigated the coccolithophores distribution the Ionian Sea and its relationship to eastern Mediterranean circulation during late fall to early winter 1997. During the investigated period, the area is characterized by the presence of a surface mixed layer, reaching a depth of 25 to 90 m. Below this layer, a marked thermo- and halocline is developed. The

sampling was planned to obtain a regular grid of samples along two transects, oriented W-E and SW-NE, and at fixed depths, from the surface to the base of the photic zone. Nine locations were investigated; surface waters were sampled at a finer vertical resolution than the deeper ones, to better assess phytoplankton spatial variability. Coccolithophorids are the dominant phytoplankton group in the investigated samples and reach concentrations up to $2x10^4$ coccospheres per liter of seawater. A total of 69 speciment of heterococcolithophorid and 37 holococcolithophorid species were recovered in the investigated samples. The species assemblage is that typical of the subtropical latitude, with a general high species diversity and a well-defined depth distribution. It is in fact possible to recognize an upper photic zone assemblage, dominated by *E. huxleyi* and characterized by higher concentration and species diversity and a lower photic zone where typically deep-living species (*F. profunda, G. flabellatus*) are present. These two zones are separated by a transition layer, where species of both zones are represented, and new ones appear. Such vertical distribution appears to be strictly related to the local hydrology, with the zone boundaries rising and falling as a function of the location of the isotherms. In particular, the first significant occurrence of *F. profunda* from surface to the deep photic zone corresponds with the start of the thermocline. Comparison of present plankton data with the surface sediment record, although displaying a

consistent pattern of species assemblage, shows some differences in the presence and relative abundance of some species (*G. oceanica*): this can be related to seasonal as well as interannual variations in the pattern and intensity of surface circulation in the investigated area (Malinverno and Ziveri, 2003).

2.2.6 Effect on the ecosystem

Coccolithophorids have a significant impact on their environment, not only respond to environmental changes but are able to change the environment in which they are found.

First, they play an important role in the carbon cycle, taking CO_2 from the water column and transforming it into organic carbon and using organic carbon for the formation of coccoliths. These are releases and then they aggregated into floating particles, when they settle down, they transport the carbon of the coccoliths to the sediments where they can dissolve (in case there are cold undersaturated waters) or accumulate forming calcareous sediments, which may give rise to calcareous deposits.

Approximately 80% of the carbon present in marine sediments is in the form of $CaCO_3$ and is mostly of biogenic origin (Broecker and Peng, 1982). In the long term, the effect of Coccolithophorids on the environment seems positive

(sequestration CO_2) but in the short term it is observed that during the formation of coccoliths, a molecule of CO_2 (powerful greenhouse gas) is generated. Although most of this gas is reused by the organism in photosynthetic processes, some of it is released into the atmosphere.

Moreover, coccoliths have the ability to disperse the light to the point that the surface blooms reduce the amount of light under them; this process could reduce the phytoplanktonic sub superficial population due to the reduction of the light, to the advantage of the Coccolithophorids. The massive blooms of Coccolithophorids also have the ability to increase the reflection of light in space (albedo), affecting the global climate.

Coccolithophorids are also involved in the sulphur cycle, producing Dimethyl sulfoniopropionate (DMSP), which seems to be related to the osmoregulation process; when this compound is released into the sea it is converted into dimethyl sulphide (DMS) and acrylic acid (Vairavamurthy *et al*., 1985). The DMS is very volatile and spreads in the atmosphere where it is oxidized; the resulting product is among the main condensation nuclei for the cloud formation process, which again influences the global climate with the increase in cloud cover (Charlson *et al.,*1987).

Important to remember that they are not normally harmful to other marine organisms in the oceans, on the contrary they constitute an excellent source of

food for small fishes and zooplanktonic organisms, especially in areas where other phytoplankton organisms are scarce.

All these characteristics suggest that the Coccolithophores have a great potential to indicate the variations of the environmental characteristics. The fact that they have a cell enclosed in a calcareous case that is preserved in sediment s allows us to find them in fossil rocks. Therefore, knowing the ecological preferences of the different species, it is possible to carry out paleoambiental reconstructions, based on the various fossil associations of both Coccolithophores and nannofossils calcareous.

2.3 CALCAREOUS NANNOFOSSILS

Calcareous nannofossils are the fossil remains of Coccolithophores, Ascidians, calcareous Dinoflagellates and Foraminifera.

They provide valuable proxies to help us understand conditions throughout geological history, because their evolution shows consistent and resilient patterns.

Nannofossils are composed of calcium carbonate, also called calcite ($CaCO_3$), and are typically less than 30μm.

A single nannofossil is called a coccosphere and is covered in many calcite plates (usually between 5 and 10 micrometers across) known as coccoliths.

The coccosphere housed the coccolithophore cell in life. After death, some may fall apart and descend as 'marine snow' to the seabed, where they settle before being preserved.

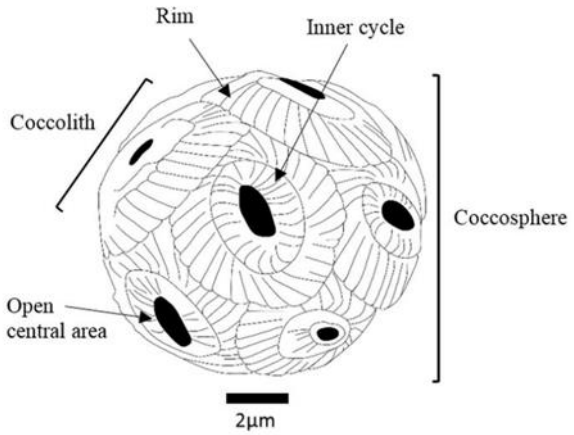

***Figure 2.6**: Key external features of calcareous nannofossil*

2.3.1 Taxonomy and classification

The shapes of the coccoliths define different nannofossil species. For example, some have spines, diverse central areas or distinctive rim shapes, even the slightest variation can denote a different species.

The taxonomy of calcareous nannofossils is entirely based on morphological characters, such as structure and form of the coccoliths and nannoliths and is therefore problematic in many aspects. The shape of the coccoliths can change in the various stages of the life cycle (polymorphism), or in function of ecological factors (ecophenotype). Moreover, some living Haptophyta produce structures very different from the typical coccoliths (*Ceratolithus* e *Florisphaera*).

However, the study of natural populations and coltures can be considered, moreover polymorphism seems to be limited to the most exotic taxa, current or fossil.

Progressive technological advances have influenced the current calcareous taxonomy and in particular, by the advent of the electron microscope, which has allowed to obtain a better morphological resolution.

The classification of nannofossils considers essentially the bipartition between coccoliths and nannoliths:

- Coccoliths are remains of algae belonging to the Haptophyta phylum and show uniform characteristics during their geological history;
- Nannoliths have a wide morphological variability, which does not allow the use of a standard taxonomic approach.

Many authors agree that the disk structure (rim) of the coccoliths is the most significant and preserved morphological character, therefore, the most appropriate for a classification at family level and at higher levels. At genus and species level, finer details on disc formation, size and structure of the central area are used.

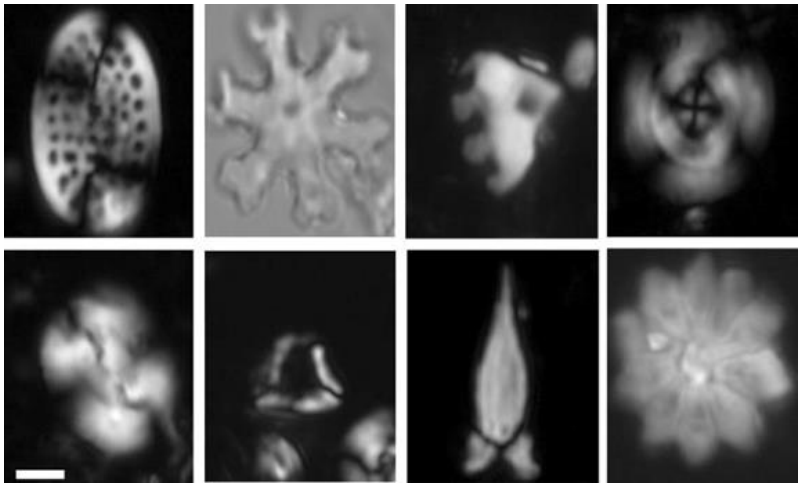

Figure 2.7*: Individual nannofossils. Scale bar represent 3µm. Top row (left to righ): Pontoshpaera multipora, Discoaster distinctus, Pemma papillatum, Reticulofenestra reticulata. Bottom row (left to right): Reticulofenestra bisecta, Lanternithus minutus, Sphenoli obtusus and Discoaster barbadiensis (Jones & Dunkley Jones, in preparation).*

2.3.2 Geological record

The earliest calcareous nannofossils are found from the late Triassic period (around 225 million years ago). It is thought that this was the first time that planktonic organisms inhabiting open oceans would export $CaCO_3$ into the deep ocean via their calcareous skeletons, which is important for the biogeochemical cycle. The emergence of calcareous nannofossils in the late Triassic started at low latitudes (near the equator) with low diversity and abundance.

Then, at the boundary between the Triassic and Jurassic periods (201 million years ago): all species of coccolithophore except *Crucirhabdus primulus* went extinct.

After this extinction event, diversity began to re-establish quickly with nannofossils rapidly taking new forms; this led to the origination of most major families in the late early Jurassic (ca. 180 million years ago).

Nannofossils seized the opportunity to adapt, colonize and flourish in almost all marine niches. In the early Jurassic, nannofossils diversified continuously, bringing a sustained increase in diversity into the Cretaceous period (starting 146 million years ago); peak diversity occurred in the Maastrichtian age (72 million to 66 million years ago). Nearing the end of the Maastrichtian, however, a sharp decrease in diversity is recorded, bringing extinction to 90%

of all calcareous nannofossil species over the infamous K–Pg boundary, the extinction event that also killed the dinosaurs.

A minimal number of small, simple species survived the catastrophic event, including *Neobiscutum* spp.

However, diversity recovered speedily, with the maximum diversity of species for the Cenozoic era (66 million years ago to the present day) transpiring around 10 million years after K–Pg event, during a time known as the Palaeocene–Eocene Thermal Maximum (Bown *et al,* 2005).

2.3.3 Importance of calcareous nannofossils

The main use of calcareous nannofossils is related to biostratigraphy, that is to the organization of sedimentary layers in biozones, identified on their fossil content without providing information on the absolute age of the biozones themselves. In particular, nannofossils are used in the biostratigraphy of the sedimentary rocks of Mesozoic and Cenozoic.

Equally important is the use of this group for paleoecological studies. Nannofossil associations contain forms whose distribution is controlled by chemical and physical conditions and therefore their variation in abundance in the stratigraphic records allows us to establish the paleoambiental variations.

Finally, we must not forget the geological and paleobiological importance of the calcareous nannoplancton. From the geological point of view, they play a lithogenetic role; they participate in quantitative meaningful way in the biogeochemical cycles of various elements (carbon, oxygen, sulfur). From the paleobiologic point of view, they represent an important part of the phytoplankton that is the beginning of the food chain in the marine waters.

Chapter Three

MATERIALS AND METHODS

3.1 STUDY AREA: THE IONIAN SEA

The Ionian Sea is an area of connection between the waters coming from the Adriatic Sea, the Eastern basin and the Western basin.

From the Adriatic Sea come dense and oxygenated waters, which discharge into the Ionian Sea as deep waters (ADW). The waters coming from the Levantine basin and from the Aegean are warm and salty and reach the Ionian Sea as intermediate waters (LIW). While, from the Strait of Sicily come the cold waters of Atlantic origin from the Western basin (MAW) confined, due to their thermoaline characteristics, in an upper layer of about 200 m.

Malanotte-Rizzoli *et al*. (1997) show how the intrusion of MAW in the first section of the eastern basin generates an anti-cyclonic vortex in the Ionian Sea area **(Fig. 3.1).**

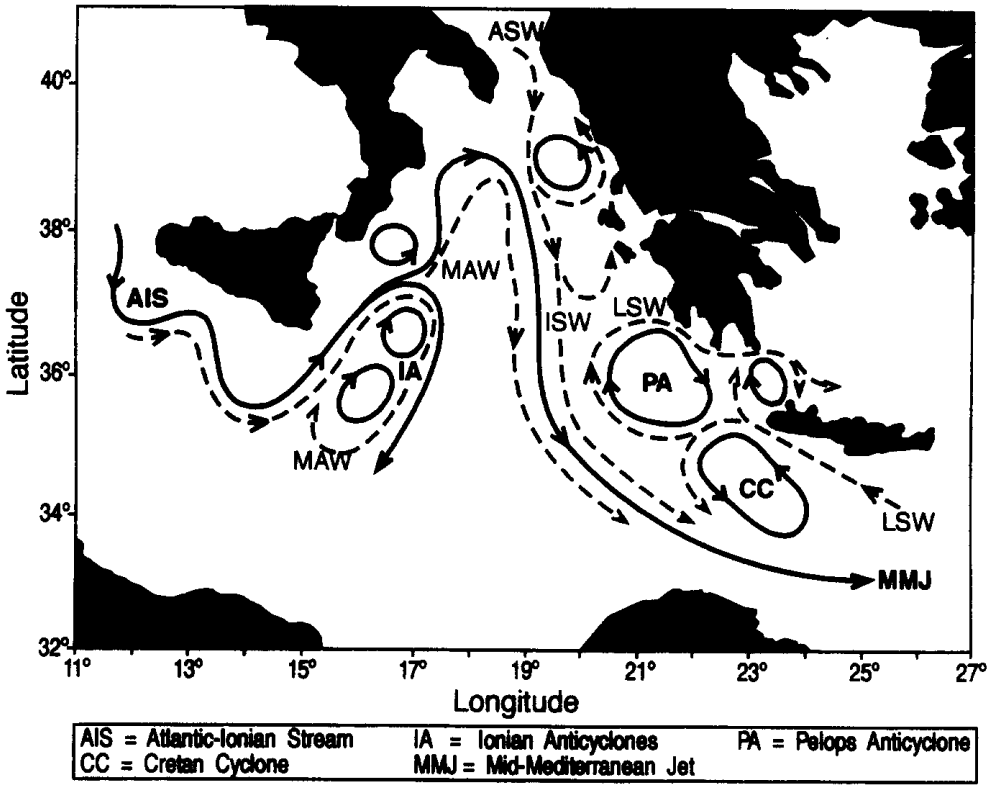

***Figure 3.1**: Schematic of the circulation and water mass pathways in different layers. Solid lines denote permanent feature, current and sub-basin gyres (Malanotte-Rizzoli, 1997)*

This vortex, that seems to have an important effect on the general circulation of water throughout the basin, is also affected by water from the East. In fact, the LIW exceeded the Island of Crete diverges to form two different currents: a primary that continues in North/West direction towards the strait of Sicily-, secondary one that proceeds in North direction, towards the Strait of Otranto. The ADW instead, generate the deepest waters of the Ionian Sea.

Gacic *et al.* (2010) also theorizes, in relation to the circulation of the currents in the Ionian Sea, a possible inversion from anticyclonic to cyclone that would have led in the past to currents whose motion was anti-clockwise, with

possible upwelling phenomena of deep waters and a different route of the LIW and MAW (**Fig 3.2**). Such a reversal would have been induced by an intensification of the river supply in the eastern part of the Mediterranean basin. The waters of the Nile would have caused this, due to stopping the downwelling of the MAW near the Island of Rhodes would have led to a blockage of the normal anti-cyclical circulation in the Ionian Sea, and consequently induced a new cyclone type circulation.

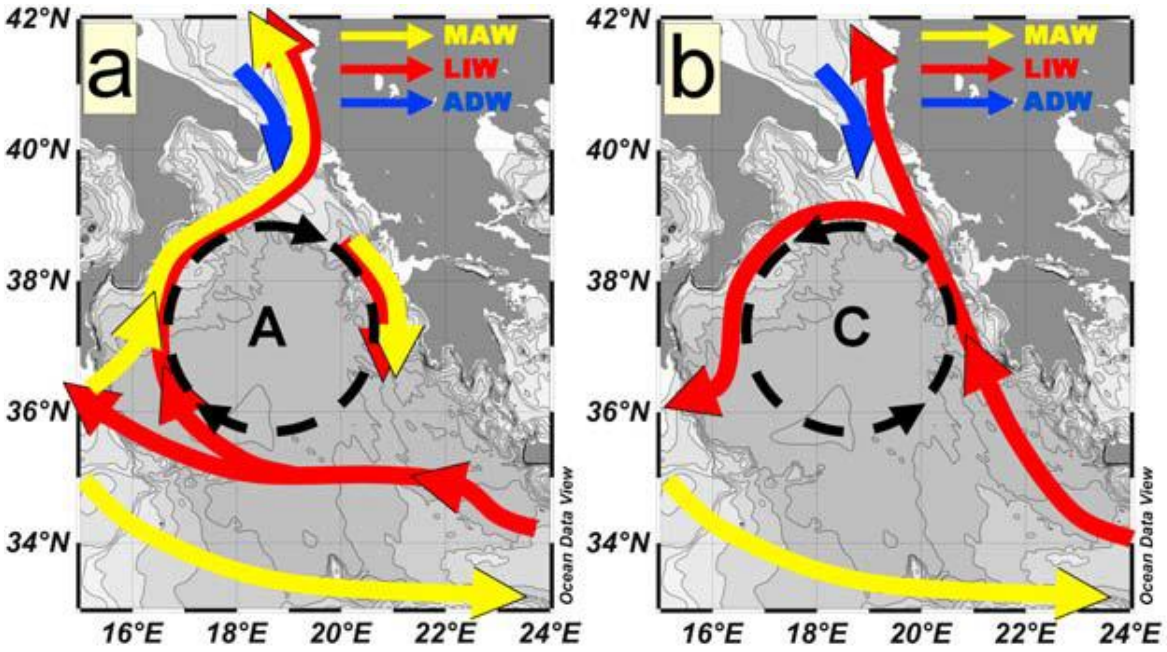

***Figure 3.2**: Schematic representation of the Adriatic-Ionian bimodal oscillating system: (a) anticyclonic mode, (b) cyclonic mode (Gacic et al., 2010)*

In relation to the deposition of sapropel, therefore, the area is very interesting as a study site, and the core M25/4-12 from this area is of considerable

importance in order to obtain new data on the deposition mechanisms of these sedimentary objects and past changes.

3.2 THE CORE M25/4-12

The 12.20 m long piston core M25/4-12 is a part of a series of four cores that were recovered from the Calabrian Ridge in the Ionian Sea in August of 1993. This was during cruise 25/4 of the R/V Meteor.

These cores were part of a study on the refinement of the Late Quaternary tephrochronological reference scale in the Eastern Mediterranean (A. Negri et al., 1999). The core was recovered at 2467m water depth, (37˚58'N 18˚11'E) (**Fig. 3.3**). The core shows dark layers, sapropels S1, S3-S10, interbedded in hemiplegic sediment along with tephra layers, Z-1 to V-4 (**Fig. 3.4**).

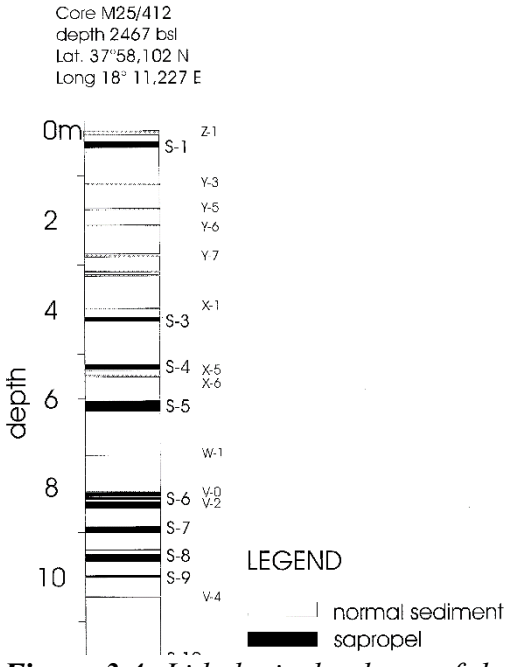

***Figure 3.4**: Lithological column of the core M25/4-12 (Negri et al., 1999)*

***Figure 3.3**: Location of the core m25/4-12 in the Ionian Sea (Google Earth)*

In the core can be observed all sapropels from S1 to S10, with the exception of S2 (Negri *et al*., 1999). Joerg Keller and Michael Kraml at the Mineralogy and Petrography Institute of the University of Freiburg (1993) made the description of the different lithological intervals in the core.

Sapropel S6, object of this work, is located in section 9, starts at 846 cmbsf, and ends at 811 cmbsf, making it at 35-centimeter-thick layer (**Fig. 3.5**).

The base (46 cm) is light beige but is immediately followed by the alternation of two Tephras (44.5 cm the first and 42.5 the second) giving the sediment a darker color. After Tephras layer, up to cm 27, the coloration is olive green. Between 26-24, cm and 21-19 cm there are two light grey bands spaced by a dark beige layer. From 19 to 17 the color returns brownish, but we notice some spots of lighter color. Lighter spot can be found also in the upper layer, despite being of darker color, up to the top of the S6 to cm 11.

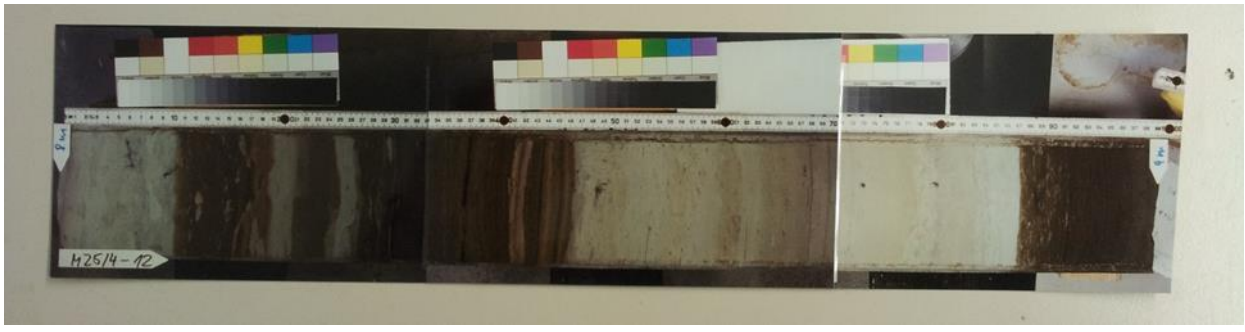

Figure 3.5: *Section 9 (Sapropel S6) of the core M25/4-12*

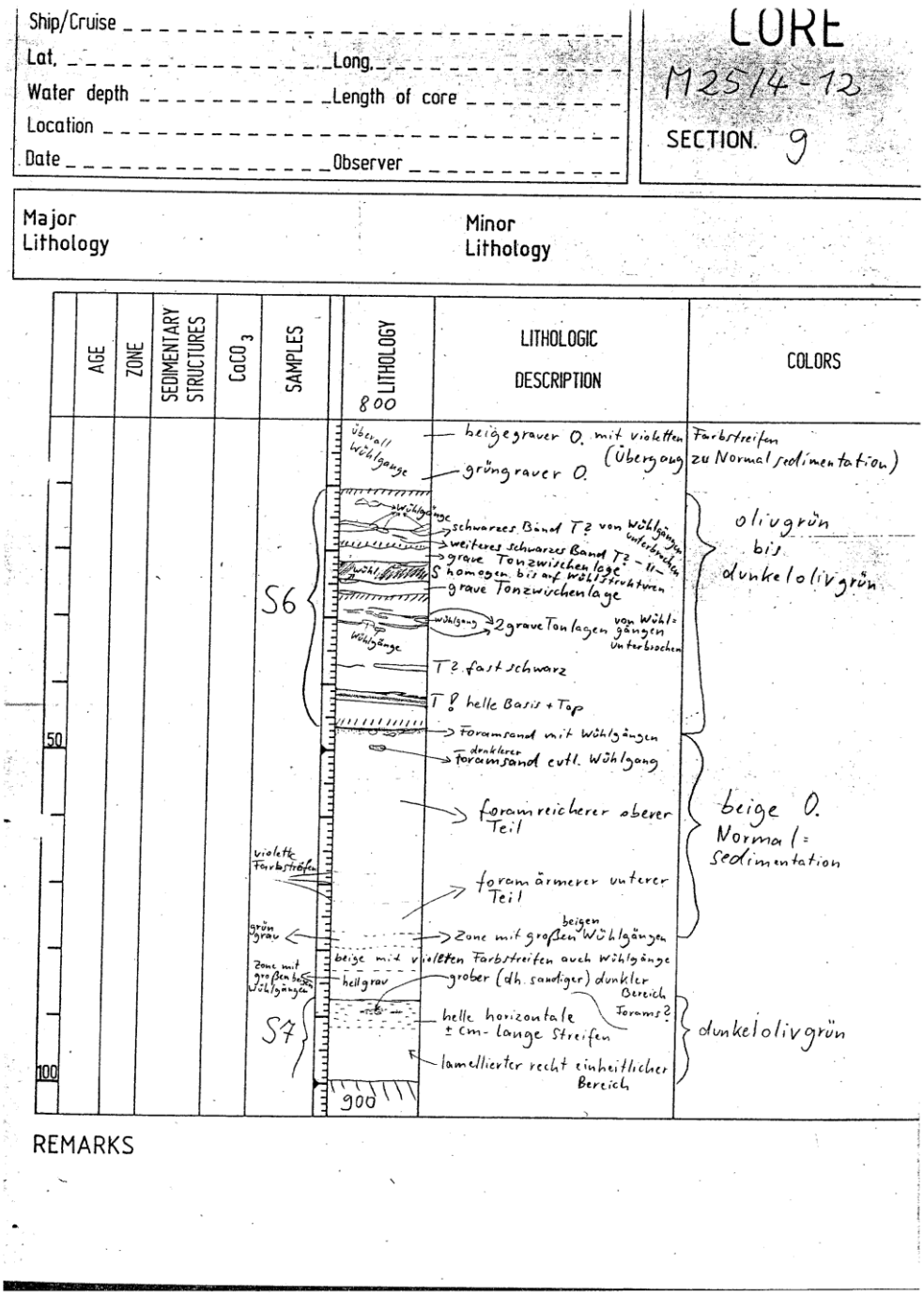

Figure 3.6: *Keller and Kraml description of section 9 (1993)*

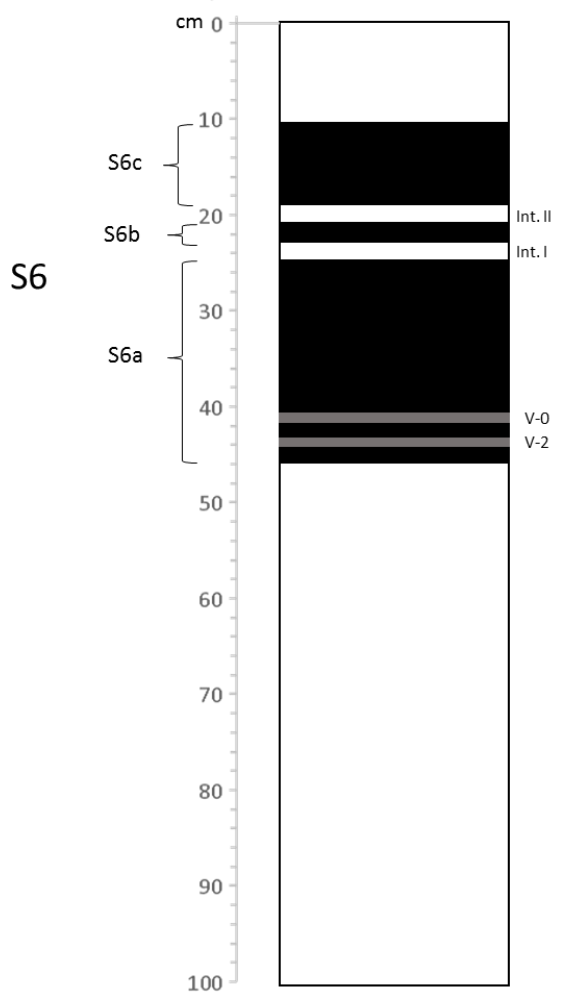

***Figure 3.7**: Illustration of section 9 (Sapropel S6) of the core M25/4-12: 46 cm base; 11 cm top; 46-26 cm S6a; 44.5-43.5 cm Tephra V-2; 42.5-41.5 cm Tephra V-0; two interruption at 26-24.5 cm and 21-19 cm; 24.5-21 cm S6b; 19-11 cm S6c*

3.3 LABORATORY TECHNIQUES

For the purpose of this work, the whole portion of sapropel S6 has been studied, which goes from cm 46 to 11, with samples taken every 1 cm. The analysis was extended also to the lower part of the base from cm 50 to 80 with an interval of 10 cm per sample, from cm 85 to 88 again every 1 cm and also to the top of the S6 from cm 0 to 10 every 1 cm.

This subdivision made possible a more in-depth study of the deposition period, also evaluating the preliminary and subsequent conditions, bringing 54 sediment samples to the analysis.

3.3.1 Settling samples

Each sample has been prepared following, and modifying some passages, the alternative method for the calculation of calcareous nannofossils accumulation rates proposed by Flores & Sierro (1997).

The procedure is as follows:

- Smash the sample of sediment.
- Weighing of an amount of dried sediment: for this analysis were used masses between 0.1 to 0.3 g.
- Place the weighed sample into a Falcon and add a volume of 15 ml of distilled water; ultrasonic for a few seconds.

- Add more distilled water a volume of 45 ml is reached.
- Ultrasonic again and shake the Falcon slightly to avoid sediment deposition.
- Take 30 ml of the mixture with a graduated glass pipette (0-30 ml), this volume is taken from the middle part of the Falcon after waiting for a few seconds to allow the settling of possible aggregates and/or large particles. Then put it inside a Becher.
- Place a coverslide in a Petri disk and put the mixture of the Becher inside the Petri, taking care not to raise the coverslide.
- Wash away any residue from the Becher.
- Keep the mixture in the Petri on a stable horizontal surface at a temperature of about 20°C for 4 hours.
- After this time, withdrawn the fluid from the Petri disk using a micropipette. To avoid removing settled particles, this withdrawal must be very slow.
- Put the Petri to dry in the oven at 70/80°C as long as necessary.
- After the disk has been dried, a cover slide is mounted with Canada balsam or any other mounting media adequate for the calcite refraction index.

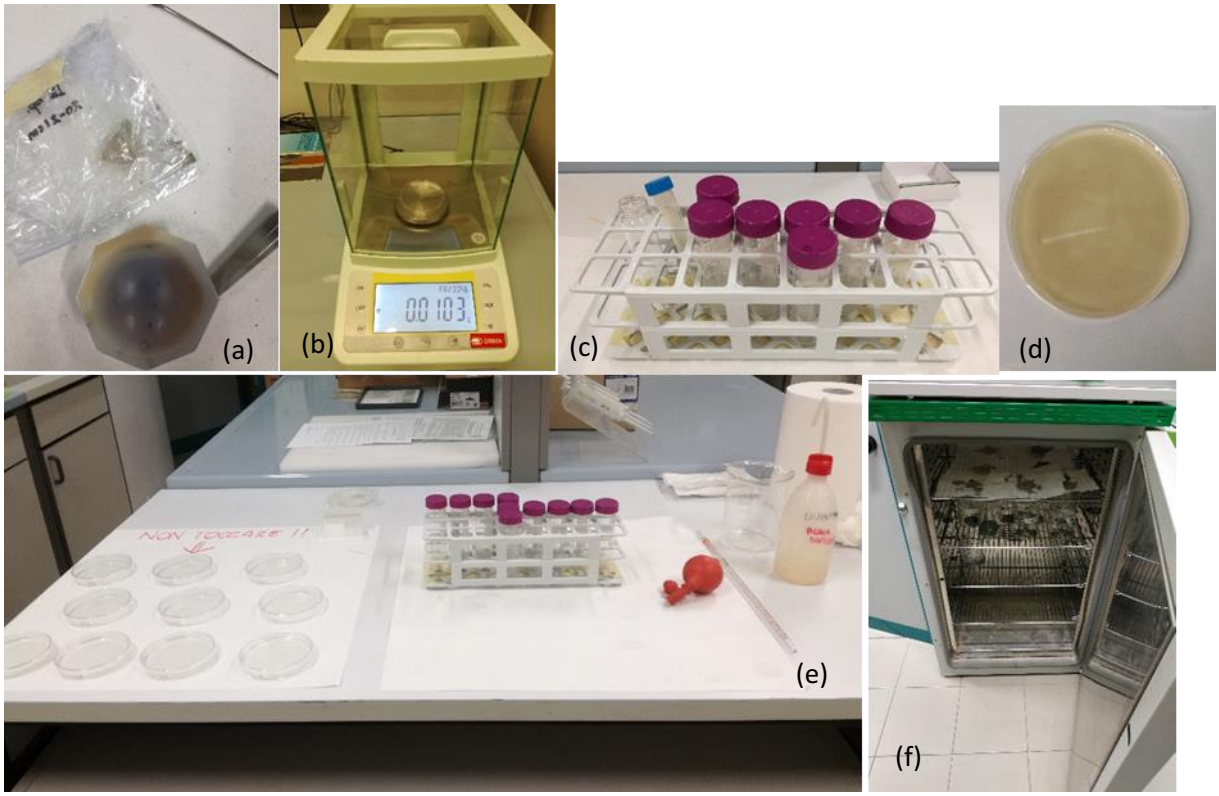

Figure 3.8: *Laboratory analyses, from the left: (a) smashing samples; (b) precision balance; (c) Falcon with the mixture; (d) Petri disk with the coverslide; (e) table of work; (f) oven*

This technique allows quantifying the amount of material per gram of sediment and/or per volume of sediment.

The aim of the technique proposed by Flores and Sierro (1997) is to obtain slides on which the nannoliths are distributed homogeneously, and to achieve the possibility of standardizing the procedure in order to save time, preparing sets of up to one hundred samples at one time.

However, as far as my experience is concerned, I have encountered problems when preparing samples using this method.

The advantage that is gained, is lost when the Petri disk is moved from a horizontal surface to the oven. Inevitably, the coverslide will shift and part of the sediment will return to suspension.

Another disadvantage is that we do not have certainty about the conservation capacity of some calcareous nannofossil species. In fac, this method requires hours of preparation: during the hours of sedimentation and those spent in the oven, less resistant species could dissolve or even evaporate once in the oven. In fact, not all my samples have succeeded perfectly, and unfortunately, I found some problems of preparation for the samples from 4-8 cm and 9-14 cm, for which I used the classic technique of smear-slide. However, of course, by doing so, I could not be able to obtain the correct analysis of the abundances for this interval. Further evidence is certainly needed to support the veracity of Flores and Sierro method.

The observation of the samples was made with a polarizing binocular microscope at a magnification of 1000X. Depending on the type of use of the polarizer, there are two mode of observation:

- cross-nicols observation (polarizer and analyzer inserted simultaneously) for the structural characteristic of calcareous nannofossils.

-parallel-nicosl observation (polarizer and analyzer inserted simultaneously but with rotating polarizer) for the morphological analyses.

***Figure 3.9**: High-powered transmitted-light microscope*

3.3.2 Qualitative and quantitative analysis

Quantitative analyses were performed by counting at least 500 species in random fields of view (**Table 1**). The relative abundance (**Table 2**) was determined in each sample, they give a good indication of the general assemblage character, but percentage data could mask inherent species-by-species variations. Although relative abundance gives indications of alterations in dominance of different species in the assemblages it contains very little information about the absolute numbers of specimens of these species in the group (Henriksson, 2000; Ferrarese *et al,* 2008).

Absolute abundance (AA) (**Table 3**) of nannofossils expressed in number of specimens per gram of sediments (nanno/g) was then estimated using the following formula (Flores and Sierro, 1997):

$$AA = \frac{N \times A \times Vtot}{f \times n \times w \times V}$$

where *N* is the number of nannofossils per gram of dry sediment; *n* the number of nannofossils counted in a random field; *A* the area of the Petri disk used (27.80 cm^2); *Vtot* the volume of water added to the dry sediment in the Falcon (45 ml), *f* the area of the visual field used in the counting (7.68 cm^2); *w* the dry sediment weight (grams) and *V* the volume of mixture withdrawn with the graduated glass pipette (30 ml).

Using this formula, the number of nannoliths per gram of sediment allowed us to estimate the amount of either one species or the total abundance of nannofossils in a given sample (Flores and Sierro, 1997).

Table 1: *Number of nannofossils per gram of sediment in each sample*

Samples	Weight (g)	Gephyrocapsa	Helicosphaer	Florisphaera	Syracosphaer	Syracosphaer	Emiliania Hux	Coccolithus p	Calcidiscus le	Reticulofenes	Reticulofenes	Rhabdosphae	Rhabdosphae	Pontosphaera	Oolitothus fra	Umbilicopsha	Umbellospha	Discosphaera	Reticulofenes	Psuedoemilia	Ceratolithus	Sphenolithus	Discoaster	Braadurospha	Tot	UPZ	Placoliths	Reworked
0-0,5 cm	0,02	373	23	22	8	0	1	5	13	65	3	3	2	2	4	4	0	0	0	0	0	1	1	0	530	21	374	2
0,5-1 cm	0,013	396	13	32	7	7	1	7	13	24	10	16	5	1	4	4	0	0	0	2	0	0	0	0	542	43	397	2
1-2 cm	0,012	382	35	46	5	9	1	4	15	16	10	10	13	0	4	5	0	0	0	1	0	1	0	0	557	46	383	2
2-3 cm	0,011	398	28	55	10	11	1	10	12	3	3	17	4	1	3	2	0	0	0	2	2	1	0	0	563	47	399	5
3-4 cm	0,013	389	25	53	18	12	1	7	13	15	2	10	3	2	4	3	0	0	1	1	1	2	0	0	562	50	390	4
4-5 cm	*	346	64	86	11	23	1	15	14	6	3	5	7	6	4	5	0	0	0	2	0	0	1	0	599	55	347	3
5-6 cm	*	400	28	84	11	21	4	10	11	3	3	6	2	5	3	4	0	1	0	4	0	1	0	0	601	48	404	5
6-7 cm	*	379	39	69	12	25	3	16	18	0	4	2	5	0	4	2	0	0	0	2	0	0	0	0	580	50	382	2
7-8 cm	*	400	27	94	9	24	1	4	9	11	4	6	5	1	3	5	1	0	0	1	0	0	0	0	605	53	401	1
8-9 cm	0,023	397	18	82	10	10	3	10	7	13	4	23	5	0	5	4	0	0	0	2	1	2	1	0	597	57	400	6
9-10 cm	*	381	36	90	17	33	1	8	7	0	1	8	4	3	4	5	0	1	0	3	0	2	0	0	604	72	382	5
11-12 cm	*	395	32	61	18	21	3	13	7	2	2	5	5	0	3	9	0	0	0	0	0	0	1	2	579	61	398	1
12-13 cm	*	357	70	81	20	21	2	12	7	0	2	4	7	0	3	8	0	0	0	3	1	0	0	0	598	63	359	4
13-14 cm	*	378	37	78	19	37	5	6	4	2	1	9	5	1	3	9	0	0	0	2	1	0	0	0	597	82	383	3
14-15 cm	0,015	391	56	89	6	4	2	9	5	5	4	16	2	0	0	6	0	1	0	0	2	0	0	1	599	35	393	2
15-16 cm	0,016	360	91	75	5	0	2	13	9	9	2	9	2	0	3	3	0	0	0	2	0	0	0	0	585	22	362	2
16-17 cm	0,019	361	86	65	4	10	2	9	12	2	0	14	2	0	1	5	0	0	0	1	0	0	1	0	575	36	363	2
17-18 cm	0,016	380	70	74	10	9	1	9	1	3	1	12	5	0	3	7	0	0	0	2	0	0	0	0	587	46	381	2
18-19 cm	0,021	375	75	66	8	11	2	3	10	2	3	10	3	0	5	6	0	0	0	2	0	0	0	0	581	43	377	2
19-20 cm	0,015	394	38	70	7	10	6	8	8	15	1	12	5	1	2	3	0	0	0	2	0	1	0	0	583	39	400	3
20-21 cm	0,02	388	44	94	9	13	3	11	7	11	0	9	6	1	4	3	0	0	0	4	0	1	0	1	609	44	391	5
21-22 cm	0,025	395	48	100	10	10	2	7	4	7	0	14	4	0	2	7	0	0	0	2	0	1	0	0	613	47	397	3
22-23 cm	0,022	394	53	87	10	9	6	4	8	9	0	10	0	2	3	6	0	0	0	4	0	1	0	0	606	38	400	5
23-24 cm	0,02	381	78	98	7	7	3	11	3	0	2	7	2	0	2	6	0	0	0	3	2	0	0	0	612	31	384	5
24-25 cm	0,021	395	72	63	6	4	4	7	5	3	1	6	0	0	4	3	0	0	0	2	0	1	0	0	576	23	399	3
25-26 cm	0,024	356	70	117	10	29	2	7	5	3	4	5	6	2	4	7	0	0	0	4	3	0	1	0	635	61	358	8
26-27 cm	0,023	366	55	121	30	14	4	7	7	6	7	4	2	2	5	3	0	0	0	2	0	0	0	1	636	58	370	2
27-28 cm	0,023	369	38	114	20	37	4	4	6	10	3	8	3	0	6	5	0	0	0	4	0	1	1	2	635	79	373	6
28-29 cm	0,025	364	53	116	18	32	4	6	7	13	0	4	0	2	2	6	0	0	0	4	1	0	1	0	633	62	368	6
29-30 cm	0,02	384	34	120	11	20	3	13	7	11	1	15	3	0	2	4	0	0	0	2	1	0	0	0	631	55	387	3
30-31 cm	0,021	362	74	106	12	17	6	10	11	4	4	4	1	1	4	7	0	0	0	1	0	0	0	0	624	45	368	1
31-32 cm	0,024	387	45	117	14	10	4	9	16	10	0	7	2	0	7	4	0	0	0	1	0	0	0	0	633	44	391	1
32-33 cm	0,025	379	50	125	14	8	7	7	21	15	1	3	1	1	5	5	0	0	0	3	0	0	0	0	645	36	386	3
33-34 cm	0,022	392	37	102	19	12	7	11	7	7	0	9	6	0	2	6	0	0	0	1	0	0	1	0	619	54	399	2
34-35 cm	0,026	395	45	106	16	8	5	11	4	8	3	6	3	1	3	7	0	0	0	2	0	0	0	0	623	43	400	2
35-36 cm	0,026	399	28	73	16	16	5	12	5	10	0	10	3	0	3	5	0	0	0	3	0	1	0	0	589	53	404	4
36-37 cm	0,025	397	26	136	14	15	8	12	5	13	5	11	1	1	2	4	0	0	0	3	0	0	0	0	653	47	405	3
37-38 cm	0,025	377	43	110	26	17	6	13	6	12	0	4	2	0	2	9	0	0	0	1	0	0	0	0	628	60	383	1
38-39,5 cm	0,026	363	36	95	54	21	4	14	2	5	0	3	2	0	3	8	0	0	0	0	0	0	0	0	610	91	367	0
39,5-41 cm	0,024	388	42	93	31	15	5	7	5	2	0	6	4	0	3	5	0	0	0	2	0	0	0	0	608	64	393	2
42-43 cm	0,028	347	66	145	25	34	4	10	6	0	0	6	5	1	3	4	0	0	0	3	0	0	0	0	659	77	351	3
43-44 cm	0,025	353	75	124	27	23	4	11	4	0	0	5	2	0	3	6	0	0	0	1	0	0	0	0	638	66	357	1
44-45 cm	0,026	374	59	126	20	14	4	6	8	0	0	4	13	0	4	5	0	0	0	1	2	0	0	0	640	60	378	3
45-46 cm	0,023	383	40	110	23	13	4	10	17	2	0	8	4	0	4	4	0	0	0	1	0	0	0	1	624	56	387	1
46-47 cm	0,025	351	36	79	21	17	3	22	31	4	3	6	7	1	5	4	0	0	0	1	1	0	0	0	592	60	354	2
47-48 cm	0,024	361	35	120	20	29	6	18	20	2	0	3	11	1	4	5	0	0	0	1	0	0	0	1	637	72	367	1
48-49 cm	0,028	370	34	110	18	21	7	20	25	0	1	3	8	0	4	5	0	0	0	0	0	0	0	0	626	59	377	0
49-50 cm	0,024	356	34	126	24	21	7	16	29	0	2	10	7	0	5	4	0	0	0	1	1	0	0	1	644	71	363	2
60-61 cm	0,025	394	36	135	21	13	6	14	10	2	1	3	4	2	2	7	0	0	0	3	0	0	0	0	653	50	400	3
70-71 cm	0,026	376	26	140	41	20	5	7	13	0	0	5	9	1	2	6	0	0	0	1	3	0	0	0	655	83	381	4
80-81 cm	0,028	388	21	101	29	19	7	13	16	3	0	4	6	1	5	6	0	0	0	1	2	0	0	0	622	69	395	3
85-86 cm	0,029	362	50	123	18	11	4	20	23	0	3	2	9	2	5	6	0	0	0	1	0	0	0	0	639	51	366	1
86-87 cm	0,025	342	66	107	19	22	4	13	22	3	0	4	9	0	2	6	0	0	0	1	0	0	0	0	620	62	346	1
87-88 cm	0,027	348	83	116	16	12	5	20	9	1	0	2	6	3	4	5	0	0	0	1	0	0	0	0	631	45	353	1

***Table 2**: Relative abundances (%)*

	Gephyroc	Helicosph	Florisphae	Syracosph	Syracosph	Emiliania	Coccolithu	Calcidiscu	Reticulofe	Reticulofe	Rhadbosp	Rhabdosp	Pontosph	Oolitothus	Umbelicos	Umbellos	Discospha	Reticulofe	Psuedoem	Ceratolith	Sphenolit	Discoaster	Braadurosphaera	Tot		Placoliths	UPZ	Reworked
0,0	70,4	4,3	4,2	1,5	0,0	0,2	0,9	2,5	12,3	0,6	0,6	0,4	0,4	0,8	0,8	0,0	0,0	0,0	0,0	0,0	0,2	0,2	0,0	100		70,6	4,0	0,4
0,5	73,1	2,4	5,9	1,3	1,3	0,2	1,3	2,4	4,4	1,8	3,0	0,9	0,2	0,7	0,7	0,0	0,0	0,0	0,4	0,0	0,0	0,0	0,0	100		73,2	7,9	0,4
1,0	68,6	6,3	8,3	0,9	1,6	0,2	0,7	2,7	2,9	1,8	1,8	2,3	0,0	0,7	0,9	0,0	0,0	0,0	0,2	0,0	0,2	0,0	0,0	100		68,8	8,3	0,4
2,0	70,7	5,0	9,8	1,8	2,0	0,2	1,8	2,1	0,5	0,5	3,0	0,7	0,2	0,5	0,4	0,0	0,0	0,0	0,4	0,4	0,2	0,0	0,0	100		70,9	8,3	0,9
3,0	69,2	4,4	9,4	3,2	2,1	0,2	1,2	2,3	2,7	0,4	1,8	0,5	0,4	0,7	0,5	0,0	0,0	0,2	0,2	0,2	0,4	0,0	0,0	100		69,4	8,9	0,7
4,0	57,8	10,7	14,4	1,8	3,8	0,2	2,5	2,3	1,0	0,5	0,8	1,2	1,0	0,7	0,8	0,0	0,0	0,0	0,3	0,0	0,0	0,2	0,0	100		57,9	9,2	0,5
5,0	66,6	4,7	14,0	1,8	3,5	0,7	1,7	1,8	0,5	0,5	1,0	0,3	0,8	0,5	0,7	0,0	0,2	0,0	0,7	0,0	0,2	0,0	0,0	100		67,2	8,0	0,8
6,0	65,3	6,7	11,9	2,1	4,3	0,5	2,8	3,1	0,0	0,7	0,3	0,9	0,0	0,7	0,3	0,0	0,0	0,0	0,3	0,0	0,0	0,0	0,0	100		65,9	8,6	0,3
7,0	66,1	4,5	15,5	1,5	4,0	0,2	0,7	1,5	1,8	0,7	1,0	0,8	0,2	0,5	0,8	0,2	0,0	0,0	0,2	0,0	0,0	0,0	0,0	100		66,3	8,8	0,2
8,0	66,5	3,0	13,7	1,7	1,7	0,5	1,7	1,2	2,2	0,7	3,9	0,8	0,0	0,8	0,7	0,0	0,0	0,0	0,3	0,2	0,3	0,2	0,0	100		67,0	9,5	1,0
9,0	63,1	6,0	14,9	2,8	5,5	0,2	1,3	1,2	0,0	0,2	1,3	0,7	0,5	0,7	0,8	0,0	0,2	0,0	0,5	0,0	0,3	0,0	0,0	100		63,2	11,9	0,8
11,0	68,2	5,5	10,5	3,1	3,6	0,5	2,2	1,2	0,3	0,3	0,9	0,9	0,0	0,5	1,6	0,0	0,0	0,0	0,0	0,0	0,0	0,2	0,3	100		68,7	10,5	0,2
12,0	59,7	11,7	13,5	3,3	3,5	0,3	2,0	1,2	0,0	0,3	0,7	1,2	0,0	0,5	1,3	0,0	0,0	0,0	0,5	0,2	0,0	0,0	0,0	100		60,0	10,5	0,7
13,0	63,3	6,2	13,1	3,2	6,2	0,8	1,0	0,7	0,3	0,2	1,5	0,8	0,2	0,5	1,5	0,0	0,0	0,0	0,3	0,2	0,0	0,0	0,0	100		64,2	13,7	0,5
14,0	65,3	9,3	14,9	1,0	0,7	0,3	1,5	0,8	0,8	0,7	2,7	0,3	0,0	0,0	1,0	0,0	0,2	0,0	0,0	0,3	0,0	0,0	0,2	100		65,6	5,8	0,3
15,0	61,5	15,6	12,8	0,9	0,0	0,3	2,2	1,5	1,5	0,3	1,5	0,3	0,0	0,5	0,5	0,0	0,0	0,0	0,3	0,0	0,0	0,0	0,0	100		61,9	3,8	0,3
16,0	62,8	15,0	11,3	0,7	1,7	0,3	1,6	2,1	0,3	0,0	2,4	0,3	0,0	0,2	0,9	0,0	0,0	0,0	0,2	0,0	0,0	0,2	0,0	100		63,1	6,3	0,3
17,0	64,7	11,9	12,6	1,7	1,5	0,2	1,5	0,2	0,5	0,2	2,0	0,9	0,0	0,5	1,2	0,0	0,0	0,0	0,3	0,0	0,0	0,0	0,0	100		64,9	7,8	0,3
18,0	64,5	12,9	11,4	1,4	1,9	0,3	0,5	1,7	0,3	0,5	1,7	0,5	0,0	0,9	1,0	0,0	0,0	0,0	0,3	0,0	0,0	0,0	0,0	100		64,9	7,4	0,3
19,0	67,6	6,5	12,0	1,2	1,7	1,0	1,4	1,4	2,6	0,2	2,1	0,9	0,2	0,3	0,5	0,0	0,0	0,0	0,3	0,0	0,2	0,0	0,0	100		68,6	6,7	0,5
20,0	63,7	7,2	15,4	1,5	2,1	0,5	1,8	1,1	1,8	0,0	1,5	1,0	0,2	0,7	0,5	0,0	0,0	0,0	0,7	0,0	0,2	0,0	0,2	100		64,2	7,2	0,8
21,0	64,4	7,8	16,3	1,6	1,6	0,3	1,1	0,7	1,1	0,0	2,3	0,7	0,0	0,3	1,1	0,0	0,0	0,0	0,3	0,0	0,2	0,0	0,0	100		64,8	7,7	0,5
22,0	65,0	8,7	14,4	1,7	1,5	1,0	0,7	1,3	1,5	0,0	1,7	0,0	0,3	0,5	1,0	0,0	0,0	0,0	0,7	0,0	0,2	0,0	0,0	100		66,0	6,3	0,8
23,0	62,3	12,7	16,0	1,1	1,1	0,5	1,8	0,5	0,0	0,3	1,1	0,3	0,0	0,3	1,0	0,0	0,0	0,0	0,5	0,3	0,0	0,0	0,0	100		62,7	5,1	0,8
24,0	68,6	12,5	10,9	1,0	0,7	0,7	1,2	0,9	0,5	0,2	1,0	0,0	0,0	0,7	0,5	0,0	0,0	0,0	0,3	0,0	0,2	0,0	0,0	100		69,3	4,0	0,5
25,0	56,1	11,0	18,4	1,6	4,6	0,3	1,1	0,8	0,5	0,6	0,8	0,9	0,3	0,6	1,1	0,0	0,0	0,0	0,6	0,5	0,0	0,2	0,0	100		56,4	9,6	1,3
26,0	57,5	8,6	19,0	4,7	2,2	0,6	1,1	1,1	0,9	1,1	0,6	0,3	0,3	0,8	0,5	0,0	0,0	0,0	0,3	0,0	0,0	0,0	0,2	100		58,2	9,1	0,3
27,0	58,1	6,0	18,0	3,1	5,8	0,6	0,6	0,9	1,6	0,5	1,3	0,5	0,0	0,9	0,8	0,0	0,0	0,0	0,6	0,0	0,2	0,2	0,3	100		58,7	12,4	0,9
28,0	57,5	8,4	18,3	2,8	5,1	0,6	0,9	1,1	2,1	0,0	0,6	0,0	0,3	0,3	0,9	0,0	0,0	0,0	0,6	0,2	0,0	0,2	0,0	100		58,1	9,8	0,9
29,0	60,9	5,4	19,0	1,7	3,2	0,5	2,1	1,1	1,7	0,2	2,4	0,5	0,0	0,3	0,6	0,0	0,0	0,0	0,3	0,2	0,0	0,0	0,0	100		61,3	8,7	0,5
30,0	58,0	11,9	17,0	1,9	2,7	1,0	1,6	1,8	0,6	0,6	0,6	0,2	0,2	0,6	1,1	0,0	0,0	0,0	0,2	0,0	0,0	0,0	0,0	100		59,0	7,2	0,2
31,0	61,1	7,1	18,5	2,2	1,6	0,6	1,4	2,5	1,6	0,0	1,1	0,3	0,0	1,1	0,6	0,0	0,0	0,0	0,2	0,0	0,0	0,0	0,0	100		61,8	7,0	0,2
32,0	58,8	7,8	19,4	2,2	1,2	1,1	1,1	3,3	2,3	0,2	0,5	0,2	0,2	0,8	0,8	0,0	0,0	0,0	0,5	0,0	0,0	0,0	0,0	100		59,8	5,6	0,5
33,0	63,3	6,0	16,5	3,1	1,9	1,1	1,8	1,1	1,1	0,0	1,5	1,0	0,0	0,3	1,0	0,0	0,0	0,0	0,2	0,0	0,0	0,2	0,0	100		64,5	8,7	0,3
34,0	63,4	7,2	17,0	2,6	1,3	0,8	1,8	0,6	1,3	0,5	1,0	0,5	0,2	0,5	1,1	0,0	0,0	0,0	0,3	0,0	0,0	0,0	0,0	100		64,2	6,9	0,3
35,0	67,7	4,8	12,4	2,7	2,7	0,8	2,0	0,8	1,7	0,0	1,7	0,5	0,0	0,5	0,8	0,0	0,0	0,0	0,5	0,0	0,2	0,0	0,0	100		68,6	9,0	0,7
36,0	60,8	4,0	20,8	2,1	2,3	1,2	1,8	0,8	2,0	0,8	1,7	0,2	0,2	0,3	0,6	0,0	0,0	0,0	0,5	0,0	0,0	0,0	0,0	100		62,0	7,2	0,5
37,0	60,0	6,8	17,5	4,1	2,7	1,0	2,1	1,0	1,9	0,0	0,6	0,3	0,0	0,3	1,4	0,0	0,0	0,0	0,2	0,0	0,0	0,0	0,0	100		61,0	9,6	0,2
38,0	59,5	5,9	15,6	8,9	3,4	0,7	2,3	0,3	0,8	0,0	0,5	0,3	0,0	0,5	1,3	0,0	0,0	0,0	0,0	0,0	0,0	0,0	0,0	100		60,2	14,9	0,0
39,5	63,8	6,9	15,3	5,1	2,5	0,8	1,2	0,8	0,3	0,0	1,0	0,7	0,0	0,5	0,8	0,0	0,0	0,0	0,3	0,0	0,0	0,0	0,0	100		64,6	10,5	0,3
42,0	52,7	10,0	22,0	3,8	5,2	0,6	1,5	0,9	0,0	0,0	0,9	0,8	0,2	0,5	0,6	0,0	0,0	0,0	0,5	0,0	0,0	0,0	0,0	100		53,3	11,7	0,5
43,0	55,3	11,8	19,4	4,2	3,6	0,6	1,7	0,6	0,0	0,0	0,8	0,3	0,0	0,5	0,9	0,0	0,0	0,0	0,2	0,0	0,0	0,0	0,0	100		56,0	10,3	0,2
44,0	58,4	9,2	19,7	3,1	2,2	0,6	0,9	1,3	0,0	0,0	0,6	2,0	0,0	0,6	0,8	0,0	0,0	0,0	0,2	0,3	0,0	0,0	0,0	100		59,1	9,4	0,5
45,0	61,4	6,4	17,6	3,7	2,1	0,6	1,6	2,7	0,3	0,0	1,3	0,6	0,0	0,6	0,6	0,0	0,0	0,0	0,2	0,0	0,0	0,0	0,2	100		62,0	9,0	0,2
46,0	59,3	6,1	13,3	3,5	2,9	0,5	3,7	5,2	0,7	0,5	1,0	1,2	0,2	0,8	0,7	0,0	0,0	0,0	0,2	0,2	0,0	0,0	0,0	100		59,8	10,1	0,3
47,0	56,7	5,5	18,8	3,1	4,6	0,9	2,8	3,1	0,3	0,0	0,5	1,7	0,2	0,6	0,8	0,0	0,0	0,0	0,2	0,0	0,0	0,0	0,2	100		57,6	11,3	0,2
48,0	59,1	5,4	17,6	2,9	3,4	1,1	3,2	4,0	0,0	0,2	0,5	1,3	0,0	0,6	0,8	0,0	0,0	0,0	0,0	0,0	0,0	0,0	0,0	100		60,2	9,4	0,0
49,0	55,3	5,3	19,6	3,7	3,3	1,1	2,5	4,5	0,0	0,3	1,6	1,1	0,0	0,8	0,6	0,0	0,0	0,0	0,2	0,2	0,0	0,0	0,2	100		56,4	11,0	0,3
60,0	60,3	5,5	20,7	3,2	2,0	0,9	2,1	1,5	0,3	0,2	0,5	0,6	0,3	0,3	1,1	0,0	0,0	0,0	0,5	0,0	0,0	0,0	0,0	100		61,3	7,7	0,5
70,0	57,4	4,0	21,4	6,3	3,1	0,8	1,1	2,0	0,0	0,0	0,8	1,4	0,2	0,3	0,9	0,0	0,0	0,0	0,2	0,5	0,0	0,0	0,0	100		58,2	12,7	0,6
80,0	62,4	3,4	16,2	4,7	3,1	1,1	2,1	2,6	0,5	0,0	0,6	1,0	0,2	0,8	1,0	0,0	0,0	0,0	0,2	0,3	0,0	0,0	0,0	100		63,5	11,1	0,5
85,0	56,7	7,8	19,2	2,8	1,7	0,6	3,1	3,6	0,0	0,5	0,3	1,4	0,3	0,8	0,9	0,0	0,0	0,0	0,2	0,0	0,0	0,0	0,0	100		57,3	8,0	0,2
86,0	55,2	10,6	17,3	3,1	3,5	0,6	2,1	3,5	0,5	0,0	0,6	1,5	0,0	0,3	1,0	0,0	0,0	0,0	0,2	0,0	0,0	0,0	0,0	100		55,8	10,0	0,2
87,0	55,2	13,2	18,4	2,5	1,9	0,8	3,2	1,4	0,2	0,0	0,3	1,0	0,5	0,6	0,8	0,0	0,0	0,0	0,2	0,0	0,0	0,0	0,0	100		55,9	7,1	0,2

***Table 3**: Absolute abundances*

	Weight (g)	G																						oliths	Reworked
0,0	0,02	1,93E+07	1,19E+06	1,1E+06	4,1E+05	0,0E+00	5,2E+04	2,6E+05	6,7E+05	3,4E+06	1,6E+05	1,6E+05	1,0E+05	1,0E+05	2,1E+05	2,1E+05	0,0E+00	0,0E+00	0,0E+00	0,0E+00	0,0E+00	5,2E+04	5,2E+04	0,0E+00	1,1E+06	1,9E+07	1,0E+05
0,5	0,013	1,54E+07	4,48E+05	1,1E+06	2,4E+05	2,4E+05	3,4E+04	2,4E+05	4,5E+05	8,3E+05	3,4E+05	5,5E+05	1,7E+05	3,4E+04	1,4E+05	1,4E+05	0,0E+00	0,0E+00	0,0E+00	0,0E+00	6,9E+04	0,0E+00	0,0E+00	0,0E+00	0,0E+00	1,5E+06	1,4E+07	6,9E+04
1,0	0,012	1,41E+07	1,14E+06	1,5E+06	1,6E+05	2,9E+05	3,3E+04	1,3E+05	4,9E+05	5,2E+05	3,3E+05	3,3E+05	4,2E+05	0,0E+00	1,3E+05	1,6E+05	0,0E+00	0,0E+00	0,0E+00	0,0E+00	3,3E+04	0,0E+00	3,3E+04	0,0E+00	0,0E+00	1,5E+06	1,3E+07	6,5E+04
2,0	0,011	1,36E+07	8,47E+05	1,7E+06	3,0E+05	3,3E+05	3,0E+04	3,0E+05	3,6E+05	9,1E+04	9,1E+04	5,1E+05	1,2E+05	3,0E+04	9,1E+04	6,1E+04	0,0E+00	0,0E+00	0,0E+00	0,0E+00	6,1E+04	6,1E+04	3,0E+04	0,0E+00	0,0E+00	1,4E+06	1,2E+07	1,5E+05
3,0	0,013	1,57E+07	8,93E+05	1,9E+06	6,4E+05	4,3E+05	3,6E+04	2,5E+05	4,6E+05	5,4E+05	7,1E+04	3,6E+05	1,1E+05	7,1E+04	1,4E+05	1,1E+05	0,0E+00	0,0E+00	0,0E+00	3,6E+04	3,6E+04	3,6E+04	7,1E+04	0,0E+00	0,0E+00	1,8E+06	1,4E+07	1,4E+05
8,0	0,023	3,02E+07	1,21E+06	5,5E+06	6,7E+05	6,7E+05	2,0E+05	6,7E+05	4,7E+05	8,7E+05	2,7E+05	1,5E+06	3,4E+05	0,0E+00	3,4E+05	2,7E+05	0,0E+00	0,0E+00	0,0E+00	0,0E+00	1,3E+05	6,7E+04	1,3E+05	6,7E+04	0,0E+00	3,8E+06	2,7E+07	4,0E+05
14,0	0,015	1,94E+07	2,46E+06	3,9E+06	2,6E+05	1,8E+05	8,8E+04	4,0E+05	2,2E+05	2,2E+05	1,8E+05	7,0E+05	8,8E+04	0,0E+00	0,0E+00	2,6E+05	0,0E+00	4,4E+04	0,0E+00	0,0E+00	8,8E+04	0,0E+00	0,0E+00	4,4E+04	1,5E+06	1,7E+07	8,8E+04
15,0	0,016	1,87E+07	4,16E+06	3,4E+06	2,3E+05	0,0E+00	9,1E+04	5,9E+05	4,1E+05	4,1E+05	9,1E+04	4,1E+05	9,1E+04	0,0E+00	1,4E+05	1,4E+05	0,0E+00	0,0E+00	0,0E+00	0,0E+00	9,1E+04	0,0E+00	0,0E+00	0,0E+00	0,0E+00	1,0E+06	1,7E+07	9,1E+04
16,0	0,019	2,18E+07	4,59E+06	3,5E+06	2,1E+05	5,3E+05	1,1E+05	4,8E+05	6,4E+05	1,1E+05	0,0E+00	7,5E+05	1,1E+05	0,0E+00	5,3E+04	2,7E+05	0,0E+00	0,0E+00	0,0E+00	0,0E+00	5,3E+04	0,0E+00	0,0E+00	5,3E+04	0,0E+00	1,9E+06	1,9E+07	1,1E+05
17,0	0,016	1,98E+07	3,21E+06	3,4E+06	4,6E+05	4,1E+05	4,6E+04	4,1E+05	4,6E+04	1,4E+05	4,6E+04	5,5E+05	2,3E+05	0,0E+00	1,4E+05	3,2E+05	0,0E+00	0,0E+00	0,0E+00	0,0E+00	9,2E+04	0,0E+00	0,0E+00	0,0E+00	0,0E+00	2,1E+06	1,7E+07	9,2E+04
18,0	0,021	2,53E+07	4,47E+06	3,9E+06	4,8E+05	6,6E+05	1,2E+05	1,8E+05	6,0E+05	1,2E+05	1,8E+05	6,0E+05	1,8E+05	0,0E+00	3,0E+05	3,6E+05	0,0E+00	0,0E+00	0,0E+00	0,0E+00	1,2E+05	0,0E+00	0,0E+00	0,0E+00	0,0E+00	2,6E+06	2,2E+07	1,2E+05
19,0	0,015	1,91E+07	1,62E+06	3,0E+06	3,0E+05	4,3E+05	2,6E+05	3,4E+05	3,4E+05	6,4E+05	4,3E+04	5,1E+05	2,1E+05	4,3E+04	8,5E+04	1,3E+05	0,0E+00	0,0E+00	0,0E+00	0,0E+00	8,5E+04	0,0E+00	4,3E+04	0,0E+00	0,0E+00	1,7E+06	1,7E+07	1,3E+05
20,0	0,02	2,62E+07	2,62E+06	5,6E+06	5,4E+05	7,7E+05	1,8E+05	6,5E+05	4,2E+05	6,5E+05	0,0E+00	5,4E+05	3,6E+05	6,0E+04	2,4E+05	1,8E+05	0,0E+00	0,0E+00	0,0E+00	0,0E+00	2,4E+05	0,0E+00	6,0E+04	0,0E+00	6,0E+04	2,6E+06	2,3E+07	3,0E+05
21,0	0,025	3,35E+07	3,59E+06	7,5E+06	7,5E+05	7,5E+05	1,5E+05	5,2E+05	3,0E+05	5,2E+05	0,0E+00	1,0E+06	3,0E+05	0,0E+00	1,5E+05	5,2E+05	0,0E+00	0,0E+00	0,0E+00	0,0E+00	1,5E+05	0,0E+00	7,5E+04	0,0E+00	0,0E+00	3,5E+06	3,0E+07	2,2E+05
22,0	0,022	2,91E+07	3,45E+06	5,7E+06	6,5E+05	5,9E+05	3,9E+05	2,6E+05	5,2E+05	5,9E+05	0,0E+00	6,5E+05	0,0E+00	1,3E+05	2,0E+05	3,9E+05	0,0E+00	0,0E+00	0,0E+00	0,0E+00	2,6E+05	0,0E+00	6,5E+04	0,0E+00	0,0E+00	2,5E+06	2,6E+07	3,3E+05
23,0	0,02	2,58E+07	4,67E+06	5,9E+06	4,2E+05	4,2E+05	1,8E+05	6,6E+05	1,8E+05	0,0E+00	1,2E+05	4,2E+05	1,2E+05	0,0E+00	1,2E+05	3,6E+05	0,0E+00	0,0E+00	0,0E+00	0,0E+00	1,8E+05	1,2E+05	0,0E+00	0,0E+00	0,0E+00	1,9E+06	2,3E+07	3,0E+05
24,0	0,021	2,64E+07	4,26E+06	3,7E+06	3,5E+05	2,4E+05	2,4E+05	4,1E+05	3,0E+05	1,8E+05	5,9E+04	3,5E+05	0,0E+00	0,0E+00	2,4E+05	1,8E+05	0,0E+00	0,0E+00	0,0E+00	0,0E+00	1,2E+05	0,0E+00	5,9E+04	0,0E+00	0,0E+00	1,4E+06	2,4E+07	1,8E+05
25,0	0,024	3,00E+07	5,21E+06	8,7E+06	7,4E+05	2,2E+06	1,5E+05	5,2E+05	3,7E+05	2,2E+05	3,0E+05	3,7E+05	4,5E+05	1,5E+05	3,0E+05	5,2E+05	0,0E+00	0,0E+00	0,0E+00	0,0E+00	3,0E+05	2,2E+05	0,0E+00	7,4E+04	0,0E+00	4,5E+06	2,7E+07	6,0E+05
26,0	0,023	2,96E+07	3,93E+06	8,6E+06	2,1E+06	1,0E+06	2,9E+05	5,0E+05	5,0E+05	4,3E+05	5,0E+05	2,9E+05	1,4E+05	1,4E+05	3,6E+05	2,1E+05	0,0E+00	0,0E+00	0,0E+00	0,0E+00	1,4E+05	0,0E+00	0,0E+00	0,0E+00	7,1E+04	4,1E+06	2,6E+07	1,4E+05
27,0	0,023	2,98E+07	2,71E+06	8,1E+06	1,4E+06	2,6E+06	2,9E+05	2,9E+05	4,3E+05	7,1E+05	2,1E+05	5,7E+05	2,1E+05	0,0E+00	4,3E+05	3,6E+05	0,0E+00	0,0E+00	0,0E+00	0,0E+00	2,9E+05	0,0E+00	7,1E+04	7,1E+04	1,4E+05	5,6E+06	2,7E+07	4,3E+05
28,0	0,025	3,19E+07	4,10E+06	9,0E+06	1,4E+06	2,5E+06	3,1E+05	4,6E+05	5,4E+05	1,0E+06	0,0E+00	3,1E+05	0,0E+00	1,5E+05	1,5E+05	4,6E+05	0,0E+00	0,0E+00	0,0E+00	0,0E+00	3,1E+05	7,7E+04	0,0E+00	7,7E+04	0,0E+00	4,8E+06	2,8E+07	4,6E+05
29,0	0,02	2,68E+07	2,10E+06	7,4E+06	6,8E+05	1,2E+06	1,9E+05	8,0E+05	4,3E+05	6,8E+05	6,2E+04	9,3E+05	1,9E+05	0,0E+00	1,2E+05	2,5E+05	0,0E+00	0,0E+00	0,0E+00	0,0E+00	1,2E+05	6,2E+04	0,0E+00	0,0E+00	0,0E+00	3,4E+06	2,4E+07	1,9E+05
30,0	0,021	2,63E+07	4,74E+06	6,8E+06	7,7E+05	1,1E+06	3,8E+05	6,4E+05	7,0E+05	2,6E+05	2,6E+05	2,6E+05	6,4E+04	6,4E+04	2,6E+05	4,5E+05	0,0E+00	0,0E+00	0,0E+00	0,0E+00	6,4E+04	0,0E+00	0,0E+00	0,0E+00	0,0E+00	2,9E+06	2,4E+07	6,4E+04
31,0	0,024	3,25E+07	3,34E+06	8,7E+06	1,0E+06	7,4E+05	3,0E+05	6,7E+05	1,2E+06	7,4E+05	0,0E+00	5,2E+05	1,5E+05	0,0E+00	5,2E+05	3,0E+05	0,0E+00	0,0E+00	0,0E+00	0,0E+00	7,4E+04	0,0E+00	0,0E+00	0,0E+00	0,0E+00	3,3E+06	2,9E+07	7,4E+04
32,0	0,025	3,38E+07	3,94E+06	9,8E+06	1,1E+06	6,3E+05	5,5E+05	5,5E+05	1,7E+06	1,2E+06	7,9E+04	2,4E+05	7,9E+04	7,9E+04	3,9E+05	3,9E+05	0,0E+00	0,0E+00	0,0E+00	0,0E+00	2,4E+05	0,0E+00	0,0E+00	0,0E+00	0,0E+00	2,8E+06	3,0E+07	2,4E+05
33,0	0,022	2,95E+07	2,46E+06	6,8E+06	1,3E+06	8,0E+05	4,7E+05	7,3E+05	4,7E+05	4,7E+05	0,0E+00	6,0E+05	4,0E+05	0,0E+00	1,3E+05	4,0E+05	0,0E+00	0,0E+00	0,0E+00	0,0E+00	6,7E+04	0,0E+00	0,0E+00	6,7E+04	0,0E+00	3,6E+06	2,7E+07	1,3E+05
34,0	0,026	3,54E+07	3,56E+06	8,4E+06	1,3E+06	6,3E+05	4,0E+05	8,7E+05	3,2E+05	6,3E+05	2,4E+05	4,7E+05	2,4E+05	7,9E+04	2,4E+05	5,5E+05	0,0E+00	0,0E+00	0,0E+00	0,0E+00	1,6E+05	0,0E+00	0,0E+00	0,0E+00	0,0E+00	3,4E+06	3,2E+07	1,6E+05
35,0	0,026	3,38E+07	2,10E+06	5,5E+06	1,2E+06	1,2E+06	3,7E+05	9,0E+05	3,7E+05	7,5E+05	0,0E+00	7,5E+05	2,2E+05	0,0E+00	2,2E+05	3,7E+05	0,0E+00	0,0E+00	0,0E+00	0,0E+00	2,2E+05	0,0E+00	7,5E+04	0,0E+00	0,0E+00	4,0E+06	3,0E+07	3,0E+05
36,0	0,025	3,59E+07	2,07E+06	1,1E+07	1,1E+06	1,2E+06	6,4E+05	9,6E+05	4,0E+05	1,0E+06	4,0E+05	8,8E+05	8,0E+04	8,0E+04	1,6E+05	3,2E+05	0,0E+00	0,0E+00	0,0E+00	0,0E+00	2,4E+05	0,0E+00	0,0E+00	0,0E+00	0,0E+00	3,7E+06	3,2E+07	2,4E+05
37,0	0,025	3,28E+07	3,30E+06	8,44E+06	1,99E+06	1,30E+06	4,60E+05	9,97E+05	4,60E+05	9,21E+05	0,00E+00	3,07E+05	1,53E+05	0,00E+00	1,53E+05	6,90E+05	0,00E+00	0,00E+00	0,00E+00	0,00E+00	7,67E+04	0,00E+00	0,00E+00	0,00E+00	0,00E+00	4,6E+06	2,9E+07	7,7E+04
38,0	0,026	3,19E+07	2,79E+06	7,36E+06	4,19E+06	1,63E+06	3,10E+05	1,09E+06	1,55E+05	3,88E+05	0,00E+00	2,33E+05	1,55E+05	0,00E+00	2,33E+05	6,20E+05	0,00E+00	0,00E+00	0,00E+00	0,00E+00	0,00E+00	0,00E+00	0,00E+00	0,00E+00	0,00E+00	7,1E+06	2,8E+07	0,0E+00
39,5	0,024	3,13E+07	2,99E+06	6,63E+06	2,21E+06	1,07E+06	3,57E+05	4,99E+05	3,57E+05	1,43E+05	0,00E+00	4,28E+05	2,85E+05	0,00E+00	2,14E+05	3,57E+05	0,00E+00	0,00E+00	0,00E+00	0,00E+00	1,43E+05	0,00E+00	0,00E+00	0,00E+00	0,00E+00	4,6E+06	2,8E+07	1,4E+05
42,0	0,028	3,54E+07	5,95E+06	1,31E+07	2,25E+06	3,07E+06	3,61E+05	9,02E+05	5,41E+05	0,00E+00	0,00E+00	5,41E+05	4,51E+05	9,02E+04	2,71E+05	3,61E+05	0,00E+00	0,00E+00	0,00E+00	0,00E+00	2,71E+05	0,00E+00	0,00E+00	0,00E+00	0,00E+00	6,9E+06	3,2E+07	2,7E+05
43,0	0,025	3,12E+07	5,85E+06	9,66E+06	2,10E+06	1,79E+06	3,12E+05	8,57E+05	3,12E+05	0,00E+00	0,00E+00	3,90E+05	1,56E+05	0,00E+00	2,34E+05	4,68E+05	0,00E+00	0,00E+00	0,00E+00	0,00E+00	7,79E+04	0,00E+00	0,00E+00	0,00E+00	0,00E+00	5,1E+06	2,8E+07	7,8E+04
44,0	0,026	3,44E+07	4,80E+06	1,02E+07	1,63E+06	1,14E+06	3,25E+05	4,88E+05	6,51E+05	0,00E+00	0,00E+00	3,25E+05	1,06E+06	0,00E+00	3,25E+05	4,07E+05	0,00E+00	0,00E+00	0,00E+00	0,00E+00	8,13E+04	1,63E+05	0,00E+00	0,00E+00	0,00E+00	4,9E+06	3,1E+07	2,4E+05
45,0	0,023	3,04E+07	2,81E+06	7,71E+06	1,61E+06	9,12E+05	2,81E+05	7,01E+05	1,19E+06	1,40E+05	0,00E+00	5,61E+05	2,81E+05	0,00E+00	2,81E+05	2,81E+05	0,00E+00	0,00E+00	0,00E+00	0,00E+00	7,01E+04	0,00E+00	0,00E+00	0,00E+00	7,01E+04	3,9E+06	2,7E+07	7,0E+04
46,0	0,025	2,88E+07	2,60E+06	5,71E+06	1,52E+06	1,23E+06	2,17E+05	1,59E+06	2,24E+06	2,89E+05	2,17E+05	4,34E+05	5,06E+05	7,23E+04	3,62E+05	2,89E+05	0,00E+00	0,00E+00	0,00E+00	0,00E+00	7,23E+04	7,23E+04	0,00E+00	0,00E+00	0,00E+00	4,3E+06	2,6E+07	1,4E+05
47,0	0,024	3,05E+07	2,61E+06	8,96E+06	1,49E+06	2,17E+06	4,48E+05	1,34E+06	1,49E+06	1,49E+05	0,00E+00	2,24E+05	8,22E+05	7,47E+04	2,99E+05	3,74E+05	0,00E+00	0,00E+00	0,00E+00	0,00E+00	7,47E+04	0,00E+00	0,00E+00	0,00E+00	7,47E+04	5,4E+06	2,7E+07	7,5E+04
48,0	0,028	3,59E+07	2,91E+06	9,42E+06	1,54E+06	1,80E+06	6,00E+05	1,71E+06	2,14E+06	0,00E+00	8,57E+04	2,57E+05	6,85E+05	0,00E+00	3,43E+05	4,28E+05	0,00E+00	0,00E+00	0,00E+00	0,00E+00	0,00E+00	0,00E+00	0,00E+00	0,00E+00	0,00E+00	5,1E+06	3,2E+07	0,0E+00
49,0	0,024	3,05E+07	2,57E+06	9,52E+06	1,81E+06	1,59E+06	5,29E+05	1,21E+06	2,19E+06	0,00E+00	1,51E+05	7,55E+05	5,29E+05	0,00E+00	3,78E+05	3,02E+05	0,00E+00	0,00E+00	0,00E+00	0,00E+00	7,55E+04	7,55E+04	0,00E+00	0,00E+00	7,55E+04	5,4E+06	2,7E+07	1,5E+05
60,0	0,025	3,56E+07	2,87E+06	1,08E+07	1,68E+06	1,04E+06	4,79E+05	1,12E+06	7,98E+05	1,60E+05	7,98E+04	2,39E+05	3,19E+05	1,60E+05	1,60E+05	5,58E+05	0,00E+00	0,00E+00	0,00E+00	0,00E+00	2,39E+05	0,00E+00	0,00E+00	0,00E+00	0,00E+00	4,0E+06	3,2E+07	2,4E+05
70,0	0,026	3,54E+07	2,16E+06	1,17E+07	3,41E+06	1,66E+06	4,16E+05	5,83E+05	1,08E+06	0,00E+00	0,00E+00	4,16E+05	7,49E+05	8,32E+04	1,66E+05	4,99E+05	0,00E+00	0,00E+00	0,00E+00	0,00E+00	8,32E+04	2,50E+05	0,00E+00	0,00E+00	0,00E+00	6,9E+06	3,2E+07	3,3E+05
80,0	0,028	3,74E+07	1,79E+06	8,60E+06	2,47E+06	1,62E+06	5,96E+05	1,11E+06	1,36E+06	2,55E+05	0,00E+00	3,40E+05	5,11E+05	8,51E+04	4,26E+05	5,11E+05	0,00E+00	0,00E+00	0,00E+00	0,00E+00	8,51E+04	1,70E+05	0,00E+00	0,00E+00	0,00E+00	5,9E+06	3,4E+07	2,6E+05
85,0	0,029	3,71E+07	4,53E+06	1,11E+07	1,63E+06	9,96E+05	3,62E+05	1,81E+06	2,08E+06	0,00E+00	2,72E+05	1,81E+05	8,15E+05	1,81E+05	4,53E+05	5,43E+05	0,00E+00	0,00E+00	0,00E+00	0,00E+00	9,06E+04	0,00E+00	0,00E+00	0,00E+00	0,00E+00	4,6E+06	3,3E+07	9,1E+04
86,0	0,025	2,93E+07	5,00E+06	8,10E+06	1,44E+06	1,67E+06	3,03E+05	9,85E+05	1,67E+06	2,27E+05	0,00E+00	3,03E+05	6,82E+05	0,00E+00	1,51E+05	4,54E+05	0,00E+00	0,00E+00	0,00E+00	0,00E+00	7,57E+04	0,00E+00	0,00E+00	0,00E+00	0,00E+00	4,7E+06	2,6E+07	7,6E+04
87,0	0,027	3,28E+07	6,91E+06	9,66E+06	1,33E+06	9,99E+05	4,16E+05	1,67E+06	7,49E+05	8,33E+04	0,00E+00	1,67E+05	5,00E+05	2,50E+05	3,33E+05	4,16E+05	0,00E+00	0,00E+00	0,00E+00	0,00E+00	8,33E+04	0,00E+00	0,00E+00	0,00E+00	0,00E+00	3,7E+06	2,9E+07	8,3E+04

3.4 SEDIMENTARY RATE, TOC AND OXYGEN ISOTOPE

Sedimentation rates for all sapropels show that sapropel S3 has the lowest sedimentation rate, at 1.36 cm/kyrs. Sapropel S5 has the highest sedimentation rate of 3.21 cm/kyrs. Sapropel S4 has two different sedimentation rates due to the tephra layer found during the sapropel. Sapropel S6 has a sedimentation rate of 2.69 cm/kyr (de Groot, 2017).

	Duration (kyrs)	Thickness	Sedimentation rate (cm/kyr)
Sapropel S1	5.1	11	2.16
Sapropel S3	6.6	9	1.36
Sapropel S4 (post-tephra layer)	4.4	10	2.27
Sapropel S4 (pre-tephra layer)	3.8	1	0.26
Sapropel S5	8.1	26	3.21
Sapropel S6	13	35	2.69

***Figure 3.10**: Sedimentation rates from Sapropel S1 to Sapropel S6 (de Groot, 2017)*

Sapropels in the Mediterranean Sea are known to contain elevated carbon concentrations, much higher than the surrounding sediment (Emeis *et al.*, 1998; Rohling *et al.,* 2015). Two different methods were used by de Groot (2017) to measure Total Organic Carbon (TOC) content in the sediment samples. The sediment samples for sapropel S1, S3, S4 and S5 were analysed with Leco first, and after evaluating at the results and finding inconsistencies, new samples were analysed by decalcifying them and using the Fisons NA1500 NCS Elemental Analyser to measure TOC content (de Groot, 2017).

The Total Organic Carbon (TOC, % weight) was measured for samples encompassing sapropel S1, S3, S4, S5 and S6, and its surrounding sediment (**Fig. 3.11**). All tested sediment shows enriched TOC during sapropels and range from 1.2% in sapropel S3, and 3.4% in sapropel S5. All TOC percentages before and after sapropels are above 0.12%, and below 1.2% (de Groot, 2017).

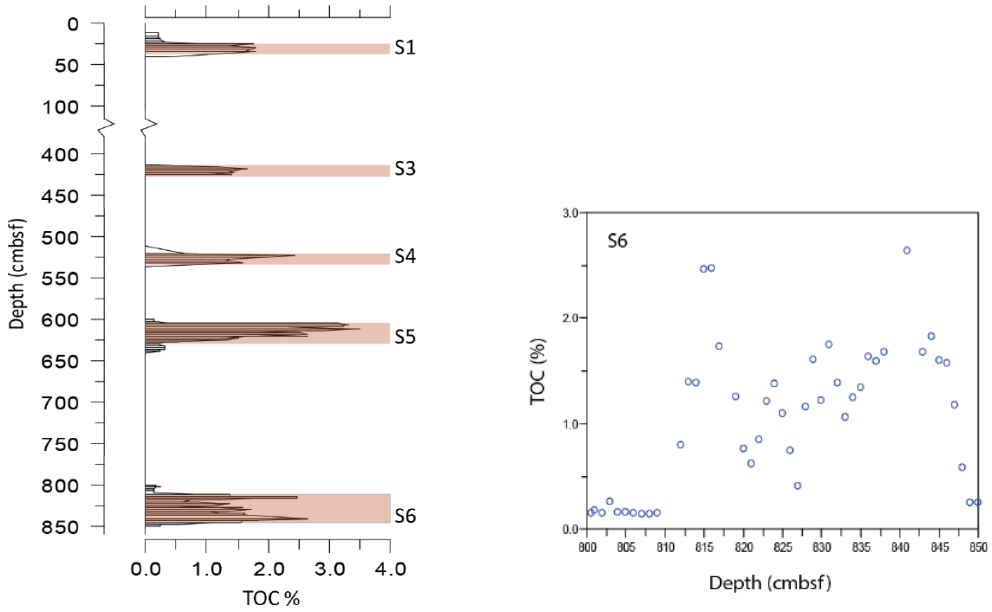

***Figure 3.11**: Total Organic Carbon content of all sapropel from the core M25/4-12 and TOC percentages from S6 (de Groot, 2017)*

Oxygen isotope measurements (**Fig. 3.12**) were carried out by Grant *et al*., (2019 pers comm). The analyses were performed on specimens of *Globigerinoides ruber* surface planktonic species which thrives during the late summer and fall (Negri et al., 1999) and *Neogloboquadrina pachyderma* a deep-sea species that dominates assemblages in transitional to polar water masses and occurs in low frequencies in warm subtropical and tropical environments (Ehrenberg, 1861).

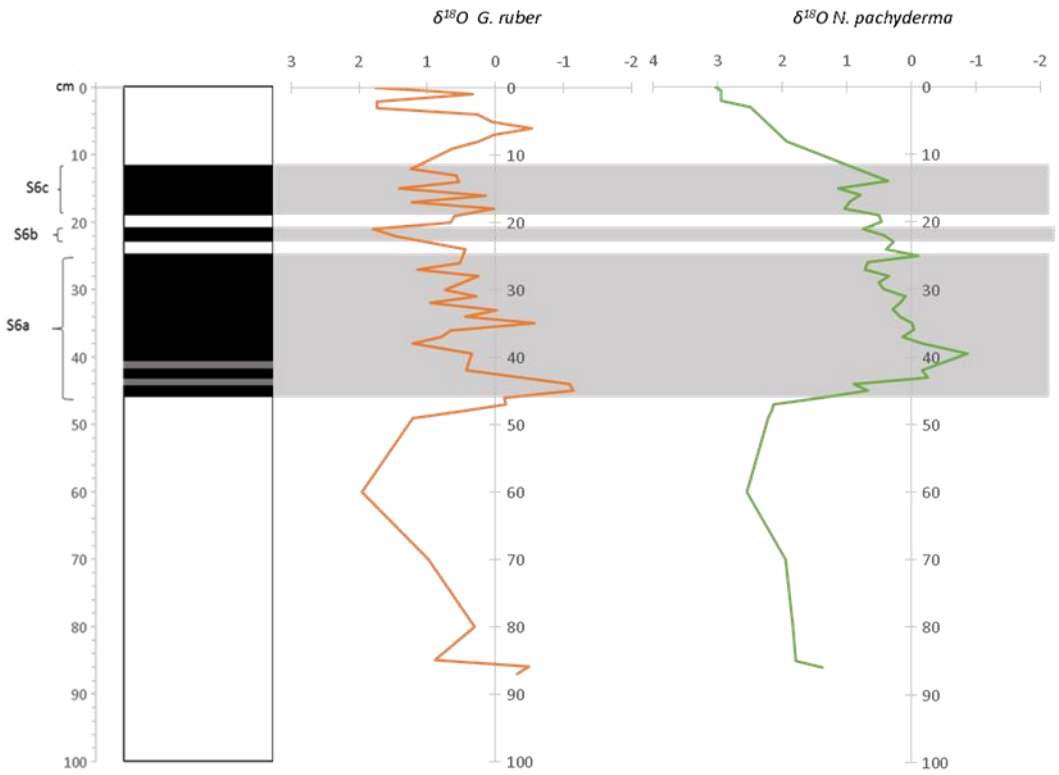

***Figure 3.12**: Stable Oxygen isotope curve based on G. ruber and N. pachyderma*

Chapter Four

RESULTS

In this part of the study, the results of the calcareous nannofossil absolute abundance analyses will be described. Here, the number of nannoliths per gram of sediment and the frequencies (%) for each species analysed is reported.

As for absolute abundance, the processing of the 4-7 cm 9-13 cm intervals was hampered by the problems encountered during the sample preparation, as discussed in the chapter "Materials and methods".

Total abundance

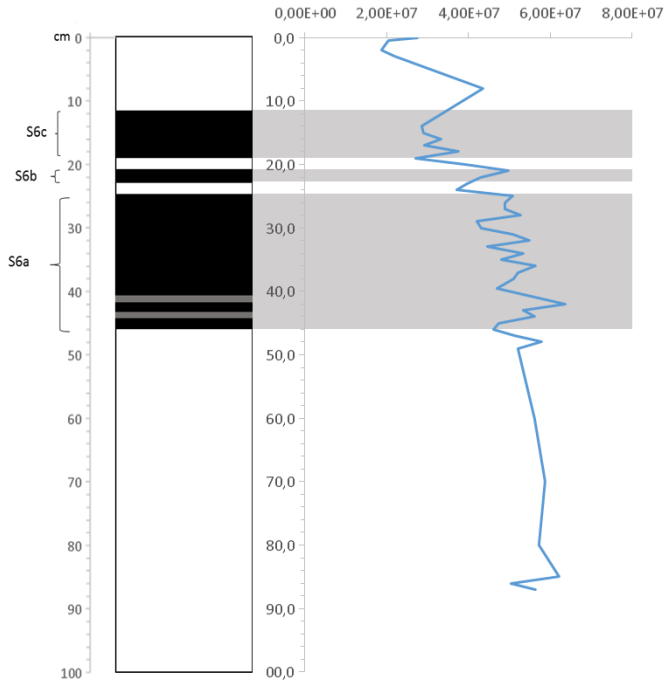

The absolute abundance of coccoliths shows constant values from the base of the sapropel to the first interruption. After the second interruption, the trend is increasing and then drastically decreasing immediately after the top of the sapropel. The general trend is decreasing toward the top of the core. The higher values are reached at 42 cm (6,36E+0,7).

Gephyrocapsa small

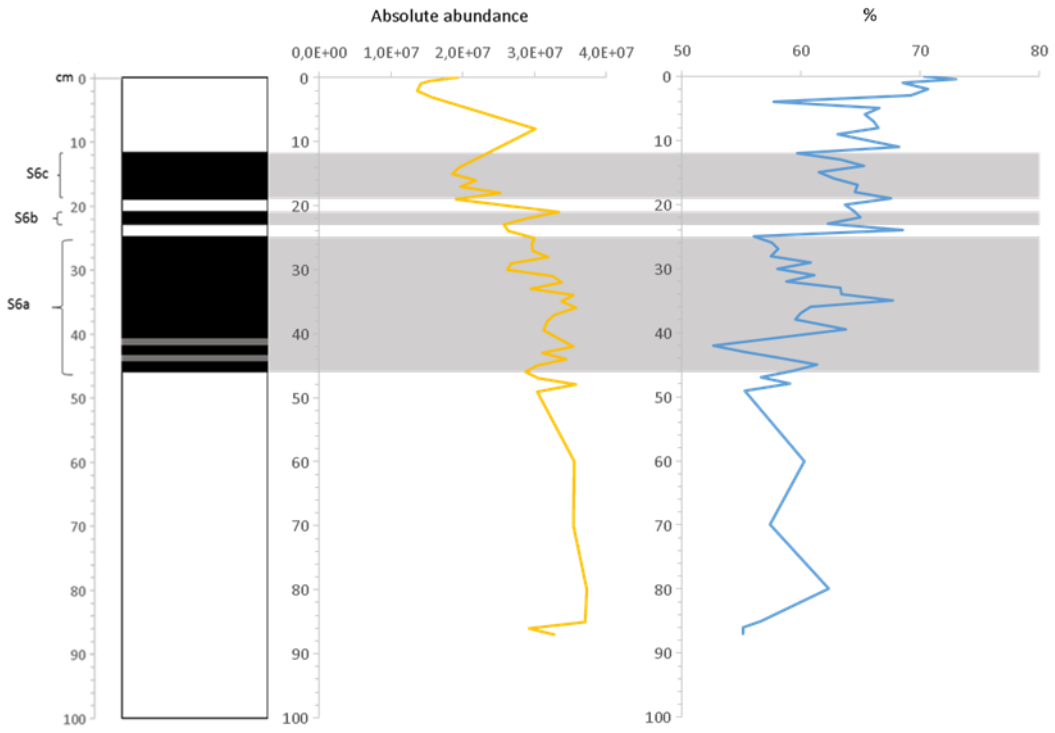

Absolute abundance: This species is the most abundant throughout all the samples, in fact it shows always high and constant values. However, a generally decreasing trend can be observed from the base to the top with minor positive peaks at 20 and 8 cm. The abundance in the S6a is generally higher than in S6c. Indeed, S6c shows a sharp decrease of *G. small.*

Percentages: A fluctuating increasing trend, contrary to absolute abundance graph, characterizes the frequency abundance of this species. Percentages are lower in the pre-sapropel and S6a while is observed an increase toward the top (inversely to what observed in the absolute abundances) the higher value

are reached at 35 and 24cm (67% and 68%) whereas the minimum at 42 cm (52%).

Helicosphaera carteri

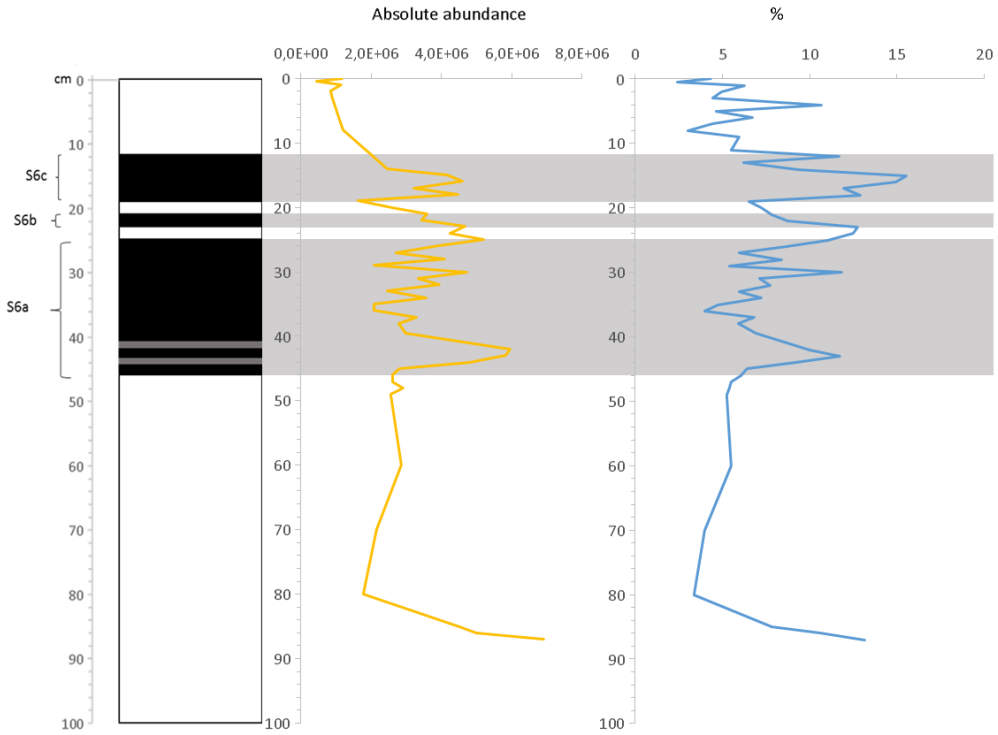

Absolute abundance: We can observe a fluctuating pattern of positive peaks alternating with negative peaks in a constant manner. The general trend is decreasing toward the top.

At the base of the sapropel, 46 cm, it has one of the most negative peaks, followed immediately at 43 cm by the peak of maximum abundance.

Other significant peaks are found in correspondence after the bases of the three section of the sapropel (S6a; S6b; S6c).

Percentages: Values oscillate between 5 and 15%. The fluctuating trend is much more marked, but it is consistent with the graph of the absolute abundances, except for the maximum peak at 22 cm which does not seem to occur here. The maximum abundance is 15.6%.

Florisphaera profunda (LPZ)

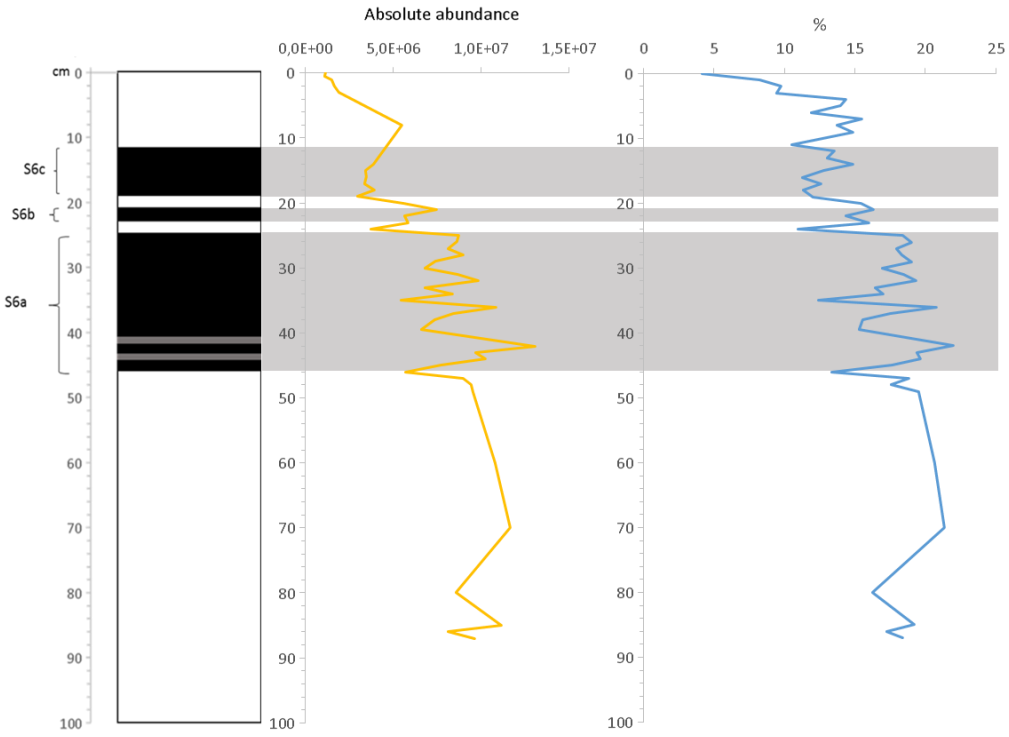

Absolute Abundance: Overall, a decreasing trend form the base to the top, the graph shows a marked fluctuating trend. Negative peaks, the major at the base of the sapropel at 46 cm, are immediately followed by positive peaks. At 42 cm we can observe the maximum abundance, while the negative peaks are observed throughout the two interruptions.

Percentages: The graph of percentages is much less marked than that of the abundances, also in this case a topward decreasing trend is observed. As for the rest it is consistent with the graph of the abundances. The maximum abundance is 22%.

Syracosphaera pulchra

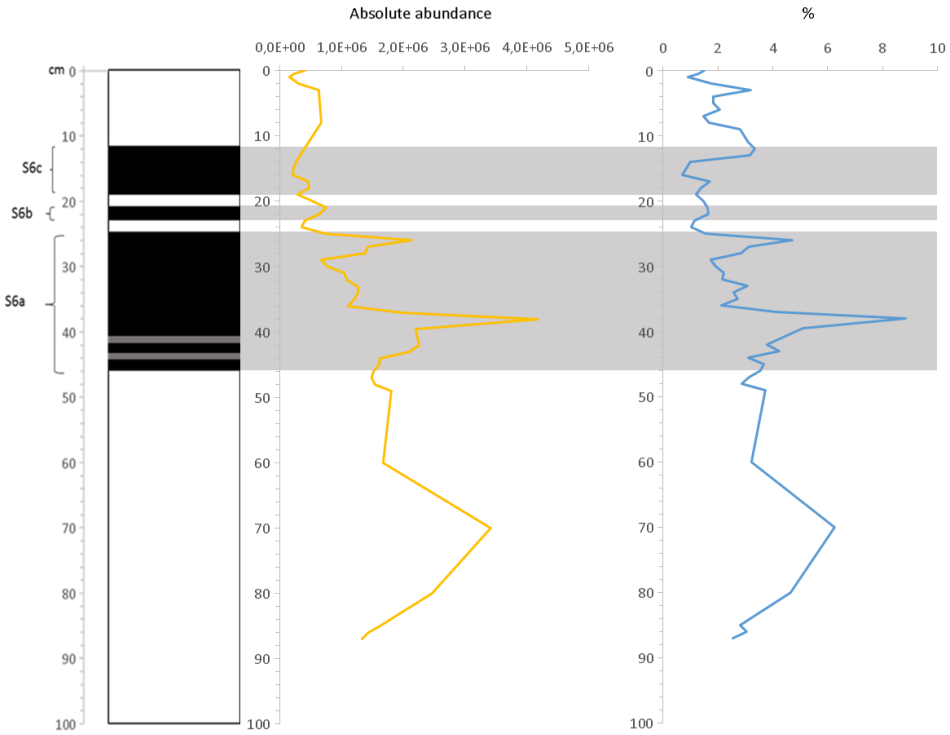

Absolute abundance: The abundance of this species is low throughout the core, and shows a general decreasing trend. A clear abundance peak is observed at 38 cm in S6a. Another important positive peak is found at 26 cm, corresponding with the first interruption.

Percentage: The graph is much more marked than that of the abundances. Although a fluctuating trend an overall decreasing trend can be observed, interrupted by two evident peaks at 43 and 26 cm. Two minor peaks occur at 13 and 4 cm. At the top of the sapropel, in the range 9-13 cm, growth is observed, which is not visible in the abundance graphic due to lack of data. The maximum abundance is 8,9%.

Syracosphaera sp.

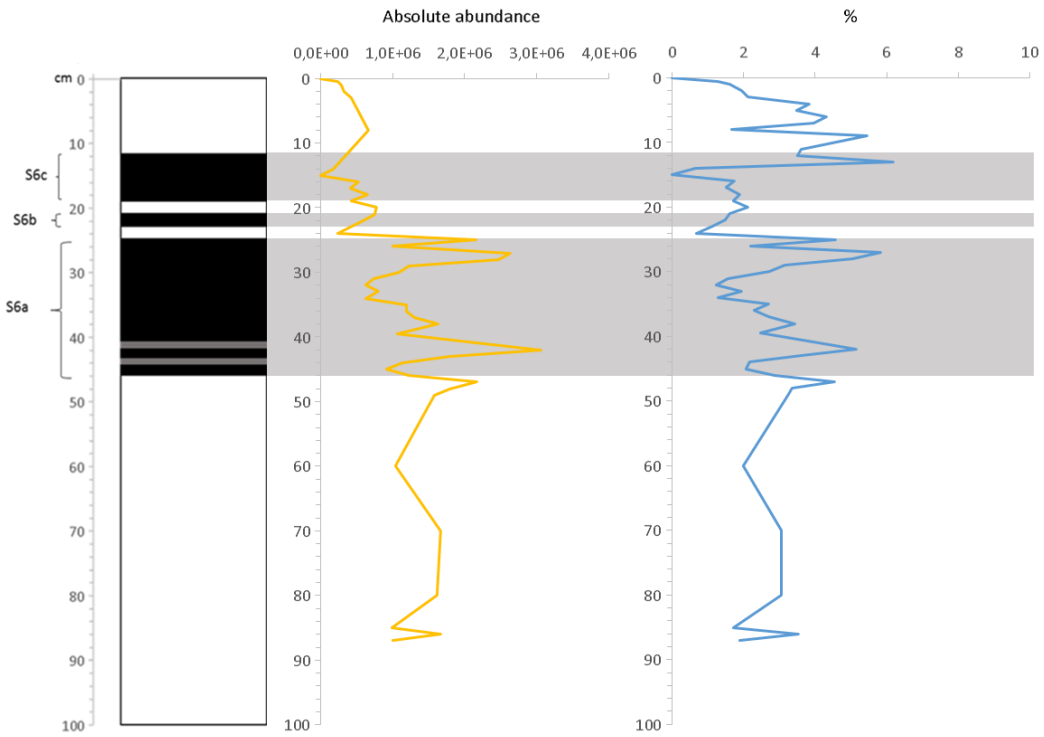

Absolute abundance: The species shows a fluctuating abundance in S6a. The highest peak is observed at 42 cm, while the others at 28 cm and 25 cm, before the first interruption. A general decreasing trend toward the top is shown, after the first interruption.

Percentage: The graph shows the peaks in a much less marked way but is consistent with the graphic of the abundances. We observe in the range 9-13 cm high values which drop drastically up to 0% to 15 cm. The maximum abundance is 6.2%.

Emiliania huxleyi

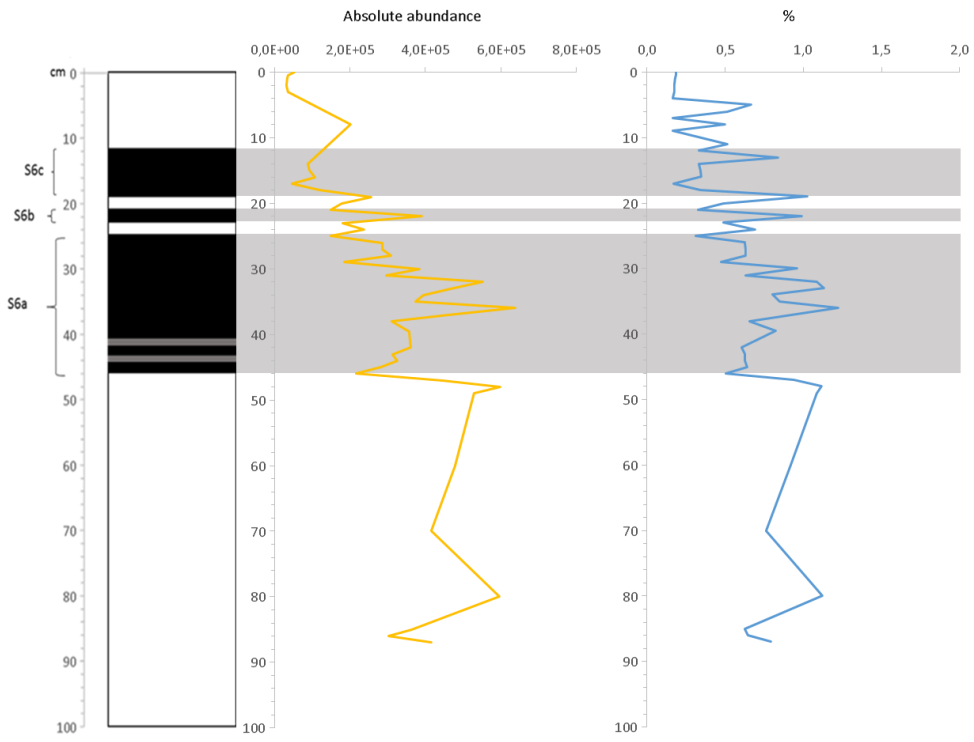

Absolute abundance: The species is very rare, in agreement with the biostratigraphic scheme by Rio *et al*., as this sample fall in the MNN21a zone characterized by rare *E. huxleyi*. The species is oscillating abundant before the sapropels onset, a sharp decrease is observed. The trend observed is clearly pointing to a topward decrease has a negative peak at the base of the sapropel at 46 cm, it remains on quite low values up to 36 cm when the peak of greater abundance of all the core is observed. From here towards the top of the sapropel the abundances are very fluctuating. We observe two other significant positive peaks at 32 and 22 cm. The values of the abundance appear to drop from 16 cm

towards the top of the sapropel, but it is not a certain analysis given the lack of data in the range 9-13 cm.

Percentage: The graph compared to that of the abundances is much less marked in the positive peaks, even if consistent with the previous analysis, exception for the peak to 19 cm much more marked in this graph. From the 16 cm we see a remarkable growth that culminates with a peak to 13 cm, in contrast with what was noted from the graph of the abundances, but this difference is to be attributed to the lack of data. The maximum abundance is 1.2%.

Coccolithus pelagicus

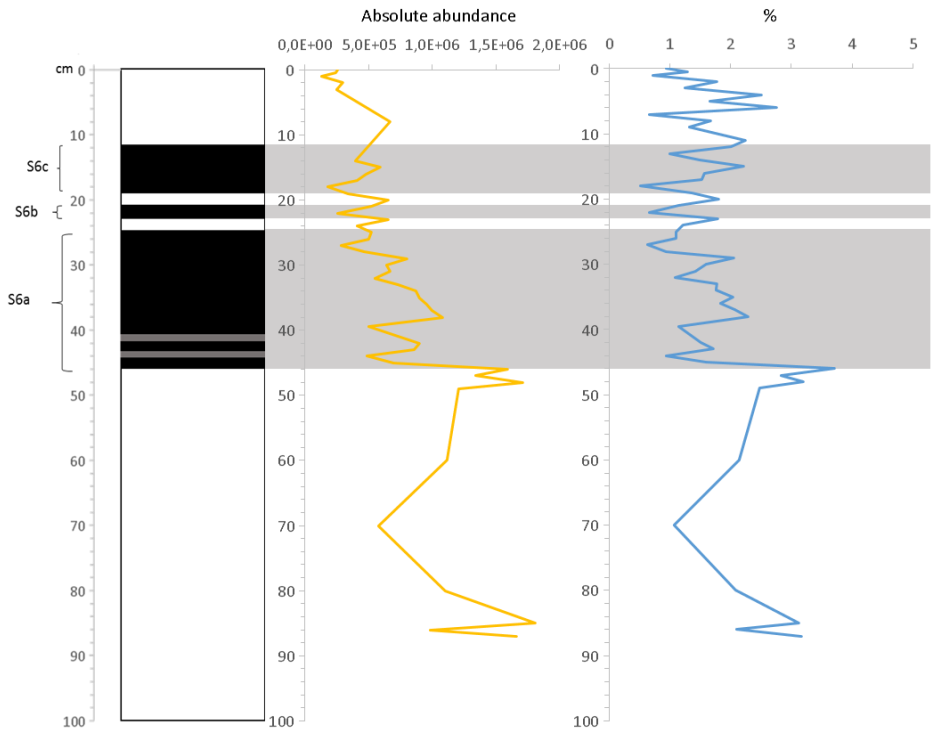

Absolute Abundance: The graph shows at the base of the sapropel the highest positive peak followed immediately by a decreasing trend toward the top. It decreases during the first interruption, then, a slight increasing toward the S6c is observed. However, the general trend shows decrease toward the top of the core.

Percentages: The percentages are consistent with the abundance. The peaks and fluctuations are more marked. The positive peaks at the base is validated and also the decreasing trend. The maximum abundance is 3.7%.

Calcidiscus leptoporus

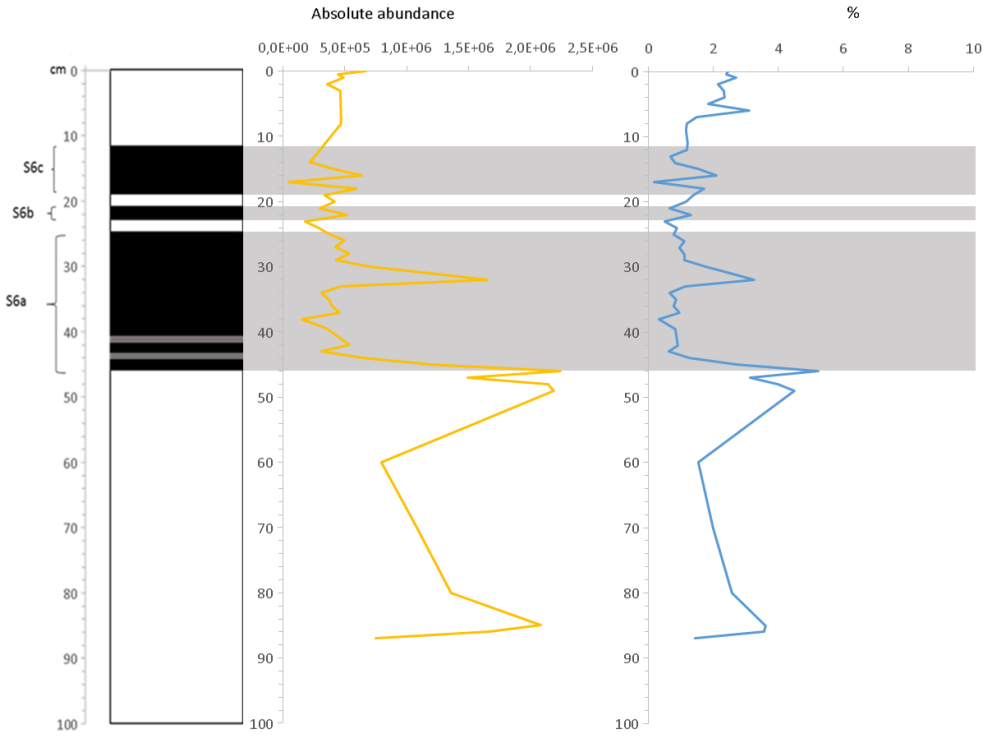

Absolute abundance: This species shows an increase in the pre-sapropel section, then it decreases in S6a, reaching a minimum at 46 cm. At 32 cm a clear positive peak, is observed and then the abundance sharply decreases, at 17 cm is reached the minimum value of 4,6E+04.

Percentages: The peaks in the percentages graph are much less marked than that of the abundances. The values are generally respected, showing a decreasing trend toward the top. The maximum abundance is 5.2%.

Rhabdosphaera clavigera

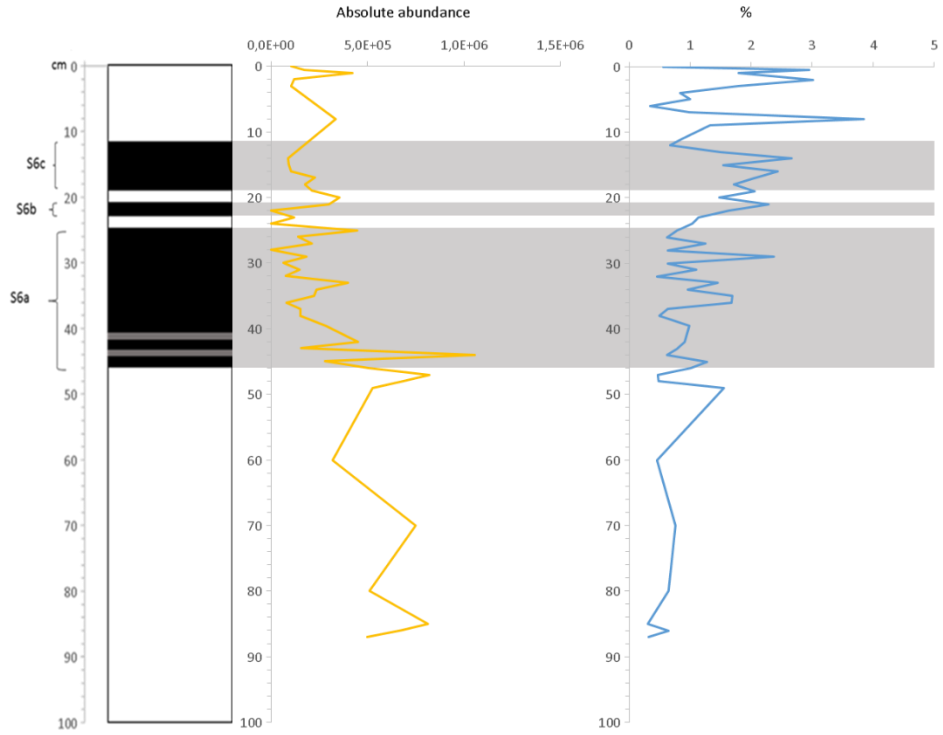

Absolute abundance: The peak of the maximum abundance of this species is at 44 cm, just after the base of the sapropel. Then its values drop, keeping a decreasing trend toward the top.

Percentages: The difference with the graph of the absolute abundances is noted at 44 cm where the peak of maximum abundance is not so marked. It shows an increasing trend toward the top of S6c. The general trend is however decreasing. The maximum abundance is 3.9%.

Rhabdosphaera stilifera

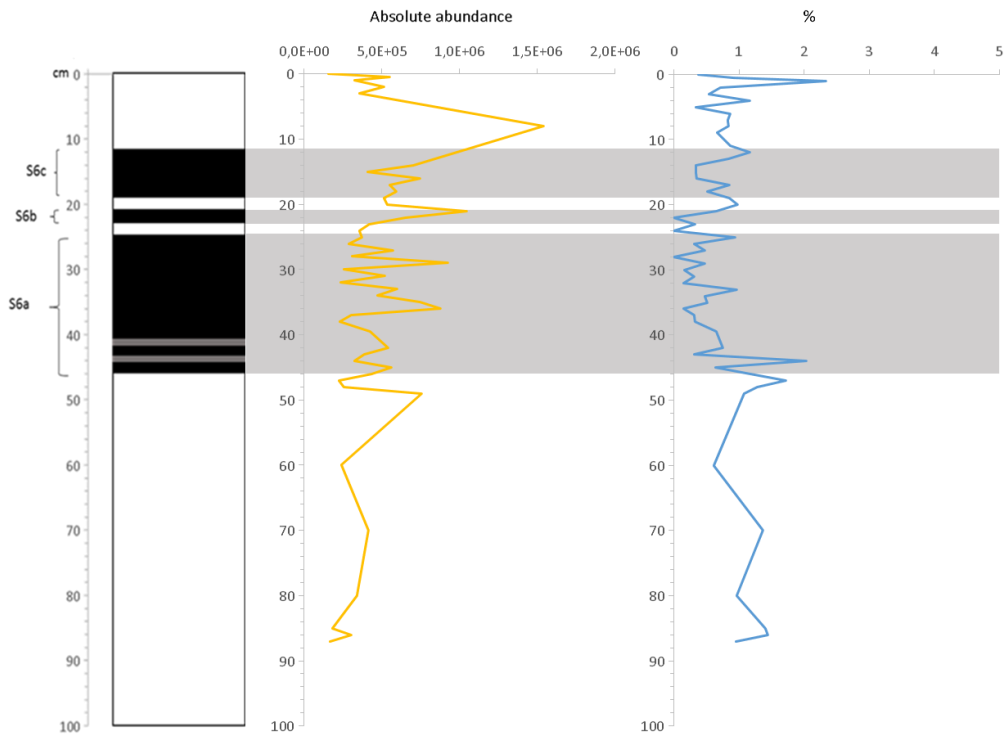

Absolute abundance: This species shows constant values toward the three section of the sapropel. The maximum abundance is observed at 8 cm, then values decrease toward the top.

Percentages: A decreasing trend is observed in S6a, then values increase toward the top of the core. There are no significant peaks of abundance, except for very negative values in S6b. The maximum abundance is 2.3%.

Reticulofenestra small (< 5µm)

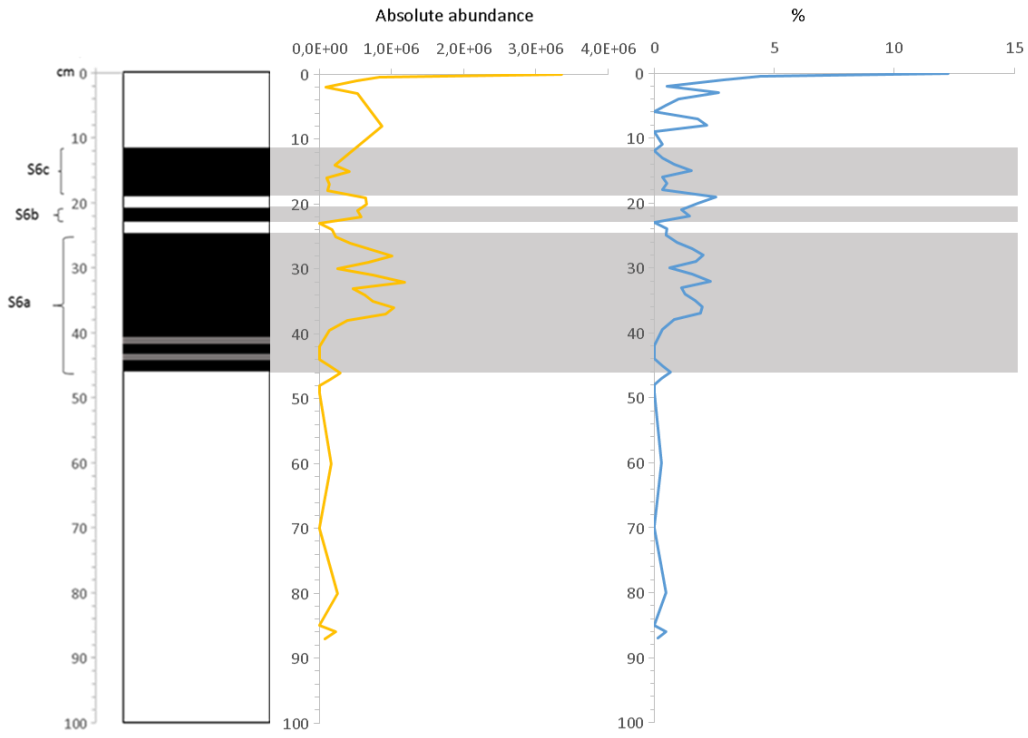

Absolute abundance: This species shows increasing trend towards S6a, the values decrease in S6b and then it shows increasing trend toward the top of the core.

Percentages: The trend of the graph is constant with that of the abundances, slightly less marked in the positive peaks. Maximum abundance is confirmed at the top of the core with much higher values than the rest. The maximum abundance is 12.3%.

Reticulofenestra medium-small (5-7µm)

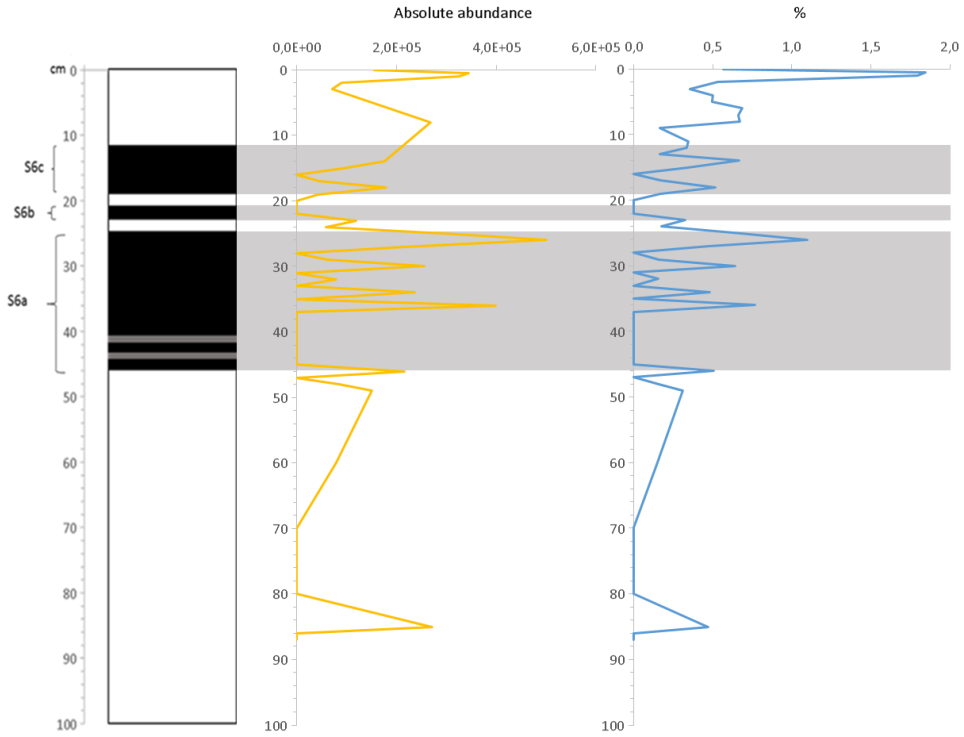

Absolute abundance: Despite the low abundance values of this species, we can observe a fluctuating trend throughout the core, with alternation of very positive peaks and very negative peaks. For most of the S6a portion the species is absent. Then it shows maximum abundance in the first interruption. Also, in the range 22-21 and 13-11 cm the species seems absent. After S6c the trend is increasing.

Percentages: The graph is constant with that of the absolute abundances, the peaks are respected even if in less marked way. In the range 13-9 cm the species shows low values, in contradiction with the diagram of the abundances. The maximum abundance is 1.8%.

Pontosphaera

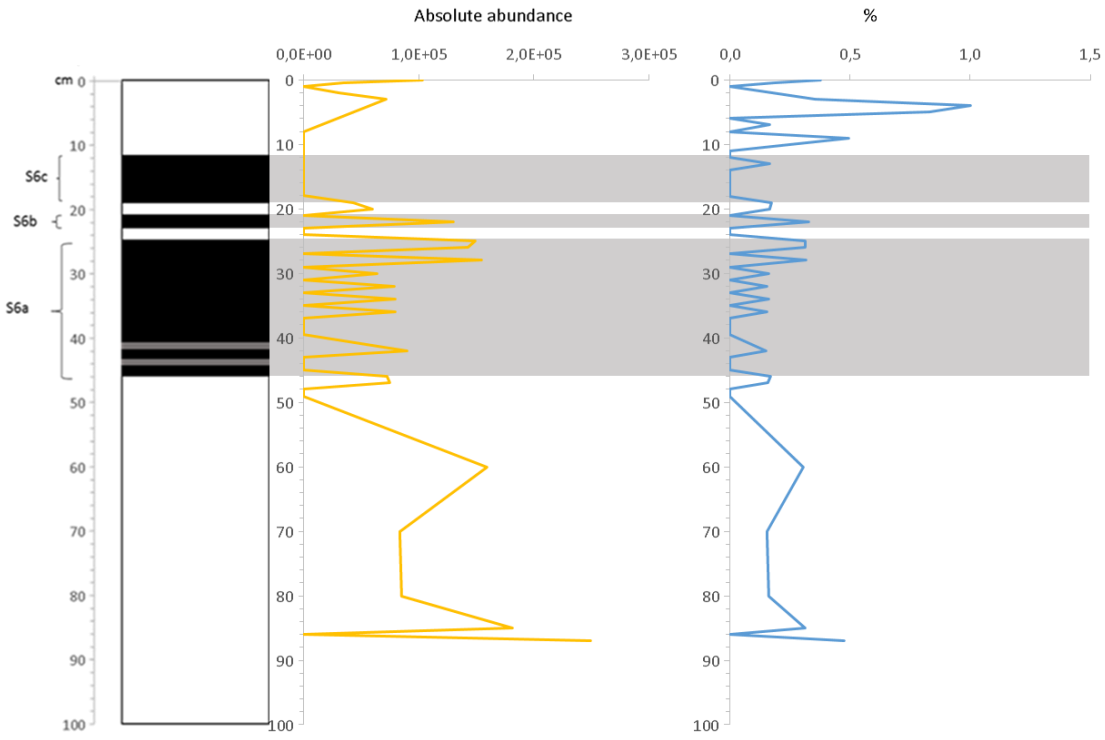

Absolute abundance: This species has very low values. At the base of the S6a it shows an initial positive peak followed by its absence in the range 45-44 cm, and for most of the S6b. This pattern of abundance is constant throughout the core. The peak of maximum abundance is observed at 87 cm outside the range of the sapropel and at 28 cm in S6a.

Percentages: The graph is constant with that of the abundances in the values. Its absences in S6b is confirm. The peak of maximum percentage abundance is described at 4 cm in contradiction with that indicated in the graph of absolute abundance. The maximum abundance is 1%.

Oolitothus fragilis

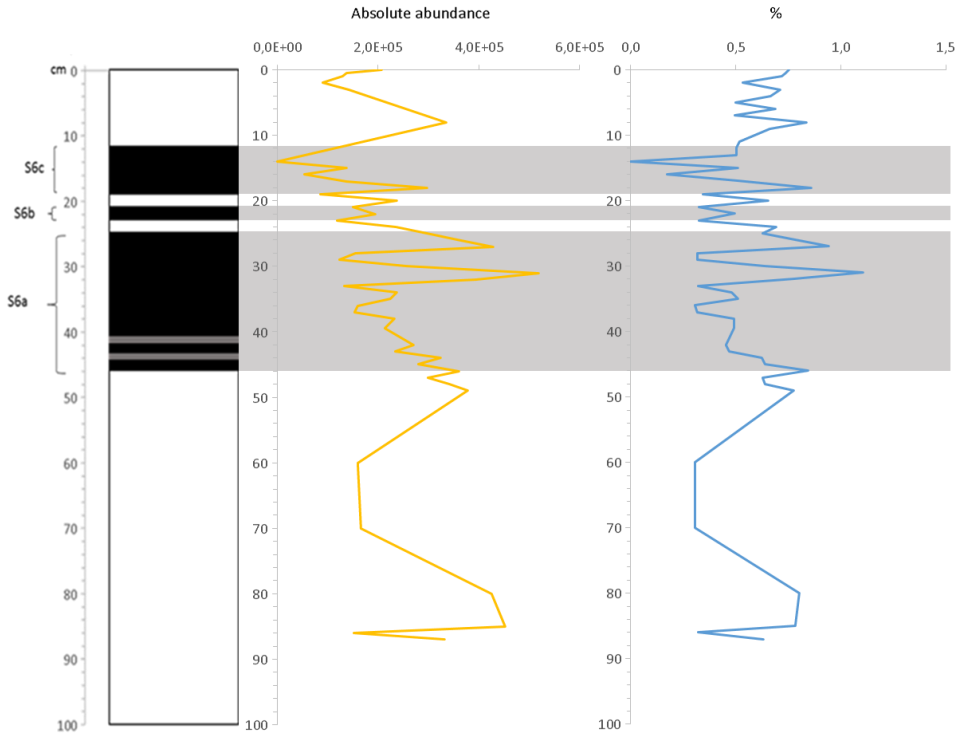

Absolute abundance: The species shows a decreasing trend toward the top. Peaks of greater abundance are observed in the middle part of S6a and at the base of S6c, showing in this section a decreasing trend.

Percentages: The graph shows values in accordance with that of the abundances. The peaks are respected even if the fluctuations are less marked. At 14 cm we can observe the most negative peak. The maximum abundance is 1.1%.

Umbilicosphaera sibogae

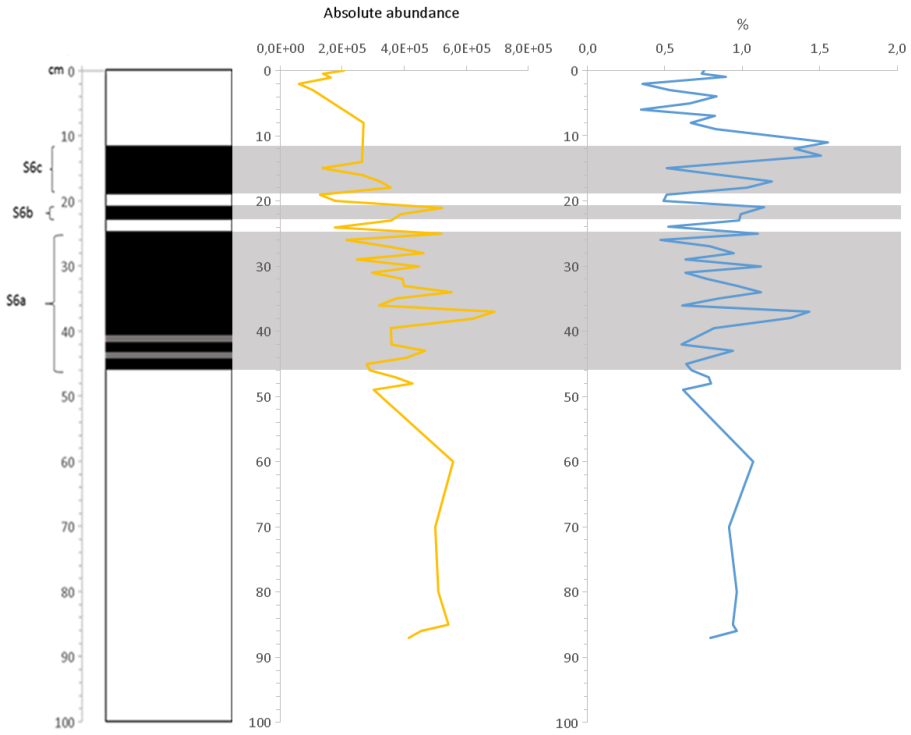

Absolute abundance: The species shows a constant downward trend from the sapropel base to the top. The peak of maximum abundance is observed at 37 cm, while the minimum is 19 cm.

Percentages: The percentage values reflect those of the absolute abundance. The positive trend is marked from 13 to 11 cm. The maximum abundance is 1.6%.

Reworked species

(Pseudoemiliania lacunosa, Ceratolithus, Sphenolithus, Discoaster)

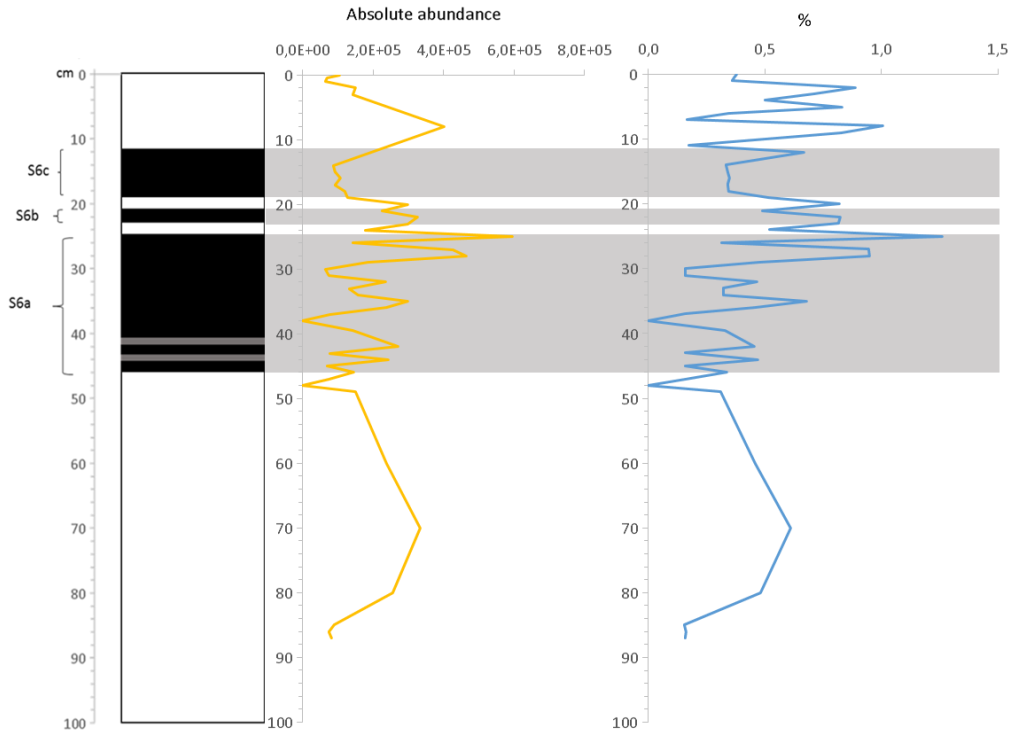

Absolute abundance: The reworked species show relatively low abundance values. They increase toward the top pf S6a, but a decreasing trend is observed. S6c is characterized by low values, that increase to cm 8.

Percentages: The trend of the percentages is the same as the graph of the abundances. After the decrease in S6c, a further positive peak at 8 cm is observed. The maximum abundance is 1.3%.

Upper Photic Zone

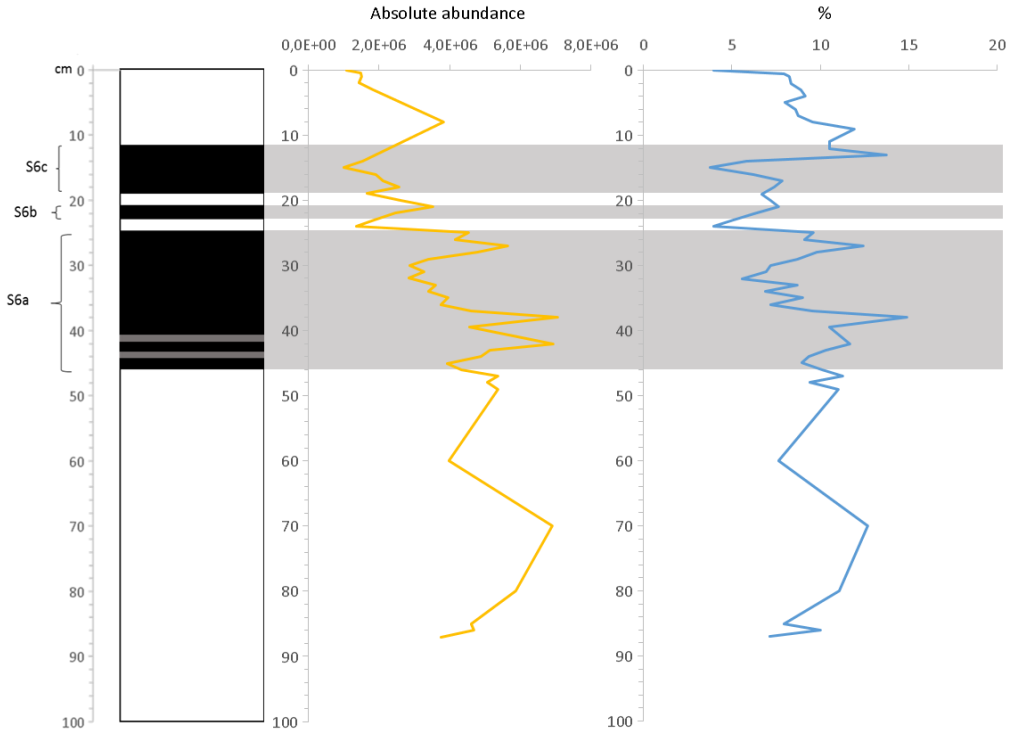

Absolute abundance: The values of the absolute abundance how a generale decreasing trend towards the core. S6b in characterized by an increasing trend, like also S6c. Lowest peaks are observed in the two interruption.

Percentages: The pattern of alternation is also confirmed by the percentages, even if some peaks are less marked. The maximum abundance is 14.9%.

Placoliths

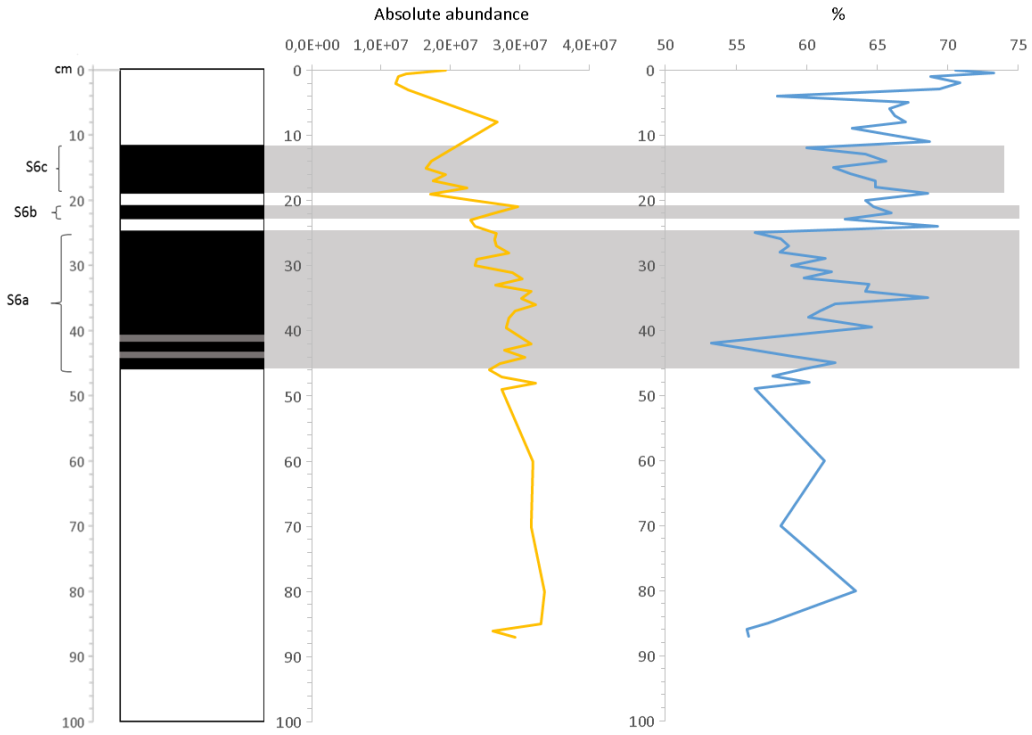

Absolute abundance: It is evident that the values of the abundance are very high and constant in almost all the portion of the sapropel, in particular S6a. The tendency is decreasing towards the top of the core. No significant positive or negative peaks are observed.

Percentage: The graph is much more marked than that of the abundances. In fact, here the peaks are much more evident and significant. The main difference is the increasing trend toward the top of the core. The maximum abundance is 73%.

Chapter Five

DISCUSSION

Sapropel S6 is a well-known glacial sapropel deposited about 180 kyr ago (Cita *et al*., 1982).

The aim of this work is to try to investigate the causes of the deposition of S6 and the paleoclimatic conditions during its formation studying the calcareous nannofossils assemblage and their ecological preferences.

Based on the results of quantitative and qualitative analysis of calcareous nannofossils of the core M25-4/12, 23 species have been identified (including *Pseudoemiliania lacunosa, Ceratolithus, Sphenolithus, Discoaster*, considered as reworked species), thanks also to the use of the database system "nannotax" (http://www.mikrotax.org/Nannotax3/) which it has been consulted for taxonomic identification. Among these 23 species those that have given a relevant signal for the purpose of this work were: *Florisphaera profunda* is the second most abundant species (22%) and indicative of the Lower Photic Zone (Okada and Honjo, 1973; Molfino and McIntyre, 1990; Castradori, 1993; Baumann, 2005; Incarbona *et al.*, 2011); *Helicosphaera carteri* abundant in all the samples and above all it was the best preserved species, indicator of high-productivity water (Cachão & Moita, 2000; Ziveri *et al*. 1995a,b; Baumann, 2005); *Coccolithus pelagicus* used as an indicator of cold temperatures and

high productivity (Cachão, 1991; Castradori, 1993,; Negri & Giunta, 2001; Baumann, 2005; Triantaphyllou *et al.,* 2009). Other species show frequencies below 2%. For convenience, they were grouped following the assemblage of Incarbona (2011): Placoliths (*Gephyrocapsa "small"* and *E. huxleyi*) and UPZ (*Syracosphaera pulchra, Umbellosphaera spp, Discosphaera tubifera, Rhabdosphaera clavigera, Rhabdosphaera stilifera, Oolithotus fragilis, Umbilicosphaera sibogae*). Placoliths signal is driven by *Gephyrocapsa spp. "small",* showing almost constant values across the whole section studied. This species is a cold-water and high productivity indicator (Gartner, 1987), resistant to diagenesis (Castradori, 1993) and dominating the assemblage in a restricted interval between 830 and 1010 cm (Negri *et al.,* 1999). Whereas UPZ are species generally living in the upper photic zone.

Comparing the graphs of Placoliths, UPZ, H. carteri, F. profunda and C. pelagicus it has been possible to identify a pattern of distribution throughout the core. The calcareous nannofossil data were further compared with stable isotope $\delta^{18}O$ (**Fig 5.2**) (Grant, 2019 pers comm, 2019) described below and with the dinoflagellate and pollen data (de Groot, 2017).

The $\delta^{18}O$ records (Grant pers. Comm, 2019) are summarized in **Figure 5.1**. In general, it is evident for both the deep water (*N.pachyderma*) and the superficial water (*G. ruber*) indicators a trend indicating cold conditions before the

sapropel, then a warm peak more evident for the superficial indicators (between 45 and 44 cm) an soon after for the deeper indicator *N. pachyderma* (cm 42-40). After this peak condition toward the top of the S6 sapropel show a cold trend, more. Although the both trends are indicative of a cooling trend, *G. ruber* indicate more evident surface water temperature fluctuations. Other important positive fluctuations values are found inside the S6a portion and just after the second interruption in the S6c and towards the top of the core. As for *N. pachyderma*, the deep-sea species, shows a linear cooling trend towards the top of the core. The *G. ruber* fluctuating trend clearly indicate that the surface water tends to warm up faster than the deep.

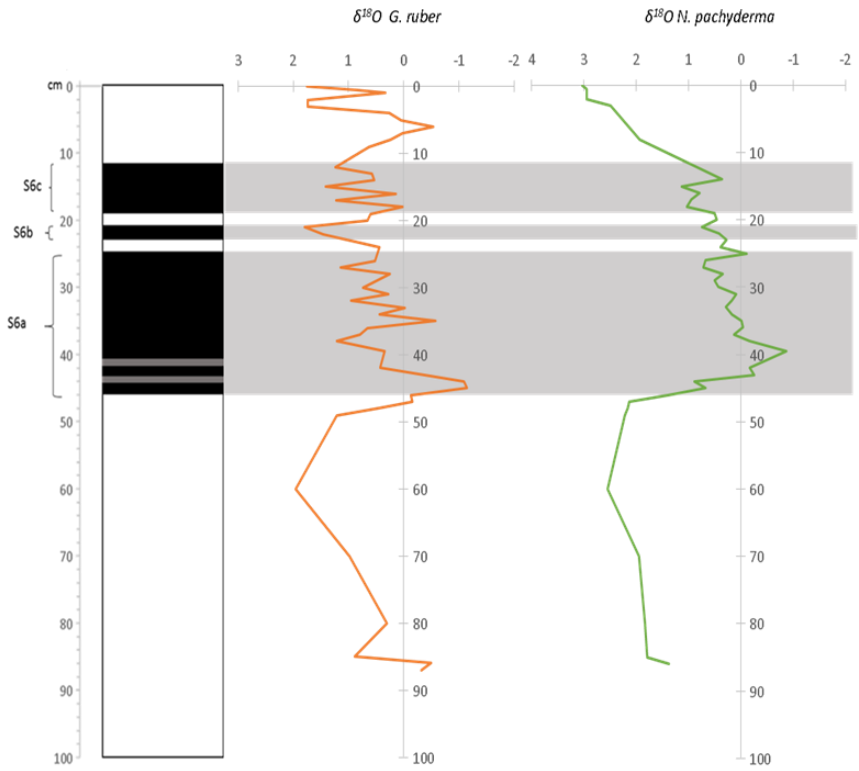

***Figura 5.1**: On the left: Illustration of Sapropel S6 of the core M25/4-12. On the right: oxygen isotope curve based on G. ruber and N. pachyderma*

The first and most important feature observed in the sapropel S6 is the trend shown by the total abundance of calcareous nannofossils assemblage (**Fig. 5.2**) that shows a general decreasing trend toward the top of the section, with evident fluctuation across the three portions of the sapropel S6 (S6a; S6b; S6c). If we observe the single graphs (**Fig 5.3**) of absolute abundance of each species analysed, this decreasing trend is verified.

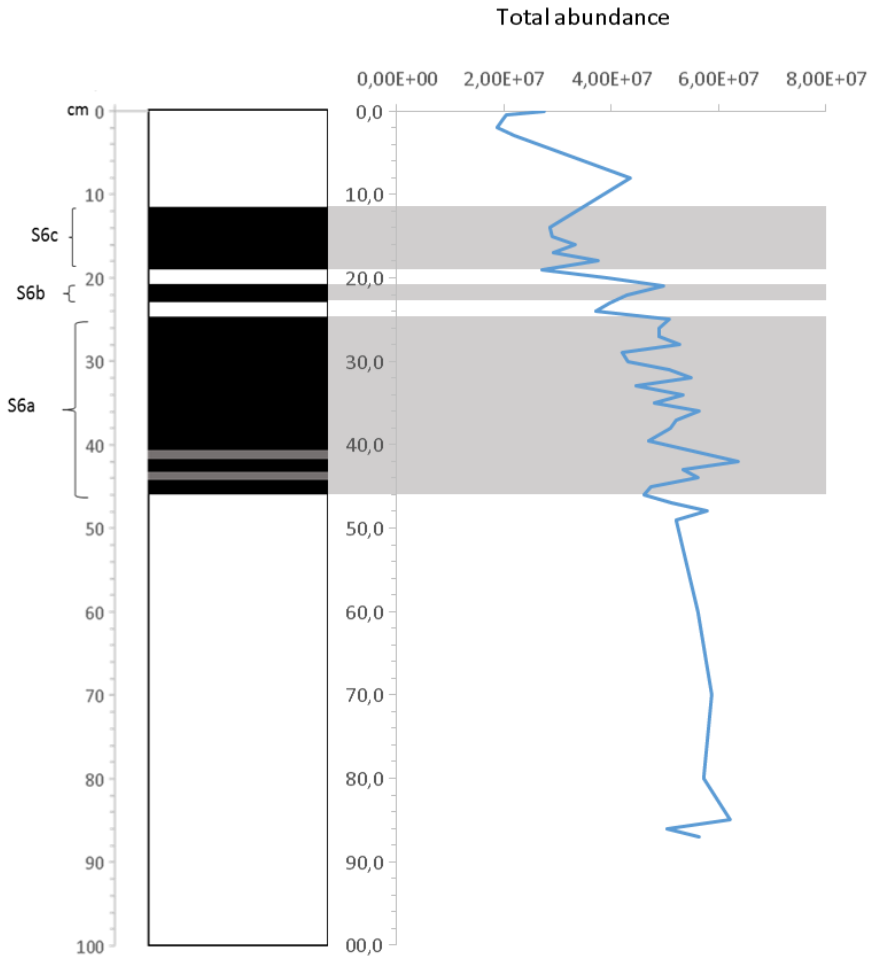

***Figure 5.2**: Total abundance of calcareous nannofossil assemblage*

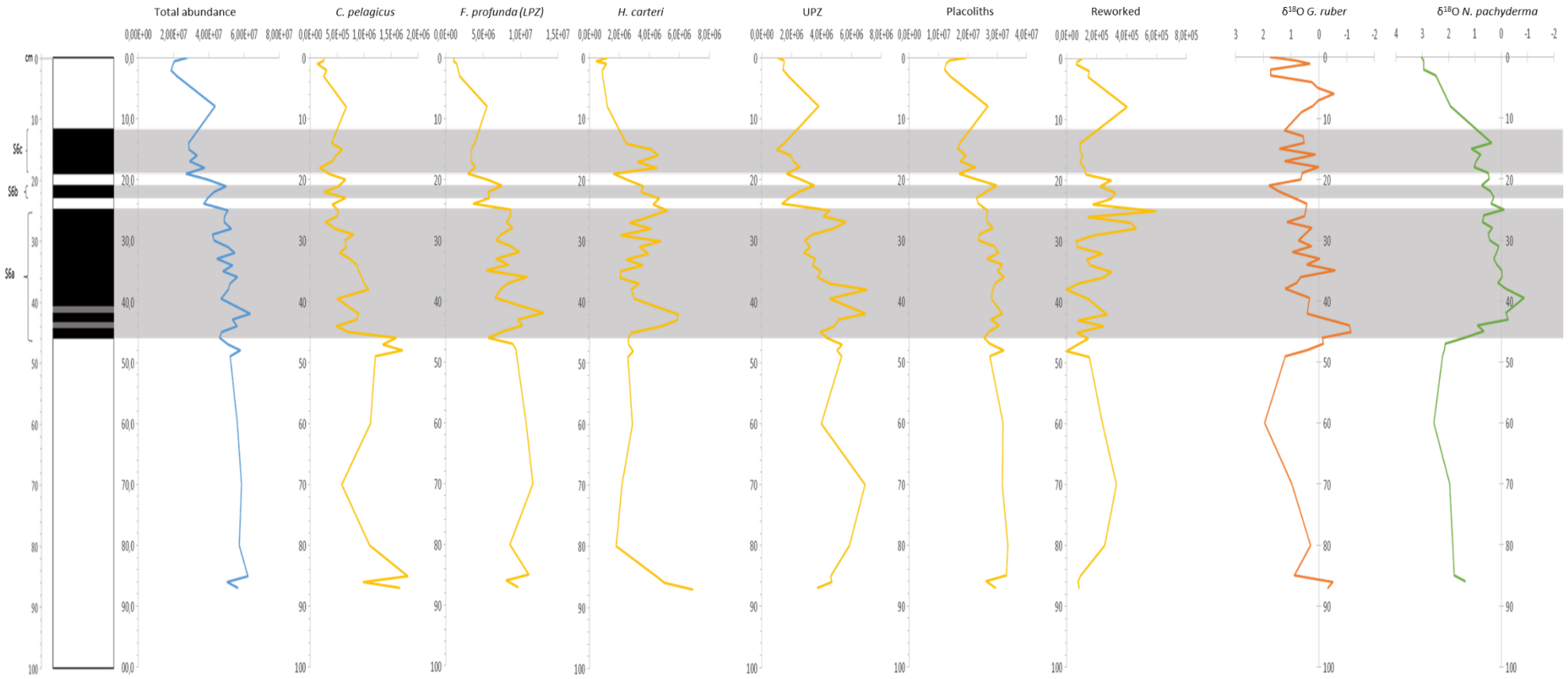

Figure 5.3: *Total abundance and calcareous nannofossils absolute abundances in detail. On the right: oxygen isotope curve*

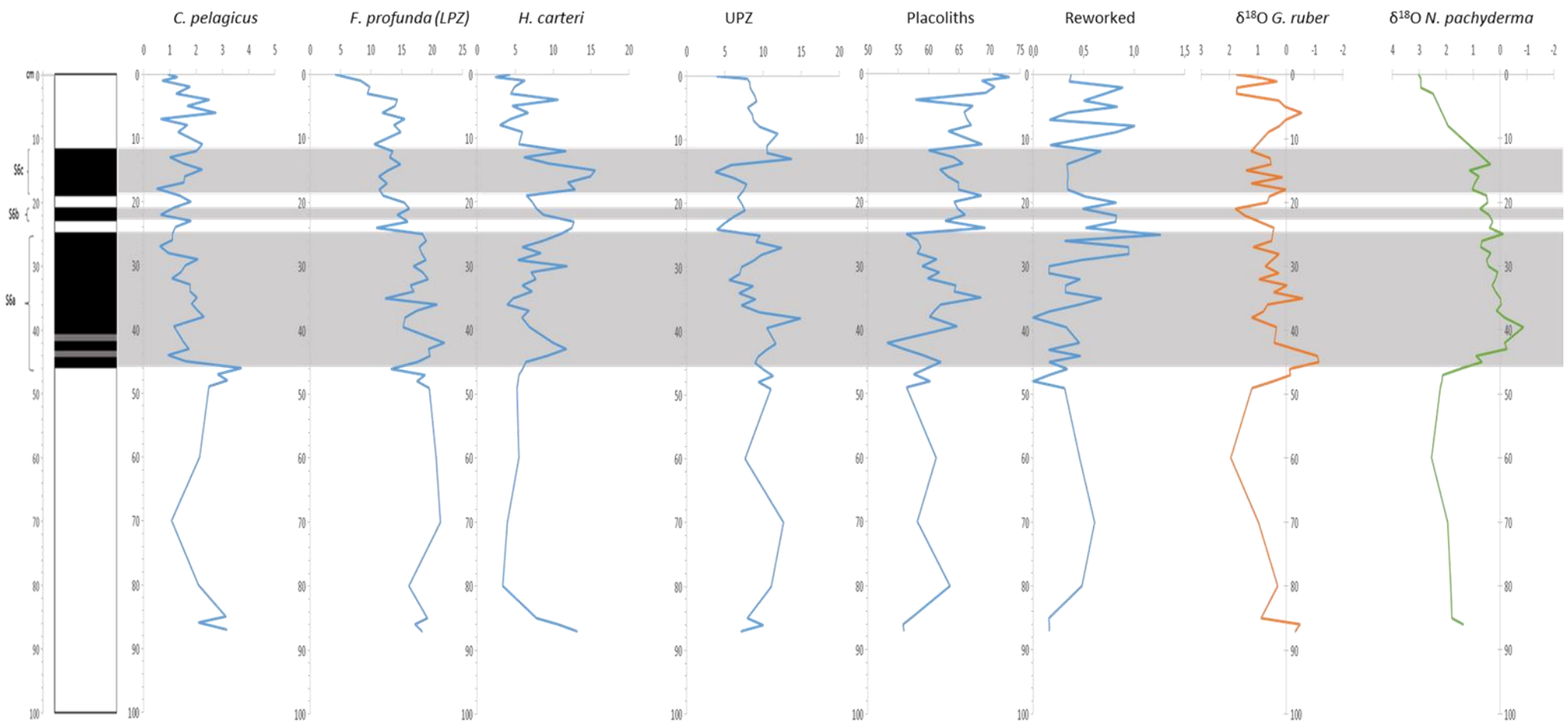

Figure 5.4: *Percentage abundance of calcareous nanofossils assemblage*

Before the sapropel beginning (section S6a) is observed an abrupt increase of *C. pelagicus* this, together with the signal of the stable isotope (*G. ruber*) indicates cold condition. In fact, according to the literature, *C. pelagicus* is a cold water species, with optimum growth conditions between 2-12°C (Castradori 1993; Bartolini 1970; Cachão, 1999; Negri *et al.*, 2002; Geisen *et al*., 2002; Baumann, 2005; Triantaphyllou *et al*., 2009). At the same time *C. pelagicus* is also indicator for nutrient enrichment of the surface oceanic waters, associated with upwelling areas and moderate turbulence (Cachão, 1999; Geisen et al, 2002; Negri *et al.,* 2002; Triantaphyllou *et al.,* 2009). The positive peak, ending at the base of the sapropel, is also observed by Negri *et al.* (2002), who suggest that the sapropel lower boundary records onset of cold and mixed water. At the same time, the *G. ruber* $\delta^{18}O$ values show high fluctuations, indicating that the superficial waters are more instable and record also short interval of fluctuating temperatures. The *N. pachyderma*, on the contrary, shows a more gradual decreasing trend toward the top of the core, indicating that, after an initial shift in temperature toward warmer values (soon after the warm peak indicated by *G. ruber* $\delta^{18}O$ at the base of S6a), the water-surface temperature decreases again. After the *C. pelagicus* peak, a positive peak of *Helicosphaera carteri* and UPZ abundances, both indicators of warmer and high-productivity water, is observed. This suggests a sudden decrease in the

salinity and/or increase in productivity (Pujos, 1992), that may indicate fresh waters discharge and so decrease in salinity and increase in turbidity. A positive correlation to *Florisphaera profunda* at the base of S6a and S6b is also observed. According to Negri *et al*. (1999) the increase in abundance of both *H. carteri* and *F. profunda* is contrasting or might be interpreted as repeated seasonal signals mixed in the sediment record. An increase of *F. profunda* is also indicator of stratification that can be correlated to the fresh buoyant water derived from river runoff.

Also, *F. profunda* abundance is decreasing across the section. Castradori (1992) suggests, like Okada and Honjo (1989) and before Okada and McIntyre (1979) that the distribution of *F. profunda* is areally and vertically limited by the isotherm of the 10°C. Therefore, to justify the decreasing trend toward the top, the cold temperature might be called responsible for this. The increase of this species at the base of S6a and S6b is probably due to the arrival of fresh and nutrient rich waters that encourage stratification and formation of a nutricline (Castradori, 1993; Baumann, 2005; Incarbona, 2011). However, the decreasing trend toward the core may be indicated that this nutricline is not well developed.

If we compare coccoliths assemblages with the analysis of dinocyst (**Fig 5.5**) made by de Groot (2017), studying the same core, it's evident that S6a base, S6b and S6c base, are characterized by high productivity water. In fact, the

species *Brigantedinium spp.* indicates upwelling and high productivity. It shows a positive correlation to *C. pelagicus, H. carteri* and UPZ. The influx of fresh water alone could explain the stratification and therefore the accumulation and availability of nutrients, which have a positive feedback on productivity (Slomp *et al*., 2002).

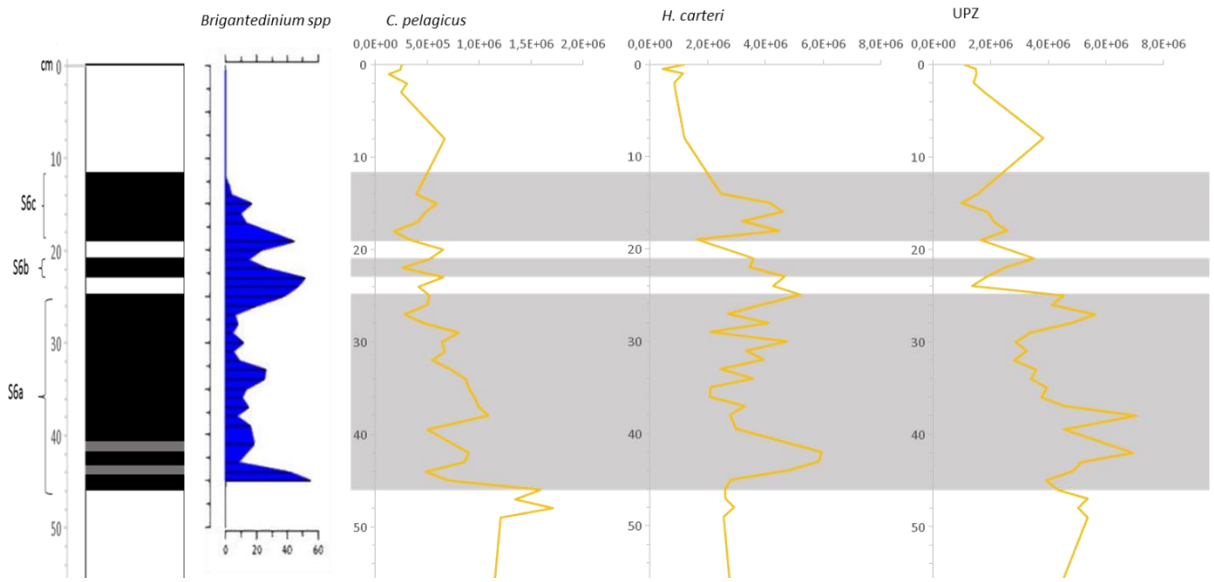

Figure 5.5*: Nannofossils abundances and dinocyst assemblage of Brigantedinium spp (dinocyst per gram sediment of S6) (modified from de Groot, 2017)*

During the first interruption, between the top of S6a and the base of S6b, we notice a decrease of *G. ruber,* probably due to a slight rise in temperatures. This is confirmed by a slight decrease of this *C. pelagicus*. Triantaphyllou *et al*. (2009) observed also a warm interval in sapropel S6, characterized by a total absence of *C. pelagicus*. However, that does not fit with this study, because *C.*

pelagicus is always present, and this can indicate that we are still in high productivity conditions. The positive peaks of *H. carteri*, UPZ and the presence of *Brigantedinium spp.* (de Groot, 2017) also confirm this.

Immediately after the first interruption, we find the section S6b, characterized again by a slight cooling of the surface waters, in fact, both the values of *G.ruber* and the abundance of *C. pelagicus* are showing an increasing trend. While *H. carteri* shows slight increase at the base, then slowly decreases towards the second interruption. UPZ also developed in the same way.

During the second interruption despite a slight warming indicated by a decrease of *G. ruber*, *C. pelagicus* shows an increasing peak, while *H. carteri* and UPZ show a slight decrease.

It could be assumed that the two interruption have led a slight rise in temperatures and even in re-oxygenation. Reworked specimens increase in the first break and slightly in the second (**Fig. 5.6**). One hypothesis to explain this behaviour could be that the core was taken in a continental slope and at the time of the deposition possibly either a dense deep waters due to a cascading event. This has led to a possible renewal of surface water. Reworked species have been compared to *Tuberculodinium vancampoae*: Fluctuations of these dinoflagellate cyst species could indicate fluctuations in temperature, salinity,

or it could be a transport signal, since it is considered a coastal species (de Groot, 2017).

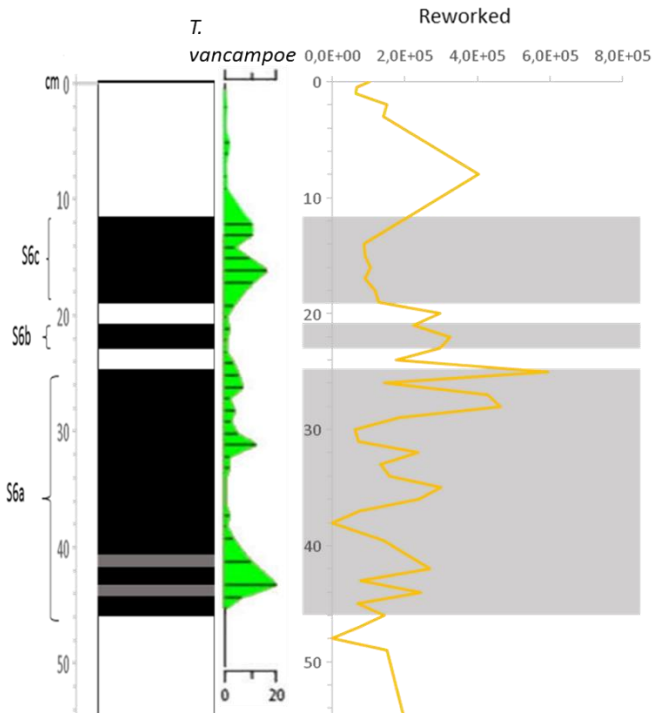

Figure 5.6 *T. vancampoae compared to nannofossils reworked assemblage (modified from de Groot, 2017)*

Temperature fluctuations are confirmed by the analysis by Emeis *et al*. (2003) in the core M40/71 (Crete). He compares the signal of oxygen isotopes with the alkenones U_{37}^{k} **(Fig 5.7**).

It can be observed that the cooler temperature of 13°C in pre-sapropel, which corresponds to *C. pelagicus* peaks of this work, is followed by a warm peak at the base of the S6a, reaching temperatures between 16 and 17°C. This

phenomenon of warmer temperature at the base is described as characteristic of all the sapropels formations studied (Emeis et al., 2003).

The fluctuations of the oxygen isotope analyses of M25/4-12 core, are in agreement with Emeis work: the coldest temperature is about 11-12°C while the warm peaks reach 17°C. The gradual heating of the surface water after the sapropel section is also confirmed.

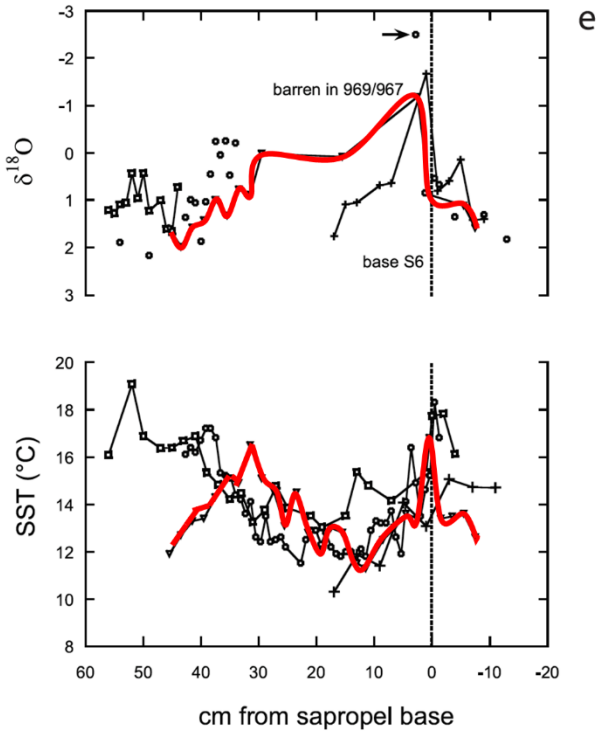

Figure 5.7: *$\delta^{18}O$ G. ruber record and SST for sapropel S6 (modified from Emeis, 2003)*

The percentages graph show in **Figure 5.4** have been taken into account due the lack of data between 13-9 cm and 7-4 cm.

A quick look at the data expressed as percentages show that the main features are observed (the succession of peaks *C. pelagicus*, and *H. carteri*).

S6 can then be divided into two parts. In the first one (S6a) calcareous nannofossils assemblage show warmer temperature and stratification, followed by progressive cooling that culminate 10 cm from the base, with temperatures of about 12°C, in agreement with Emeis *et al.* (2003) SST data. In this section high percentage of *F. profunda* were observed, indicating stratification and developing of a DCM, that instead is not observed in the upper part.

In the second section of sapropel (S6b-S6c) *H. carteri* is more abundant.

Considering that upward in the section is observed a decrease of the total abundance, this evidence that in a generally decreasing abundance *H. carteri* relatively increases probably indicating that the productivity if this species is independent from temperature, its increase is probably due to a discharge of fresh water from melting ice, due to the warmer surface temperature (**Fig 5.7**) which however does not favour stratification conditions such as to form a DCM. The high values of TOC measurement and the increase Placoliths trend

confirm that in the upper part of the photic zone high productivity conditions occur.

Finally, pollen abundances generally lower than in the other cold sapropels (S4) (de Groot, 2017) depicts an intermediate condition between humid and arid being the arboreal pollens (*Quercus* and *Pinus*) more abundant than the herbaceous ones, in particular *Artemisia*. These conditions are in agreement with the findings of this thesis and point to an unconventional sapropel characterized by cooler condition but not across the whole interval. And in particular, the inception is characterized as, all the other sapropels (Emeis *et al*., 2003) by a warm spike that probably is the primary cause for the stratification. An increase in productivity is also evident starting slightly before the beginning of sapropel, it continues with a DCM developed for the first part (S6a) and then after the interruption another relative peak expressed only by *H. carteri* in an interval characterized by a general decrease in the calcareous nannofossil productivity, indicates river discharge, turbidity but this discharge is not carrying enough nutrient to support a DCM .

Chapter Six

CONCLUSION

The aim of this work was to investigate sapropel S6 cause of deposition using the calcareous nannofossil as a paleoceanographic tool.

The calcareous nannofossils assemblage show a general decreasing trend towards the top, although, observing the relative abundances, it is evident that sapropel is characterized by different calcareous nannofossil assemblages. In particular the lower part of the S6a, is characterized by the development of a DCM, indicated by the abundance of *F. profunda*. On the other hand, S6b and S6c show an opposite behaviour, in fact, Placoliths increase, no DCM is observed but surface productivity is still high.

A comparison with literature data, confirms the glacial origin of S6.

A warm peak followed by a gradual topward cooling in S6a and then a return to warmer temperatures close the top of interval S6b-c is evidenced.

The temperature does not appear to be the sapropel S6 deposition engine, but it plays an important role for the water masses behaviour. In fact, fresh water discharge indicated by the increase of reworked specimens and *H.carteri* is claimed as responsible of a buoyant blanket that prevents mixing at the bottom.

A warm temperature spike (17°C) is the trigger for the productivity increase (peaks of *C. pelagicus* and *H.carteri*, increased relative frequency of *F. profunda*) at the base of the sapropel and is probably the cause of the initial condition of oxygen consumption (and the consequent DCM formation. then a general decrease in coccolith abundance suggest a decrease of primary productivity, but probably the sapropel anoxic conditions are maintained at bottom by stratification.

This suggest that the deposition of S6 is due to the combined effect of both high productivity and sea bottom anoxia due to stratification.

Finally, the two subsequent peaks of *C. pelagicus* and *H. carteri* respectively, is a pattern found also in other sapropels, whose meaning will have to be deeply investigated in the future and that is expected to play an important role in the understanding of the sapropel deposition dynamic

REFERENCES

Andruleit, H., Stäger, S., Rogalla, U., & Čepek, P. (2003). Living coccolithophores in the northern Arabian Sea: ecological tolerances and environmental control. Marine Micropaleontology, 49(1-2), 157-181.

Bartolini, C. (1970). Coccoliths from sediments of the western Mediterranean. Micropaleontology, 129-154.

Baumann, K.-H., Andruleit, H., Böckel, B., Geisen, M., & Kinkel, H. (2005). The significance of extant coccolithophores as indicators of ocean water masses, surface water temperature, and palaeoproductivity: a review. *Paläontologische Zeitschrift*, *79*(1), 93–112. https://doi.org/10.1007/bf03021756

Berland, B. R., Benzhitski, A. G., Burlakova, Z. P., Georgieva, L. V., Izmestieva, M. A., Kholodov, V. I., & Maestrini, S. Y. (1988). Conditions hydrologiques estivales en Méditerranée, répartition du phytoplancton et de la matière organique. Oceanol. Acta, 9(1988), 163-177.

Bernard, Francis, 1948, Recherches sur le cycle du Coccolithus fragilis Lohm., Flagell6 dominant des mers chaudes: Jour. du Cons. Permanent Internat. pour L'Exploration de la Mer, vol. 15, no. 2, pp. 177-188.

B Birkhead, M., & Pienaar, R. N. (1994). The flagellar apparatus of Prymnesium nemamethecum (Prymnesiophyceae). Phycologia, 33(5), 311-323.radley, W. H. (1938). Mediterranean sediments and Pleistocene sea levels. Science, 88(2286), 376-379.

Brand, L. E. (2006). Physiological ecology of marine. Coccolithophores, 39.

Brand, L. E., & Guillard, R. R. L. (1981). The effects of continuous light and light intensity on the reproduction rates of twenty-two species of marine phytoplankton. Journal of Experimental Marine Biology and Ecology, 50(2-3), 119-132.

Brand, L. E., Sunda, W. G., & Guillard, R. R. (1986). Reduction of marine phytoplankton reproduction rates by copper and cadmium. Journal of experimental marine biology and ecology, 96(3), 225-250.

Broecker, W. S., & Peng, T. H. (1982). Tracers in the Sea, 690 pp. Lamont-Doherty Geological Observatory, Palisades, NY.

Bown, P. R. (1997). Mesozoic calcareous nannoplankton classification. Journal of nannoplankton research, 19, 21-36.

Bown, P. R. (2005). Calcareous nannoplankton evolution: a tale of two oceans. Micropaleontology, 51(4), 299-308.

Cachão, M., & Moita, M. T. (2000). Coccolithus pelagicus, a productivity proxy related to moderate fronts off Western Iberia. *Marine Micropaleontology*, *39*(1–4), 131–155. https://doi.org/10.1016/S0377-

8398(00)00018-9
Calvert, S.E, 1983. Geochemistry of Pleistocene sapropel and associated sediments from the Eastern Mediterranean. Oceanol. Acta6, 255-267.
Canfield, D. E. (1994). Factors influencing organic carbon preservation in marine sediments. Chemical geology, 114(3-4), 315-329.
Casford, J. S. L., Rohling, E. J., Abu-Zied, R. H., Fontanier, C., Jorissen, F. J., Leng, M. J., Schmiedl, G., & Thomson, J. (2003). A dynamic concept for eastern Mediterranean circulation and oxygenation during sapropel formation. *Palaeogeography, Palaeoclimatology, Palaeoecology*, *190*, 103–119. https://doi.org/10.1016/S0031-0182(02)00601-6
Castradori, D. (1993). Calcareous nannofossil biostratigraphy and biochronology in eastern Mediterranean deep-sea cores. *Rivista Italiana Di Paleontologia e Stratigrafia*, *99*(1), 107–126. https://doi.org/10.13130/2039-4942/8948
Charlson, R. J., Lovelock, J. E., Andreae, M. O., & Warren, S. G. (1987). Oceanic phytoplankton, atmospheric sulphur, cloud albedo and climate. Nature, 326(6114), 655-661.
Cramp, A., & O'Sullivan, G. (1999). Neogene sapropels in the Mediterranean: A review. *Marine Geology*, *153*(1–4), 11–28. https://doi.org/10.1016/S0025-3227(98)00092-9
De Lange, G. J., Van Santvoort, P. J. M., Langereis, C., Thomson, J., Corselli, C., Michard, A., ... & Anastasakis, G. (1999). Palaeo-environmental variations in eastern Mediterranean sediments: a multidisciplinary approach in a prehistoric setting. Progress in Oceanography, 44(1-3), 369-386.
Ehrenberg, C.G., (1861). Ueber die TiefgrundVerhiiltnisse des Oceans am Eingange der Davisstrasse und bei Island. (K. Preuss. Akad. Wiss. Berlin, Monatsber., Jahr 1861 (1862), p. 275-315 - fide ELLIS & MESSINA).
Emeis, K.-C., Schulz, H., Struck, U., Rossignol-Strick, M., Erlenkeuser, H., Howell, M. W., Kroon, D., Mackensen, A., Ishizuka, S., Oba, T., Sakamoto, T., & Koizumi, I. (2003). Eastern Mediterranean surface water temperatures and δ 18 O composition during deposition of sapropels in the late Quaternary . *Paleoceanography*, *18*(1), n/a-n/a. https://doi.org/10.1029/2000pa000617
Emeis, K. C., Schulz, H. M., Struck, U., Sakamoto, T., Doose, H., Erlenkeuser, H., ... & Paterne, M. (1998). 26. Stable isotope and alkenone tmperature records of saproprl from site 964 and 967: constraining the physical environment of sapropel formation in the Eastern Mediterranean Sea. In Proceedings of the Ocean Drilling Program Scientific Results (Vol. 160).

Flores, J. A., & Sierro, F. J. (1997). Revised technique for calculation of calcareous nannofossil accumulation rates. *Micropaleontology*, *43*(3), 321–324. https://doi.org/10.2307/1485832

Gačić, M., Borzelli, G. E., Civitarese, G., Cardin, V., & Yari, S. (2010). Can internal processes sustain reversals of the ocean upper circulation? The Ionian Sea example. Geophysical research letters, 37(9).

Gartner, S. (1988). Paleoceanography of the mid-Pleistocene. Marine Micropaleontology, 13(1), 23-46.

Geisen, M., Probert, I., & Young, J. R. (2002). Coccolithophores for Exhibition : a Note. *Journal of Nannoplankton Research*, *24*, 3–7. http://hdl.handle.net/10013/epic.16147

Holligan, P. M., Fernández, E., Aiken, J., Balch, W. M., Boyd, P., Burkill, P. H., ... & Purdie, D. A. (1993). A biogeochemical study of the coccolithophore, Emiliania huxleyi, in the North Atlantic. Global biogeochemical cycles, 7(4), 879-900.

Hulburt, E. M., Ryther, J. H., & Guillard, R. R. L. (1960). The phytoplankton of the Sargasso Sea off Bermuda. ICES Journal of Marine Science, 25(2), 115-128.

Incarbona, A., Ziveri, P., Sabatino, N., Manta, D. S., & Sprovieri, M. (2011). Conflicting coccolithophore and geochemical evidence for productivity levels in the Eastern Mediterranean sapropel S1. *Marine Micropaleontology*, *81*(3–4), 131–143. https://doi.org/10.1016/j.marmicro.2011.09.003

Inouye, I., & Kawachi, M. (1994). The haptonema. Systematics association special volume, 51, 73-73.

Jordan, R. W. (1989). Coccolithophorid communities in the North-East Atlantic.

Klaveness, D., & Paasche, E. Y. S. T. E. I. N. (1979). Physiology of coccolithophorids. Biochemistry and physiology of protozoa, 1, 191-213.

Kleijne, A., D. Kroon, and W. Zevenboom, 1989: Phytoplankton and foraminiferal frequencies in northern Indian Ocean and Red Sea surface waters, Proc. Snellius II Symp, Neth., J. Sea, Res. 24, 531-539.

Knappertsbusch, M., Cortes, M. Y., & Thierstein, H. R. (1997). Morphologic variability of the coccolithophorid Calcidiscus leptoporus in the plankton, surface sediments and from the Early Pleistocene. *Marine Micropaleontology*, *30*(4), 293–317.
https://doi.org/10.1016/S0377-8398(96)00053-9

Kullenberg, B. (1952). On the salinity of the water contained in marine sediments (Vol. 6). Elanders boktr

Kutzbach, J. E., & Liu, Z. (1997). Response of the African monsoon to orbital

forcing and ocean feedbacks in the middle Holocene. Science, 278(5337), 440-443.
Lisiecki, L. E., & Raymo, M. E. (2005). Paleoceanography 20. PA1003, 10
Lourens, L. J., Antonarakou, A., Hilgen, F. J., Van Hoof, A. A. M., Vergnaud-Grazzini, C., & Zachariasse, W. J. (1996). Evaluation of the Plio-Pleistocene astronomical timescale. Paleoceanography, 11(4), 391-413.
Lourens, L. (2004). 21 The Neogene Period. A geologic time scale 2004, 409-440.
Löwemark, L., Lin, Y., Chen, H. F., Yang, T. N., Beier, C., Werner, F., ... & Kao, S. J. (2006). Sapropel burn-down and ichnological response to late Quaternary sapropel formation in two～400 ky records from the eastern Mediterranean Sea. Palaeogeography, Palaeoclimatology, Palaeoecology, 239(3-4), 406-425.
Malanotte-Rizzoli, P., Manca, B. B., D'Alcalà, M. R., Theocharis, A., Bergamasco, A., Bregant, D., Budillon, G., Clvitarese, G., Georgopoulos, D., Mlchelato, A., Sansone, E., Scarazzato, P., & Souvermezoglou, E. (1997). A synthesis of the Ionian Sea hydrography, circulation and water mass pathways during POEM-phase I. *Progress in Oceanography*, *39*(3), 153–204. https://doi.org/10.1016/S0079-6611(97)00013-X
Malinverno, E., Ziveri, P., & Corselli, C. (2003). Coccolithophorid distribution in the Ionian Sea and its relationship to eastern Mediterranean circulation during late fall to early winter 1997. *Journal of Geophysical Research C: Oceans*, *108*(9), 1–16. https://doi.org/10.1029/2002jc001346
Marshall, H. G. (1978). Phytoplankton distribution along the eastern coast of the USA. Part II. Seasonal assemblages north of Cape Hatteras, North Carolina. Marine Biology, 45(3), 203-208.
McIntyre, A., & Bé, A. W. (1967, October). Modern coccolithophoridae of the Atlantic Ocean—I. Placoliths and cyrtoliths. In Deep Sea Research and Oceanographic Abstracts (Vol. 14, No. 5, pp. 561-597). Elsevier.
Mercone, D., Thomson, J., Abu-Zied, R. H., Croudace, I. W., & Rohling, E. J. (2001). High-resolution geochemical and micropalaeontological profiling of the most recent eastern Mediterranean sapropel. Marine Geology, 177(1-2), 25-44.
Mjaaland, G. (1956). Some laboratory experiments on the coccolithophorid Coccolithus huxleyi. Oikos, 7(2), 251-255.
Michelle, P. (2017). *Sapropel S4 and S6 : A comparison between interglacial and glacial organic-rich sediments from the Ionian Sea*. *May*.
Milliman, J. D. (1980). Coccolithophorid production and sedimentation, Rockall Bank. Deep Sea Research Part A. Oceanographic Research

Papers, 27(11), 959-963.
Mitchell-Innes, B. A., & Winter, A. (1987). Coccolithophores: a major phytoplankton component in mature upwelled waters off the Cape Peninsula, South Africa in March, 1983. Marine Biology, 95(1), 25-30.
Monteiro, F. M., Bach, L. T., Brownlee, C., Bown, P., Rickaby, R. E., Poulton, A. J., ... & Gutowska, M. A. (2016). Why marine phytoplankton calcify. Science Advances, 2(7), e1501822.
Murat, A., 1984. Sequences et Paleoenvironments marins quaternaires. Une marge active: l'Arc Hellenique Oriental. Unpubl. Ph.D. thesis, Univ. of Perpignan, 191 pp.
Negri, A., Capotondi, L., & Keller, J. (1999). Calcareous nannofossils, planktonic foraminifera and oxygen isotopes in the late Quaternary sapropels of the Ionian Sea. *Marine Geology*, *157*(1–2), 89–103. https://doi.org/10.1016/S0025-3227(98)00135-2
Negri, Alessandra, & Giunta, S. (2001). Calcareous nannofossil paleoecology in the sapropel S1 of the Eastern Ionian sea: Paleoceanographic implications. *Palaeogeography, Palaeoclimatology, Palaeoecology*, *169*(1–2), 101–112. https://doi.org/10.1016/S0031-0182(01)00219-X
Oggioni, E., & Zandini, L. (1987). Response of benthic foraminifera to stagnant episodes—a quantitative study of Core BAN 81-23, eastern Mediterranean. Marine geology, 75(1-4), 241-261.
Okada, H., & Honjo, S. (1973, April). The distribution of oceanic coccolithophorids in the Pacific. In Deep Sea Research and Oceanographic Abstracts (Vol. 20, No. 4, pp. 355-374). Elsevier.
Paasche, E. (1968). Biology and physiology of coccolithophorids. Annual Reviews in Microbiology, 22(1), 71-86
Pinardi, N., & Masetti, E. (2000). Variability of the large scale general circulation of the Mediterranean Sea from observations and modelling: A review. *Palaeogeography, Palaeoclimatology, Palaeoecology*, *158*(3–4), 153–173. https://doi.org/10.1016/S0031
Rayns, D. G. (1962). Alternation of generations in a coccolithophorid, Cricosphaera carterae (Braarud & Fagerl.) Braarud. Journal of the Marine Biological Association of the United Kingdom, 42(3), 481-484.0182(00)00048-1
Robinson, A. R., Leslie, W. G., Theocharis, A., & Lascaratos, A. (2001). Mediterranean Sea Circulation. *Encyclopedia of Ocean Sciences*, 1689–1705. https://doi.org/10.1006/rwos.2001.0376
Rohling, E. J., Marino, G., & Grant, K. M. (2015). Mediterranean climate and oceanography, and the periodic development of anoxic events (sapropels). *Earth-Science Reviews*, *143*, 62–97.

https://doi.org/10.1016/j.earscirev.2015.01.008
Rohling, Eelco J. (1991). A Simple Two-Layered Model for Shoaling of the Eastern Mediterranean Pycnocline Due to Glacio-Eustatic Sea Level Lowering. *Paleoceanography*, *6*(4), 537–541. https://doi.org/10.1029/91PA01328
Ruddiman, W. F., & Kutzbach, J. E. (1989). Forcing of late Cenozoic Northern Hemisphere climate by plateau uplift in southern Asia and the American west. *Journal of Geophysical Research*, *94*(D15). https://doi.org/10.1029/jd094id15p18409
Ryan, W. B. F., Cita, M. B., & Observatory, L. G. (1976). *unravelled by the so-called paleoenvironmentalists or paleoceanographers . It extends well beyond one hundred million years and reveals some startling circumstances , which although poorly comprehended right now , might eventually be perceived as quantita*. *2420*.
Sancetta, C. (1994). Mediterranean sapropels: Seasonal stratification yields high production and carbon flux. *Paleoceanography*, *9*(2), 195–196. https://doi.org/10.1029/94PA00090
Stanley, D. J., & Maldonado, A. (1977). Nile Cone: Late Quaternary stratigraphy and sediment dispersal. Nature, 266(5598), 129-135.
Taylforth, J. E., McCay, G. A., Ellam, R., Raffi, I., Kroon, D., & Robertson, A. H. F. (2014). Middle Miocene (Langhian) sapropel formation in the easternmost Mediterranean deep-water basin: Evidence from northern Cyprus. *Marine and Petroleum Geology*, *57*, 521–536. https://doi.org/10.1016/j.marpetgeo.2014.04.015
Tappan, H. N. (1980). The paleobiology of plant protists. Wh Freeman.
Ten Haven, H. L., Baas, M., Kroot, M., De Leeuw, J. W., Schenck, P. A., & Ebbing, J. (1987). Late Quaternary Mediterranean sapropels. III: Assessment of source of input and palaeotemperature as derived from biological markers. Geochimica et Cosmochimica Acta, 51(4), 803-810.
Thierstein, H. R. (1998). Coccoliths in the Late. *October*, *13*(5), 517–529.
Townsend, D. W., Keller, M. D., Holligan, P. M., Ackleson, S. G., & Balch, W. M. (1994). Blooms of the coccolithophore Emiliania huxleyi with respect to hydrography in the Gulf of Maine. Continental Shelf Research, 14(9), 979-1000.
Triantaphyllou, M. V., Antonarakou, A., Kouli, K., Dimiza, M., Kontakiotis, G., Papanikolaou, M. D., Ziveri, P., Mortyn, P. G., Lianou, V., Lykousis, V., & Dermitzakis, M. D. (2009). Late Glacial-Holocene ecostratigraphy of the south-eastern Aegean Sea, based on plankton and pollen assemblages. *Geo-Marine Letters*, *29*(4), 249–267. https://doi.org/10.1007/s00367-009-0139-5

Van der Wal, P., Kempers, R. S., & Veldhuis, M. J. (1995). Production and downward flux of organic matter and calcite in a North Sea bloom of the coccolithophore Emiliania huxleyi. Marine ecology progress series, 126, 247-265.

Vairavamurthy, A., Andreae, M. O., & Iverson, R. L. (1985). Biosynthesis of dimethylsulfide and dimethylpropiothetin by Hymenomonas carterae in relation to sulfur source and salinity variations. Limnology and Oceanography, 30(1), 59-70.

Vismara Schilling, A. (1986). Foraminiferi bentonici profandi associati a eventi anossici del Pleistocene medio e superiore nel Mediterraneo orientale. Rivista italiana di paleontologia e stratigrafia, 92(1), 103-148.

Westbroek, P., Young, J. R., & Linschooten, K. (1989). Coccolith production (biomineralization) in the marine alga Emiliania huxleyi. The Journal of protozoology, 36(4), 368-373.

Williams, D. F., & Thunell, R. C. (1979). Faunal and oxygen isotopic evidence for surface water salinity changes during sapropel formation in the eastern Mediterranean. Sedimentary Geology, 23(1-4), 81-93

Winter, A. L., Jordan, R. W., & Roth, P. H. (1994). Biogeography of living coccolithophores in ocean waters.

Winter, A., & Siesser, W. G. (Eds.). (2006). Coccolithophores. Cambridge University Press.

Young, J. R., Geisen, M., Cros, L., Kleijne, a, Sprengel, C., Probert, I., & Østergaard, J. (2003). A guide to extant coccolithophore taxonomy . *Journal of Nannoplankton Research*, *Special Issue 1*, 125.

Young, J. R. (1987). Higher classification of Coccolithophores. International Nannofossil Association Newsletter, 9, 36-38.

Young J.R., Sarsia, 79 (1994), Variation in Emiliania huxleyi coccolith morphology in samples from the Norwegian EHUX experiment, 1992 pp. 417-425

Ziveri, P., Thunell, R. C., & Rio, D. (1995). Seasonal changes in coccolithophore densities in the Southern California Bight during 1991–1992. Deep Sea Research Part I: Oceanographic Research Papers, 42(11-12), 1881-1903.

APPENDIX

Ecology of calcareous nannofossils species from the literature (all photos are taken from http://www.mikrotax.org/Nannotax3/).

Gephyricapsa small

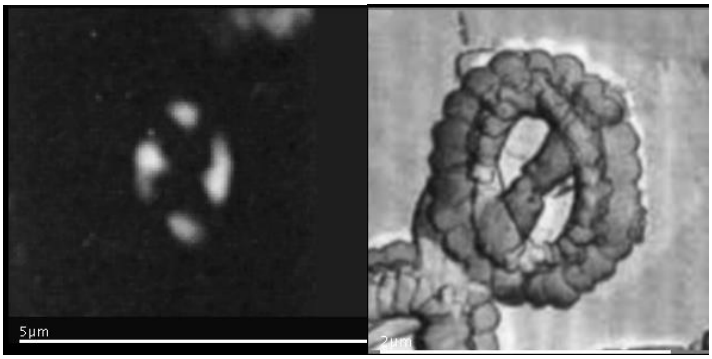

(Matsuoka & Okada 1989)

- ✓ Characteristic of the transitional climatic zone (Mcintyre and Be', 1967).
- ✓ Indicator of surface water characterized by high productivity (Gartner 1987).
- ✓ Reflection of oceanographic disturbances induced by the increase in equatorial ascents, in turn triggered by the increase in the formation rate of deep waters in the Arctic Ocean. Cold-temperate water temperature (17°C) with high nutrients content. Opportunist species. (Gartner 1988).
- ✓ Literature data concerning the different species of the genus *Gephyrocapsa* are useful. Due to the classification is too simplified; the extrapolation of ecological preferences is prevented. All species of *Gephyrocapsa* are resistant to diagenesis (Castradori 1993).
- ✓ "Small" *Gephyrocapsa* dominate the assemblage in a restricted interval between 830 and 1010 cm (Negi, Capotondi and Keller, 1999).
- ✓ Paleotemperatures proxy: qualitative SST changes have been derived previously from the relative abundances of certain *Gephyrocapsa* species (Weaver & Pujol, 1988; Takahashi & Okada 2000). Observed down-core patterns were consistent with the expected glacial-interglacial temperature variability, reflecting decreased temperatures during glacial periods.

- ✓ Bollman et al. (2002) introduced a global sea surface temperature calibration based on the relative abundance of different morphotypes within the coccolithophore genus *Gephyrocapsa*. The authors showed that this temperature transfer function has potential for the reconstruction of paleotemperatures in the temperature range from 14.0°C to 29.4°C.
- ✓ *Gephyrocapsa small* and *G. muellerae* are also presented together because are both indicative of productivity (moderate to high) in the upper photic zone (Bollmann, 1997; Wells and Okada, 1997; Flores et al., 2003; Boeckel et al., 2006).
- ✓ Considering the ecological preferences of *F. profunda* and *Gephyrocapsa spp.*, opposite trends between their records should be expected (Narciso *et al.,* 2010).

Helicosphaera carteri

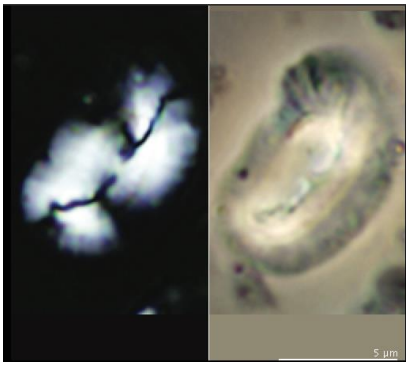

(Boesiger et al., 2017)

- ✓ Indicators of cold waters (Bartolini, 1970)
- ✓ Rare in the living (Mcintrye, Be' and Roche, 1970).
- ✓ Cosmopolitan species, not temperature related (Routh and Coulburn, 1982).
- ✓ Increases due to its best resistance to diagenesis, some authors disagree with this statement (Thiersen, 1990).
- ✓ Relationship to surface turbidity (Tephra) (Castradori and Violanti, 1991).
- ✓ Abundance increase in upwelling zones (Cachão, 1991).
- ✓ Related to the turbidity takes over other species less able to adapt to low brightness (Castradori, 1991).

- ✓ Increased frequency of *H. carteri* indicates a sudden decrease in the salinity and/or increase in productivity (Pujos, 1992).
- ✓ Inverse relationship between abundances and salinity in Eastern Mediterranean (Muller, 1995).
- ✓ Increased fluxes of *H. carteri* when overall coccolithophore fluxes were high. High coccolithophorid productivity is in fact also suggested by the increased abundance of *H. carteri*. (Ziveri et al. 1995a,b).
- ✓ In the Bermuda modern coccolithophore assemblages was recorded that *H. carteri* increases in conditions of high temperature and light intensity and when nutrients are lowered with respect to the amount required by *Emiliania huxleyi* (Haidar and Thierstein, 1997).
- ✓ Increased abundance indicates a sudden decrease in salinity and/or increase in productivity. Increase in condition of high temperatures and light intensity, and when nutrients are lowered. The increase in abundance of both *H. carteri* and *F. profunda* is somewhat contrasting or might be interpreted as repeated seasonal signals mixed in the sediment record (Negri, Capotondi, Keller 1999).
- ✓ Shows a warm water higher productivity distribution (Baumann, 2005).

Florisphaera profunda

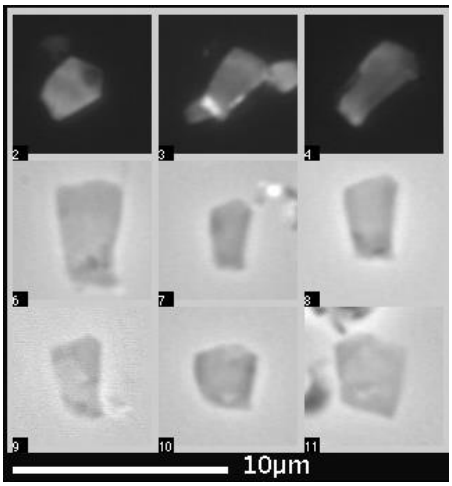

(JRYoung, unpubl)

- ✓ Lives in the lower euphotic zone and prefers low light and high nutrients. Its habitat is restricted to waters below 100 m and warmer than 10°C in the Pacific (Okada and Honjo, 1973) and in the Atlantic (Okada and Mcintyre, 1979).
- ✓ The lower photic zone species *Florisphaera profunda* is a reliable proxy of the nutricline-thermocline (Okada and Honjo, 1973; Molfino and McIntyre, 1990); thus, high relative abundances indicate stable stratification of the water column and low productivity in the surface layer (Triantaphyllou, 2014).
- ✓ Lives under 100m, lower part of the photic zone, in condition of low light and high nutrients. Distribution limited at the isotherm 10°C. Indicator of deep nutricline. (Castradori, 1993).
- ✓ The percentage of abundance of *F. profunda* in surface sediments seem to be a function of the primary productivity and, thus, providing a robust transfer function for paleoproductivity estimates (Beaufort et al. 1997).
- ✓ Relationship between the increase of *F. profunda* abundance and increase of water transparency. Increase during cold season. Prefers nutrient-depleted water, characterized also by low light intensity and low temperature. Blooms together with other species. (Negri, Capotondi, Keller, 1999).

- ✓ Deepwelling species, indicators of deep nutricline and thermocline. Most abundant and variations within their occurrences were explained in terms of changes in nutricline depth. Excellent indicator for reconstructing past changes in the thermocline dynamics. Peaks in *F. profunda* abundance rather sternly corresponding to minim of coccolith accumulation rate. (Baumann, 2005).
- ✓ Located in the photic zone below 30 m and does not appear to be related to nitrate and phosphate concentrations but rather to the turbidity and low light intensity of the area (Balestra *et al*., 2008).
- ✓ Associated with the deep photic zone with well-stratified and nutrient-rich waters (Marino *et al.,* 2008).
- ✓ Index of stratiphication condition (Triantaphyllou *et al*., 2009).
- ✓ Proxy for the development of a DCM. Abundance sensitive to modifications in the depth of the nutricline. Increase of *F. profunda* implies a shift in the nutricline towards the lower photic zone and the development of a vertical zonation in the coccolith assemblages that is typical at lower and middle latitude. Higher contribution of *F. profunda*, with respect to *E. huxleyi* and UPZ taxa, possibly due to the deepening of the thermocline. *F. profunda* is the most important species of the 'lower photic zone' (Incarbona *et al*., 2011).

Emiliania huxleyi

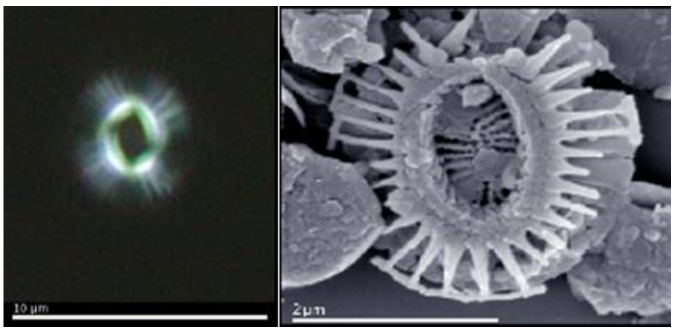

(JRYoung, unpubl)

- ✓ Fluctuations in abundance could be related to periods characterised by surface water conditions unfavourable to other species (Castradori, 1993).

- ✓ Most abundant in the Atlantic Ocean, can live at temperature under 0°C, in low nutrients condition and in the first 20 m of the water column (Balch, Holligan, Ackleson and Voss, 1991).
- ✓ Can stand the low level of salinity of the Black Sea. Cosmopolitan species (Burky, 1974).
- ✓ Most abundant under 20°C and upper 25°C. Present in the entire photic zone (Honjo and Okada, 1974).
- ✓ Ubiquitous, can live under 6°C (McIntrye, Be' and Roche, 1970).
- ✓ Considered cosmopolitan, eurihalyne, eurytherm in literatures (Winter 1985).
- ✓ Quick response to nutrient enrichment (Triantaphyllou et al. 2009).
- ✓ Controls the high production of coccolithophores. R-strategy taxa. Proxy of high productivity condition in the upper part of the water column. (Incarbona et al. 2011)

Coccolithus pelagicus

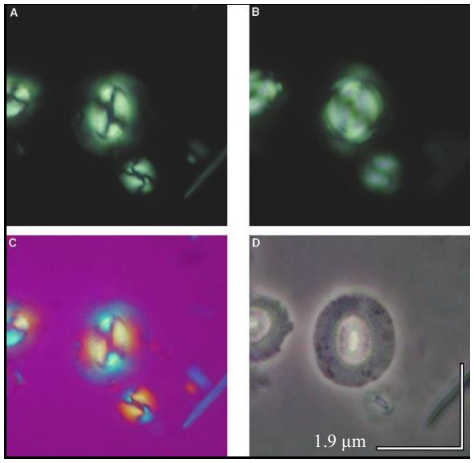

(JRYoung, unpubl)

- ✓ Cold species (Bartolini 1970).
- ✓ Cold water at high latitude in northern hemisphere. Indicator of temperature decrease (Castradori 1993).
- ✓ Optimum growth conditions between 2-12°C. Indicator for nutrient enrichment of the surface oceanic waters. Cold T from -1.7 to 15°C. Moderate turbulence. Affinity for upwelling areas (Cachao, 1999).

- ✓ Associated with cold weather conditions, is found between 26-14,8 kyr BP and 12,4-10,5 kyr BP (Buccianti and Esposito, 2002).
- ✓ Absent in the subantartic zone. High abundance in the North Atlantic T<10°C (Baumann 2005).
- ✓ Abundance is related to conditions of moderately high-water turbulence and nutrient availability (Negri, Morigi, Giunta, 2002).
- ✓ Shows preference for cold water, high nutrient concentrations and high dynamism (Marino *et al.*, 2008).
- ✓ Proxy of cold water and surface productivity (Triantaphyllou et al 2009).

Calcidiscus leptorus

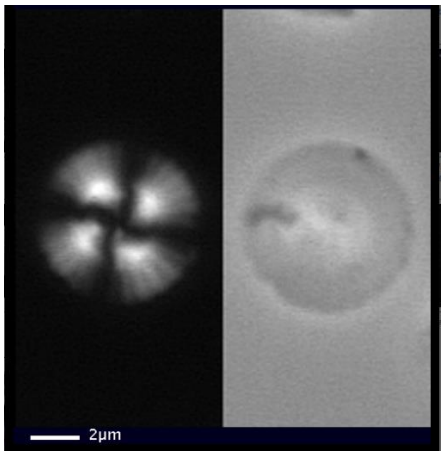

- ✓ Ubiquitous, distributed in the photic zone (Honjo, 1976).
- ✓ Moderate resistance to diagenesis. Prefers waters rich in nutrients. It is not related to the temperature (Castradori, 1993).
- ✓ Interglacial presence indicates relative increase in nutrients (Flores *et al.,* 1995).
- ✓ Associated with warm surface waters (Buccianti and Esposito, 2002).
- ✓ Associated with warm and oligotrophic waters; the low abundance of the "small" morphotype is in agreement with the affinity for the subtropical gyre of the taxa (Marino *et al.,* 2008).

Syracosphaera pulchra

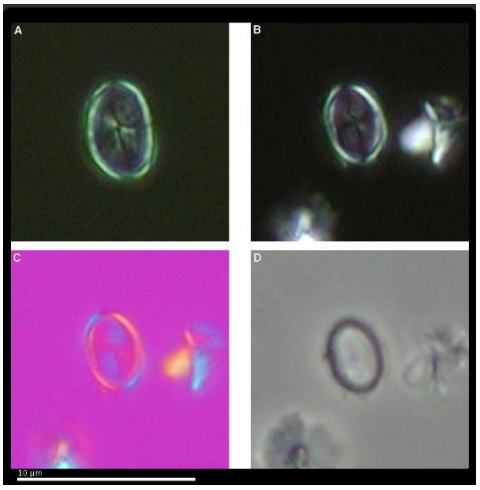

(JRYoung, unpubl)

- ✓ Medium resistance to diagenesis, wide range of distribution, prefers hot water temperatures (Castradori, 1993).
- ✓ Characteristic of less productive water (Roth and Berger, 1975).
- ✓ Characteristic of tropical and subtropical association (McIntyre, 1972).
- ✓ Distributed in the upper photic zone (Reid, 1980; Incarbona, 2011).
- ✓ Warm water, low productivity (Baumann, 2005).

Syracosphaera spp.

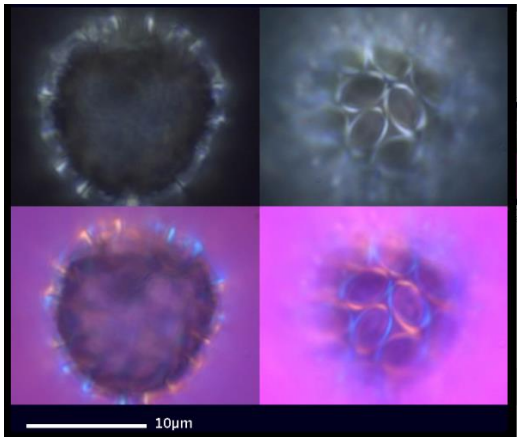

(JRYoung, unpubl)

- ✓ Negative related to *H. Carteri* and *C. leptorus*. Not so well adapted to high productivity condition (Castradori, 1993).
- ✓ The presence in relatively cold water indicates that parameters such as salinity and nutrient amounts control the concentration (Flores *et al*., 1995).
- ✓ Is located in the upper photic zone (Balestra *et al*., 2008; Incarbona, 2011).

Rhabdosphaera spp.

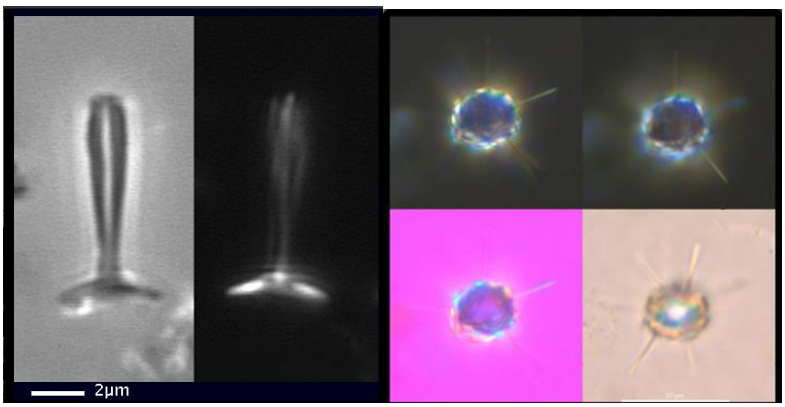

(R. clavigera (Young, 1998); R. stilifera (JRYound, unpubl))

- ✓ *R. clavigera* is found more often around -150 m of depth (perhaps limited by light); *R. stilifera* is more frequent in the top 100 m of the water column (Kimor and Wood, 1975).
- ✓ *R. clavigera:* most abundant species on the surface in the southern part of the Transitional zone; typical of upper photic zone (Okada and McIntyre, 1977). Distribution between 3-29°C (Okada and McIntyre, 1979).
- ✓ *R. clavigera*: oceanic and warm water, found under 150m of depth, maybe limited by the light (Conley, 1979).
- ✓ *R. clavigera*: develops mainly during summer when the ecological indices indicate normal or oligothropic condition, typical species of warm oligotrophic environment (Castradori, 1993).
- ✓ *R. stilifera*: most abundance up to 100m (Kimar and Wadd, 1975)
- ✓ *R. stilifera*: Proxy for warm water and stratification, and for oligotrophic condition (Castradori, 1993)
- ✓ Opportunistic group able to survive also in low nutrient conditions (Roth and Coulbourn 1982).
- ✓ In addition Ziveri et al. (1995a) recorded *Rhabdosphaera spp.* in modern assemblages over a wide range of SSTs (14–20ºC).
- ✓ The sympathetic fluctuations of *Rhabdosphaera spp*. and *F. profunda* coupled to a decrease in the total abundance of nannofossils appear to support the presence of a DCM, in agreement with Castradori (1993) (Negri, Capotondi and Keller, 1999).

Umbilicopshaera sibogae

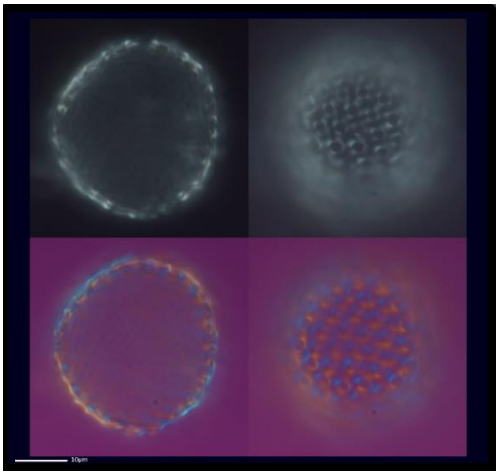

(JRYoung, unpubl)

- ✓ Prefers warm water (Okada and McIntyre, 1977).
- ✓ Distributed between 12 and 30°C (Okada and McIntyre, 1979).
- ✓ Most abundant between 8 and 20°C South in water with a medium-high level of nutrients. (Roth and Berger, 1975).
- ✓ Is located north of the 40°S, particularly abundant at low latitudes, tends to grow with SST (Hiramatsu and De Deckker, 1995).
- ✓ Is found from 10.5 kyr BP to the present day during the interglacial phase (Buccianti and Esposito, 2002).

PLATE

I. *Gephyrocapsa small*

II. *Helicosphaera carteri*

III. *Florisphaera profunda*

IV. *Coccolithus pelagicus*

V. *Syracosphaera pulchra*

VI. *Syracosphaera sp.*

VII. *Calcidiscus leptoporus*

VIII. *Rhabdosphaera clavigera*

IX. *Reticulafenestra sp.*

X. *Pontosphaera sp.*

XI. *Umbilicosphaera sp.*

XII. *Sphenolithus sp.*

I

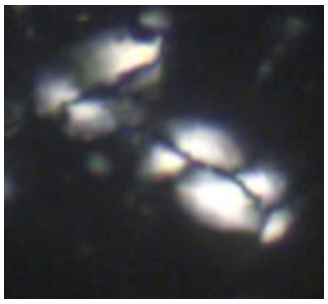

II

III

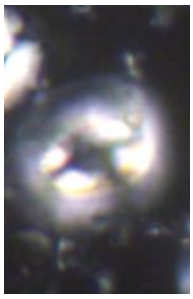

IV

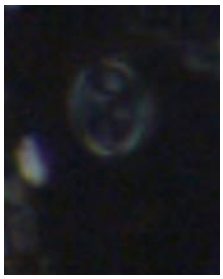

V

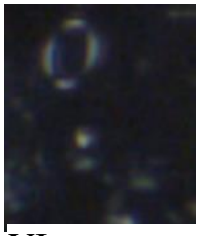

VI

VII

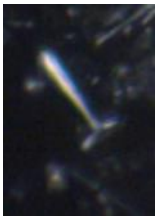

VIII

IX

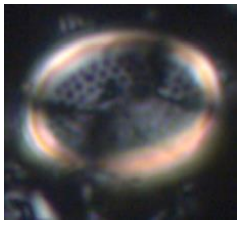

X

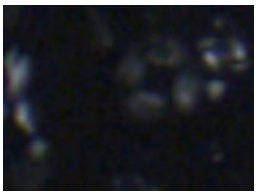

XII

XIII